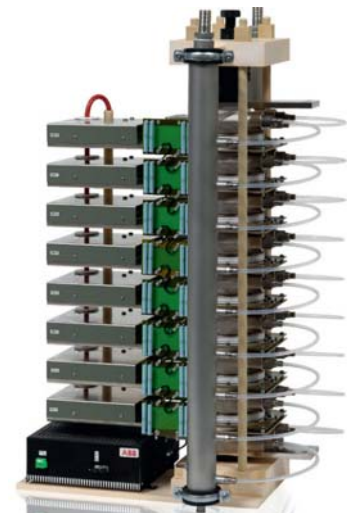
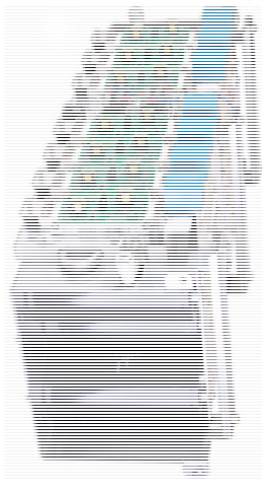
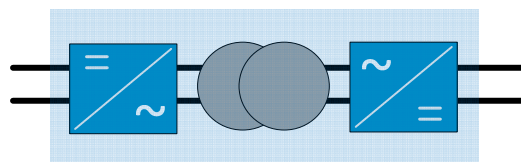


State of the Art

High power DC/DC Converters

Technologies



CGD 10-nov-2015

V-1.3

This report is part of Power Collection and Distribution in Medium Voltage DC Networks project.

Version	Init	Date	Description
1.0	CGD	21-09-2015	Document created
1.1	CGD	29-09-2015	PCK comments implemented
1.2	CGD	02-10-2015	PCK comments implemented
1.3	CGD	10-11-2015	PCK and CLB comments implemented

Contents

0. Introduction	10
1. Fundamental functionalities and technical requirements	12
2. Ranking of design drivers	17
3. Basic circuit concepts from demonstrators	22
4. Demonstrators for high power applications.....	28
a. Who has done what to solve functionalities?	28
b. DC Turbine concepts	33
i. Dual active bridge and Series Resonant converter 2007.....	33
ii. Full bridge 2009	34
iii. Single active bridge 2012.....	36
iv. Full bridge 2006	37
v. Matrix 2012	38
vi. Modular transformer less 2013.....	39
vii. High gain transformer less 2009.....	40
viii. High gain transformerless 2012.....	40
ix. High gain transformerless 2015.....	41
c. Traction demonstrators	42
i. Traction Cycloconverter 2007	42
ii. Traction SRC 2002.....	45
iii. Traction LLC 2014	47
iv. Traction SRC 2011.....	51
v. Traction DAB and SRC 2013.....	53
vi. Traction SRC 2007.....	58
vii. Traction DAB and LLC 2012	61
viii. Traction Cycloconverter 2009	63
d. Solid State Transformers	65
I. SST SiC 2011	65
II. SST DAB 2011	67
III. SST DAB 2010	69
e. Medium Voltage Distribution.....	71
I. SST DAB 2014.....	71
5. Medium Frequency Transformers	75

a.	Core	75
b.	Windings	78
c.	Insulating Material.....	78
d.	Design considerations.....	79
e.	ETH Zurich transformer prototypes.....	79
6.	Semiconductor Overview	83
a.	Line Frequency Diode	84
b.	Fast Rectifying Diode	84
c.	IGCT	85
d.	IGBT	86
e.	IEGT (Injection Enhanced Gate Transistors)	87
f.	Press pack vs. power modules.....	87
g.	Converter integration aspects	88
h.	Loss comparison of different semiconductors based on a 5[MW] 3L-NPC inverter	89
i.	Recent advances in power electronic semiconductors	91
j.	Valve mechanical concepts	91
7.	Cooling.....	99
a.	Air cooling for semiconductors [54]	99
i.	Natural and forced air cooling.....	99
b.	Liquid cooling for semiconductors [54]	100
ii.	Mounting direction and venting [54]	102
iii.	Turbulent flow [54].....	102
iv.	Thermosyphon Cooling [54]	103
v.	Phase transition Cooling [54]	104
c.	Natural and forced oil cooling for transformers [58]	105
8.	Insulation coordination	107
9.	Conclusions	109
10.	Bibliography	113
11.	Appendix	118

List of Figures

Fig. 1 Selection proces	10
Fig. 2 Where SOA belongs to	11
Fig. 3 Line diagram of turbine converter	12
Fig. 4 Specification range for turbine DC/DC converter	13
Fig. 5 Wind turbine system with MVDC output.....	14
Fig. 6 Concept of operation of day in the life	15
Fig. 7 Converter segmentation	15
Fig. 8 Control and Protection.....	16
Fig. 9 Common challenges	18
Fig. 10 ABB PCS 6000	21
Fig. 11 Topologies implemented in demonstrators	23
Fig. 12 Areas of applications for the demonstrators	23
Fig. 13 Half-Bridge SRC	23
Fig. 14 Full Bridge SRC	23
Fig. 15 NPC SRC.....	24
Fig. 16 Half-Bridge LLC.....	24
Fig. 17 Full-Bridge DAB	24
Fig. 18 NPC DAB	25
Fig. 19 Three phase Dual Active Bridge	25
Fig. 20 Modular AC/DC converter with cycloconverter+rectifier.....	26
Fig. 21 Modular AC/DC converter with rectifier+inverter+rectifier	26
Fig. 22 Modular Three Phase SST	27
Fig. 23 Relevant research centers	29
Fig. 24 Selected demonstrator projects	32
Fig. 25 Studied topologies in [3]	33
Fig. 26 Efficiency and control diagram	33
Fig. 27 Studied topologies in [7]	34
Fig. 28 Model of turbine converter	34
Fig. 29 Model of turbine control blocks	35
Fig. 30 Lab setup and transformer used in [7]	35
Fig. 31 N-parallel connected SAB dc-dc converters from [35]	36
Fig. 32 Control and lab setup from [36]	36
Fig. 33 Selected topology in [37]	37
Fig. 34 Control and lab setup used in [37].....	37
Fig. 35 Selected topology in [8]	38
Fig. 36 Control and lab setup used in [8].....	38
Fig. 37 Proposed topology in [38].....	39
Fig. 38 Control and lab setup in [38]	39
Fig. 39 Topology and lab setup.....	40
Fig. 40 Topology and lab setup.....	40

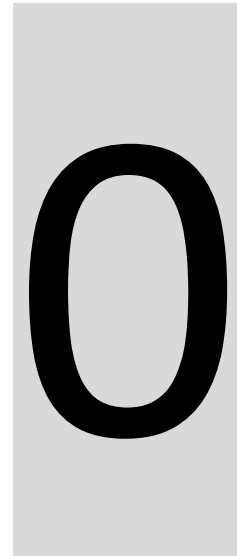
Fig. 41 Topology and lab setup.....	41
Fig. 42 Photo of demonstrator [21].....	42
Fig. 43 Photo of the sixteen medium frequency transformers [21].....	42
Fig. 44 Converter circuit used in [21]	42
Fig. 45 Control principle	44
Fig. 46 Basic configuration of coaxial transformer [13].....	45
Fig. 47 Physical arrangement of transformer [13]	45
Fig. 48 Converter circuit used in [13]	45
Fig. 49 Photo of HV PEBB.....	47
Fig. 50 Photo of LV PEBB.....	47
Fig. 51 MF Transformer	47
Fig. 52 Photo of developed PET demonstrator	47
Fig. 53 Converter circuit used in [12]	47
Fig. 54 Photo of the tank, including 9 MF transformers.....	47
Fig. 55 Control diagram	50
Fig. 56 Prototype of MF transformer	51
Fig. 57 Winding arrangement of MF transformer	51
Fig. 58 Converter circuit used in demonstrator [14]	51
Fig. 59 3L NPC Series Resonant [17]	53
Fig. 60 3L NPC Dual Active Bridge [17]	53
Fig. 61 Assembly of SRC Module (front and back view) [17].....	55
Fig. 62 Assembly of DAB module (Front and back view) [17]	55
Fig. 63 Summary of power densities and efficiencies at rated power of both designed converters and the respective volume and loss shares [17]	56
Fig. 64 Photo of MF prototype [16].....	58
Fig. 65 Lab setup [16]	58
Fig. 66 Converter circuit used in demonstrator [16]	58
Fig. 67 Insulation system, the right side is a schematic cut through the housing section marked with white arrows in the bottom picture of the left side.....	58
Fig. 68 Photo of SRC MF prototype	61
Fig. 69 Photo of DAB MF prototype	61
Fig. 70 Converter circuit used in [22].....	61
Fig. 71 Photo of MF transformer prototype.....	63
Fig. 72 Converter circuit used in [15]	63
Fig. 73 SiC Enabled SST Prototype	65
Fig. 74 SST Prototype.....	67
Fig. 75 Converter circuit used in demonstrator [24]	67
Fig. 76 Uniflex - Photo MF Transformer	69
Fig. 77 Photograph of 25 kVA transformers with the power electronics in place on the converter baseplate	69
Fig. 78 Converter circuit used Uniflex demonstrator [25].....	69
Fig. 79 Converter circuit used in RWTH Aachen [2]	71
Fig. 80 RWTH-Photo of MV DC/DC Demonstrator	71

Fig. 81 Amorphous Iron Core [5]	72
Fig. 82 DAB Closed loop control	73
Fig. 83 DAB First Harmonic Aproximation Model.....	73
Fig. 84 Core type transformer	76
Fig. 85 Shell type transformer	76
Fig. 86 Matrix type transformer	76
Fig. 87 Conductor topologies a) Solid and b)Circular Litz, c) Rectangular Litz and d) foil	78
Fig. 88 ETH Zurich U-Core type transformer	80
Fig. 89 ETH Zurich Shell type transformer concept	80
Fig. 90 ETH Zurich Matrix type transformer concept	81
Fig. 91 Different packages	84
Fig. 92 3L-NPC VSC.....	90
Fig. 93 Total loss distribution.....	90
Fig. 94 ABB One phase leg of a 3-level VSI	92
Fig. 95 ABB Phase leg with 8 IGCTs.....	92
Fig. 96 Siemens IGCT Phase module in SINAMICS GM/SM150 drives.....	92
Fig. 97 Westcode NPC phase leg	93
Fig. 98 Westcode Diode Valve	93
Fig. 99 Westcode IGBT valve	93
Fig. 100 Single leg structure of 3L-NPC-VSC and 3L-ANPC-VSC.....	93
Fig. 101 Possible configuration of an 18[MW], 6.6 kV variable speed drive.....	93
Fig. 102 GVA Thyristor pulser	94
Fig. 103 Thyristor Controlled Reactors	94
Fig. 104 Static VAR compensator.....	94
Fig. 105 Oil cooled thyristor valve [50].....	95
Fig. 106 IGCT-based cascaded converter cells showing the main components [51]	95
Fig. 107 IGBT valve [52]	96
Fig. 108 GVA IGBT valve.....	96
Fig. 109 Modular Unit used in HVDC applications.....	97
Fig. 110 Equivalent circuit for a single valve.....	97
Fig. 111 Typical Valve Unit.....	98
Fig. 112 IGBT heat sink with bonded process.....	99
Fig. 113 Forced air cooling using a radial fan [54]	99
Fig. 114 Semikron water cooled heatsink [54]	100
Fig. 115 Danfoss Mold Module, direct liquid cooled with highly efficient double sided Shower Power Turbulators	100
Fig. 116 Stack of presspack diodes cooled using Vortex	100
Fig. 117 Mounting direction and venting	102
Fig. 118 Use of coils in liquid cooling system	103
Fig. 119 Use of microchannels in liquid cooling system.....	103
Fig. 120 Thermosyphon Cooling System	103
Fig. 121 MMC cell cooling with hermosiphon system.....	103
Fig. 122 Pool boiling	104

Fig. 123 Cross section of a 2-phase immersion-cooled GTO traction inverter [57]	104
Fig. 124 Liquid cooling with heat pipes	105
Fig. 125 Oil cooling systems for transformers	106
Fig. 126 Standard Waveshapes [59]	108

List of tabels

Tabel 1 List of functionalities.....	14
Tabel 2 Ranking of design drivers.....	19
Tabel 3 List of demonstrators.....	30
Tabel 4 List of concepts	31
Tabel 5 Properties of magnetic materials	76
Tabel 6 List of medium frequency transformers	77
Tabel 7 List of fast rectifying diodes	85
Tabel 8 ABB press pack diodes	85
Tabel 9 List of ABB IGCT.....	86
Tabel 10 List of IGBTs	87
Tabel 11 List of IEGTs.....	87
Tabel 12 Materials and compatibility of liquids	102



0. Introduction

The main purpose of this report is to show the state of the art of dc/dc converters applied in high power/high voltage demonstrators. A catalogue of circuits has been assembled in a different document and it contains 35 topologies up to this point. This report down scales to a few topologies and increases the confidence for an optimal topology. Finally, a selection report is going to point the favorite candidate circuit. The intended audiences of this document are project supervisors, post-doc researches and other phd students involved in dc/dc converter design.

This report presents the challenges that appeared during selection, design, integration and development of state of the art prototypes. Areas like topologies, semiconductors, magnetics or cooling are investigated.

At the present time a few traction and SST demonstrators are covered. Different transformers, semiconductors valves and cooling concept are presented. Where it was possible to find, control strategies and insulation coordination are shown. The main focus has been on hardware issues. It is not intended to close this report, but improve it and update it with future aspects.

When reading this report, the reader should have in mind the goal of this document, which is to increase the confidence of selecting a certain topology.

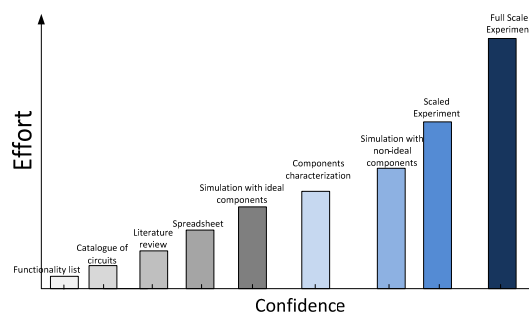


Fig. 1 Selection proces

The future versions of this report will be updated with following topics, according to literature review:

- Optimization designs of medium frequency transformers
- Characterization of semiconductors in soft switching
- Control models for DC turbines
- Loss model for semiconductors and transformer

Bellow figure indicates where this report fits in the overall project plan:

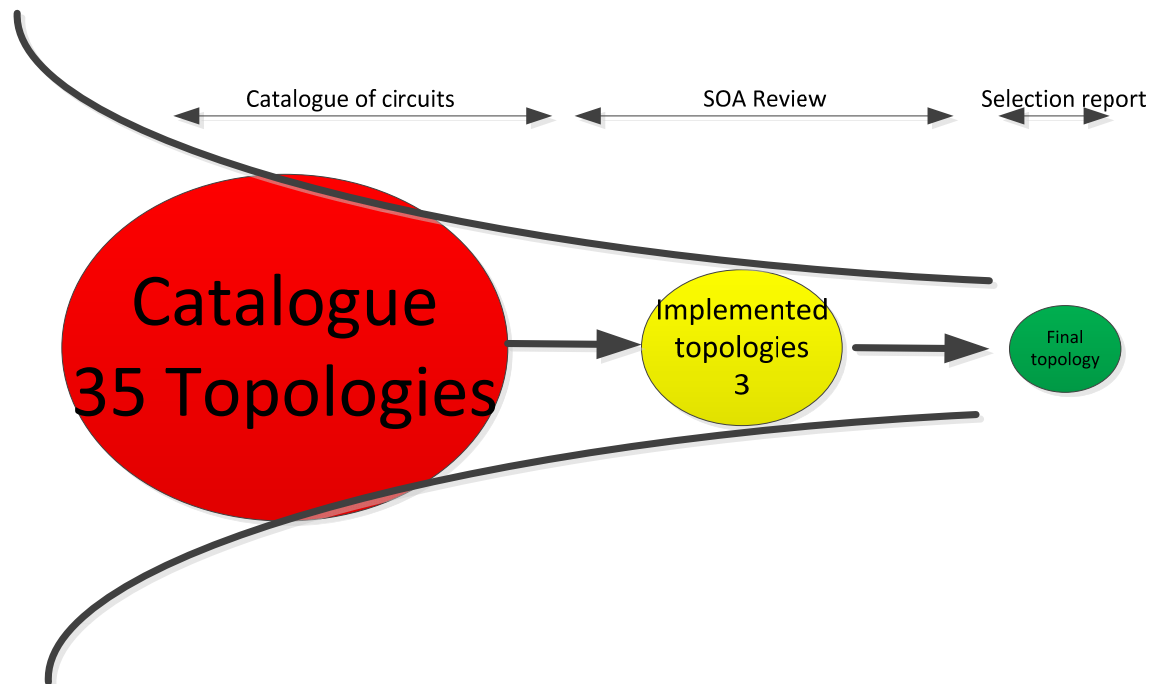


Fig. 2 Where SOA belongs to

1

1. Fundamental functionalities and technical requirements

HVDC wind farms with MVDC collection grids promise lower losses and bill of materials. One of the key components is the DC/DC converter located in the turbines. A proposed line diagram is shown in Fig. 3. The turbine converter will control a number of vital functionalities and it will have a high impact on the systems efficiency and cost. Considering that offshore wind converters operate in very hard environments exposed to salt, humidity, temperature variations and so on, the converter must be designed to deliver high levels of availability and high quality standards. The issue in this case is that there are no high power demonstrators available and no serious tracking records, to allow establishment of standards for dc-dc converters in offshore application. Fig. 3 presents the proposed line diagram of turbine converter and MVDC collection grid.

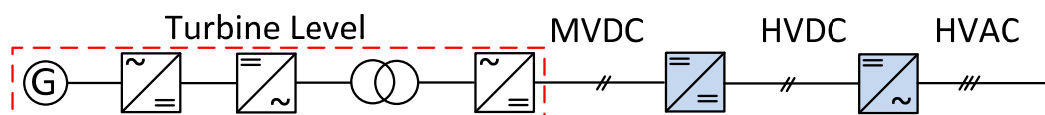


Fig. 3 Line diagram of turbine converter

Therefore, this state of the art report is focusing mainly on high power medium voltage DC/DC converter topologies which were implemented in demonstrators. Applications like traction converters, solid state transformers, medium voltage distribution and others have been selected as points of inspiration for the future topology that will be implemented at the turbine level for MVDC collection grid.

A clarification of converter specifications and parameters is necessary (see Fig. 4). Having in mind that current offshore wind turbines have nominal powers starting from 3[MW] up to 8[MW], the nominal range in this case should be somewhere between 5 and 15[MW].

Before going into details, it is necessary to make a list of functionalities and technical requirements that such a converter should fulfill. Then answers to the question of who has done what to solve the particular set of functionalities will be addressed.

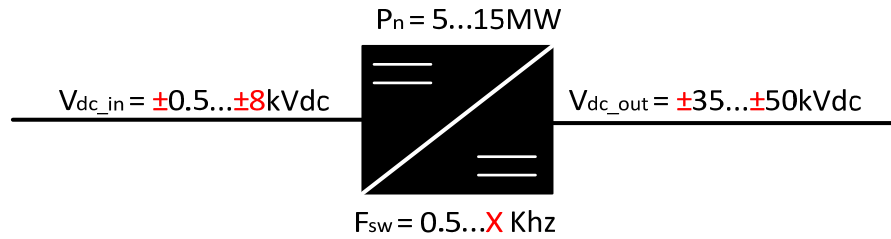


Fig. 4 Specification range for turbine DC/DC converter

The above considerations lead to a series of fundamental functional and technical requirements, for the topology that is going to be used:

No	Type	Function
F-01	System functionality	Convert and transform electrical energy from LVDC to MVDC (not necessarily from MVDC to LVDC)
F-02		Provide galvanic isolation between LVDC and MVDC sides
F-03		Connect to a generator/rectifier LVDC bus
F-04		Connect to an MVDC collector network
F-05		Energization of LVDC bus from MVDC network
F-06		De-energization of LVDC bus for service
F-07		Energization of MVDC network from the LVDC bus(?) (optional)
F-08		Bipolar output +/- kV
F-09	Power flow management	Control the power transfer between DC Link and the MVDC network in full operational range, to agreed stationary and dynamic performance [including disturbance rejection, low ripple, limit harmonic emissions, withstand network voltage harmonics]
F-10	Controllability	Control the LVDC voltage level to agreed stationary and dynamic performance.
F-11		Turbine operation in $\pm 10\%$ MVDC voltage variation, to agreed stationary and dynamic performance [including disturbance rejection, ripple, harmonics]
F-12		Respond to changes in MVDC network voltage by calculating DC/DC converter active power setpoint values
F-13		Respond to setpoints for LVDC voltage, MVDC power, connect/disconnect
F-14		Receive commanded states from [other controller] for LVDC contactor, for MVDC disconnector/breaker, for charge/discharge, run/stop
F-15		Receive setpoints from [other controller] for LVDC voltage, for MVDC power
F-16	Robustness to transients during converter load spectrum	Achieve proper voltage and current sharing on LV and MV semiconductors
F-17		Ensure proper operation with fast and stable recoveries after system faults and disturbances
F-18		Protect the DC/DC converter from excessive voltage/current from MVDC network.
F-19		Protect the MVDC network from excessive voltage/current from DC/DC converter.
F-20		Withstand MVDC voltage (stationary and temporary)
F-21		Withstand load current levels on LVDC and MVDC sides (stationary and temporary)
F-22		Withstand network short-circuit current contribution level (low grid impedance)
F-23		Governance of MVDC network fault ride-through sequence
F-24		Turbine converter short-circuit current contribution must not exceed specifications of collection network
F-25		Disconnect MVDC Bus from DC Collection network when voltage is too low/high for too long
F-26		Fault current discrimination from load current level
F-27		Protection and safe disconnection from DC Collection network during internal and external short circuit scenarios

F-28	Meet specifications	Operate with agreed efficiency and tolerance
F-29		Provide availability; operate above agreed reliability level
F-30		Stay within agreed mass, xyz dimensions, centre of gravity
F-31		Provide means for transportation and installation
F-32	Maintenance and diagnosis	Provide access for inspection, maintenance, repair
F-33		Provide diagnostics/upload access for new control sw
F-34		Provide feedback signals to [other controller] for DC/DC converter controller state [health, derate] & measured and monitored internal signals
F-35	Safety	Implement correct insulation levels, clearance and creepage distance
F-36		Contain internal fault energy, including fires originating from electrical faults
F-37		Protect humans by respect of electrical safety standards and service protocols
F-38	EMI/EMC	Limit EMC emissions (conducted/radiated) to agreed levels
F-39		Withstand EMC imissions
F-40		Limit acoustic noise emission to agreed levels
F-41	Grounding	A means to reduce the risk of electric shock and prevention of accumulation of hazardous static electrical charges
F-42	Cooling	WTG Transfer heat (from losses) to surroundings/cooling media
F-43		Connect to cooling liquid pipes; cooling air/gas inlet/outlet or heat exchanger;
F-44	Environment	Withstand ambient air (temperature, gas composition, air density, humidity [lpxx])
F-45		Withstand vibrations from environment
F-46		Withstand cooling media (liquid, air/gas)
F-47	Aux. SMPS	Receive auxiliary LVAC power for use within DC/DC converter.
Tabel 1 List of functionalities		

The primary function of the grid side converter is to control the power transfer between MVDC network and the DC link.

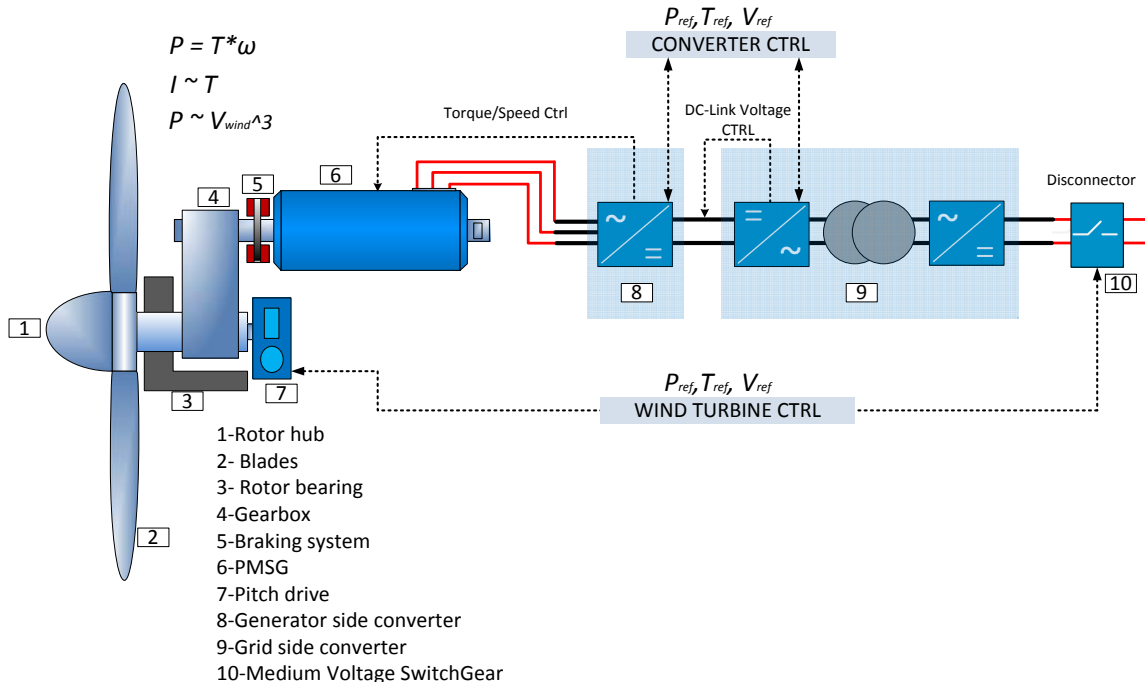


Fig. 5 Wind turbine system with MVDC output

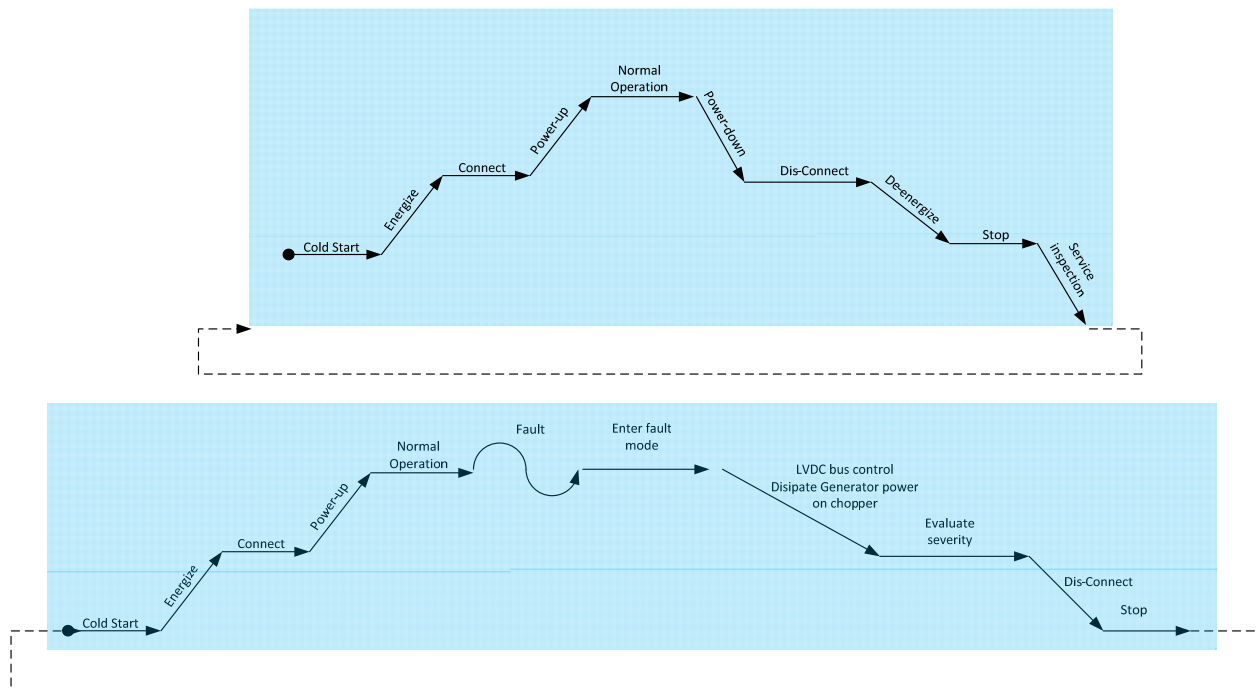


Fig. 6 Concept of operation of day in the life

General functionalities of the converter have been described in **Error! Reference source not found..** The objective was to allow a break-down of the system into sub-systems, and functions allocated for every component. This is going to reduce the scope of this project and provide criteria for selection of one converter solution over another.

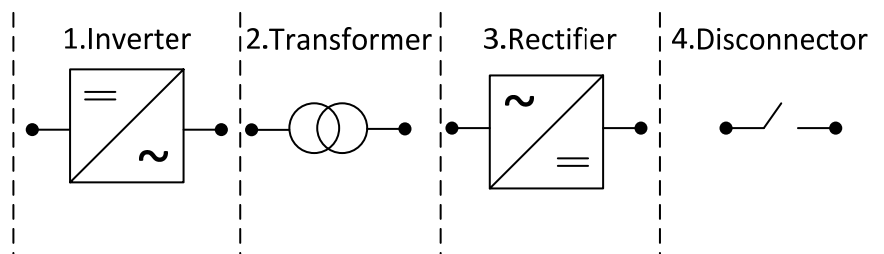


Fig. 7 Converter segmentation

LV Valve

LV valves connected in parallel, switching at frequencies above 1 kHz, delivering MW output power with high efficiency, proper cooling and low failure rate are achievable.

No	Function
1	Transform LVDC to LVAC
2.	Transfer power from LVDC to LVAC
3.	Withstand LVDC and LVAC transients
4.	Withstand LVAC short circuit current
5.	Control LVDC bus
6.	Provide even loss sharing on the switching semiconductors
7.	Provide proper semiconductor cooling

Transformer

A monolithic transformer can be realized with-with low failure rate, high efficiency, adequate power density, -for 10MW, 5/50 kV, 1 kHz sinewave excitation, using amorphous core material and Litz based windings.

No	Function
1.	Transform LVAC to MVAC
2.	Transfer power from LVAC to MVAC
3.	Provide galvanic isolation from LVAC to MVAC
4.	Provide good coupling between primary and secondary side
5.	Have low stray capacitance
7.	Provide proper core and windings cooling

MV Valve

Economic and reliable MV valves can be realized with series connected fast rectifying diodes, symmetric voltage sharing, low parasitics and proper cooling.

No	Function
1.	Transform MVAC to MVDC
2.	Transfer power from MVAC to MVDC
3.	Withstand MVAC and MVDC voltage transients
4.	Withstand MVDC short circuit current
5.	Provide even voltage sharing on the diodes
6.	Provide proper diodes cooling

Disconnecter

As the DC/DC converter can limit and react fast enough during short-circuit conditions, DC breakers are not needed and disconnectors are the only needed switch gear for the turbine.

No	Function
1.	Connect/Disconnect Turbine converter from MVDC
2.	Withstand short circuit and overcurrent on MVDC
3.	Withstand MVDC transients

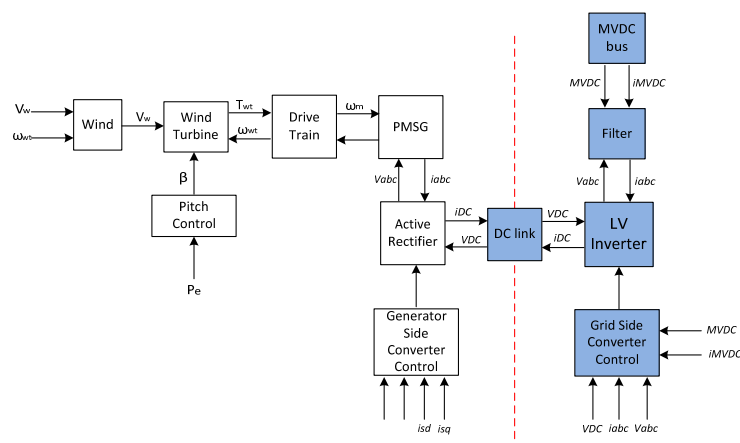


Fig. 8 Control and Protection

2

2. Ranking of design drivers

During the process of review and state of the art, the focus was mainly on built and tested high power medium voltage demonstrators. Most of the work is done on traction application, with maximum power tested up to 1.2[MW] by ABB [1], while on medium voltage distribution SST, valuable work is performed by RWTH Aachen [2]. Even if the writers claim that a 5[MW] demonstrator is built on a three phase converter, up to this point there is tracking record for a single phase 2.2[MW] setup.

Regarding tracking record for offshore wind turbine applications, as expected there isn't so much practical work. There are indeed many concepts ([3], [4], [5], [6], [7], [8]), but there are no setups tested and built at powers higher than even 100 KW. Most of the experimental work is focused on functionality assessment of different topologies and concept, but also on efficiency and performance.

In order to rank the design drivers, it's necessary to understand that different application areas require different specifications. For instance, in traction, it is expected that the DC/DC converters will be connected to two different kind of single phase grids: 16 kV and 25 kV. The power range might go up to 5[MW]. It's kind of a similar story for medium voltage distribution SSTs. According to the literature review ([9], [10], [11]) the SST will connect to 30 kV grids and step down the voltage to LV levels. Power levels are also expected to go up to 10[MW].

Traction will require high power density, so the converter will save space and weight in the locomotive. According to literature review, all the demonstrators([12], [13], [14], [15], [16], [17],

[18]) are built in a modular fashion. Redundancy is an important aspect, and N+1 modules are incorporated. As it seems in traction, high power density is the main design driver.

For medium voltage distribution SSTs, it seems that the main design driver is bi-directionality. The SST converter will have to deliver power both ways, while trying to compete with standard 50hz transformers on weight, volume and maybe on reliability.

It's quite a different story for offshore wind turbines. Considering the rough environment, humidity levels, distance from shore, considerable smaller space and size, it is expected that the design specifications will be much tougher. Power levels could go up to 15[MW], while MV side voltage could go up to 100 kV. The converter should have high efficiency and high power density, while offering really good availability and maintenance.

So, if traction converters are mainly designed to accomplish high power density and SST's are driven by bi-directionality and functionalities, the offshore wind turbine converter has to be **designed for reliability**.

Reliability, maintenance costs and availability must be the main design drivers. Even the smallest service for offshore installations immediately results in very high costs [19]. At the same time the loss of energy production due to servicing is a significant loss of profit, especially for the large wind parks, where failures can also affect the operation of other generators. Therefore, strong efforts must be taken to achieve high reliability in the power electronics converter system of the wind turbine.

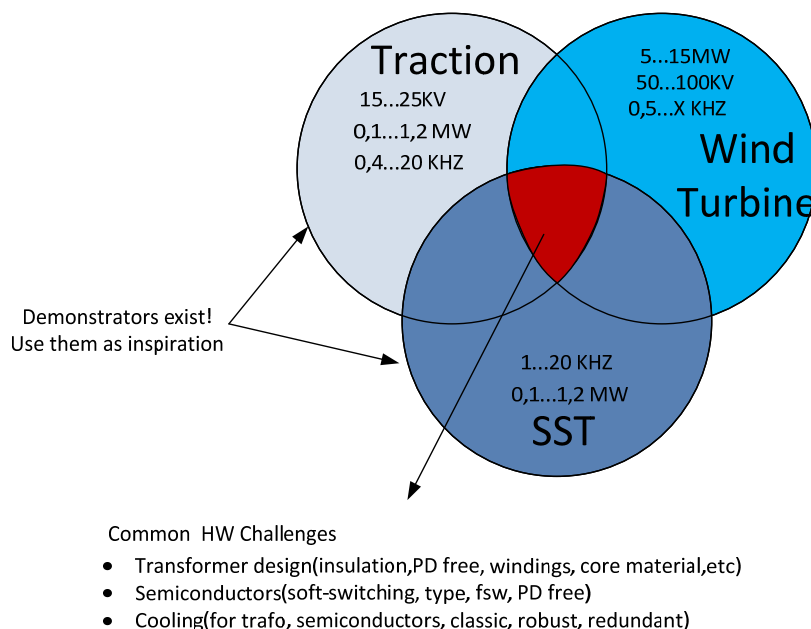


Fig. 9 Common challenges

In other words, efforts to decrease OPEX (*operational expenditure*) should be higher than decreasing CAPEX (*capital expenditures*). Below, a suggestion of design driver ranking is presented:

No	Design driver	Weighted rank
a.	Availability (leading to loss generation [[MW]h])	5
b.	Electrical losses (efficiency)	4
c.	Ratings (name plate power, voltage, temperature...)	4
d.	Repair costs (excluding scheduled maintenance)	2
e.	Power density (volume and weight)	1

Tabel 2 Ranking of design drivers

a. System reliability

Initially, the system cost, efficiency and size were the main decision factors with regards to preferred power electronics system solutions. The main focus was on the behavior of the converter during transients, faults (over-voltage, short circuit), loss of grid or instability. But moving from onshore to offshore installations puts system reliability, maintenance costs and availability at highest priority, when it comes to design drivers [19].

Design for reliability is a fundamental part of an advanced development process and already starts at the concept phase. So, from the beginning, aspects like stress, environment conditions, failure mode, etc. should be addressed. The DfR contains more tools and practices that are executed during the design stages.

Tools like FMEA (Failure Mode and Effect Analysis), RCA (Root Cause Analysis) or RP (Reliability Prediction) need to be used.

During FMEA, potential failures need to be investigated and estimate the risk of their occurrence. Afterwards, corrective actions/methods should be identified.

During RP, estimation of failure rates for different systems can be addressed. It allows the designer to compare different topologies, structures and where attention should be focused.

Therefore, the Design for Reliability process will help to:

- Identify suitable technology
- Identification of Critical system parts
- Predict Failure Rate
- Implement robust design
- Design for Maintenance

Availability

Here are a few ways to increase availability:

- Redundancy for active components and cooling
- Avoid aging
- Investigate humidity impact
- Special Start-up procedures
- High protection levels
- Condition the environment favorably for critical components
- Design-out the top-runner failures
- Implement predictive maintenance

b. Ratings

HV Potential Distributor [30...100 kV]

Medium Voltage will have a big impact on valve design, as it will decide the number of series connected switches, therefore the mechanical complexity. It will be challenging to design a low leakage inductance, low stray capacitance and limit partial discharges at voltages close to 100 kV. This design parameter is clearly higher than other applications like traction or medium voltage distribution.

Another area of impact will be the transformer insulation. Investigations of different materials should be done. In traction, high insulation levels are achieved either by potting or HV cables. According to literature, materials like mica tape, oil tape, epoxy, nomex, glass bubble filled PV, silicon based materials are normally used to have safe insulation.

High voltage means high levels of insulation, thus complex mechanical arrangement of windings. Insulation has di-electric losses and different cooling methods should be used in order to get the heat out.

Power [5...15[MW]]

Power factor will influence mainly the size and weight of LV valves and transformer core and windings area. Paralleling of semiconductors on LV valves will increase mechanical complexity and cooling.

c. Repair Costs

Importance aspects of maintenance and service need to be address, so costs could be decreased. For example, the design of the LV or MV valves should consider a good serviceability. The valve design should enable high power density without sacrificing service and maintenance aspects. The components that need to be replaced should be transportable by a single person by boat or helicopter if needed. Control hardware and software should allow remote access for off-site troubleshooting as well as software updates. In Fig. 10, a good example of serviceability and maintenance is given. ABB'S PCS 6000 IGCT valves can be exchanged fast and in a convenient way, without disconnecting bus bars or cooling pipes [19].



Fig. 10 ABB PCS 6000

Other ways to decrease maintenance costs could be:

- Design the converter with a low number of semiconductors, so reliability is increased
- System components should be operated below rated temperature and online monitoring of these limits. Also, to meet the failure rate, the components should operate under conditions that contribute with a known life time consumption, whether it be high/low losses, temperature, humidity, vibration, radiation, voltage, etc.
- Utilize derating in the design
- Modularity to some extent

d. Power density

Smaller size and weight at high power levels means high power density. High efficiency (>98%) plus high power density will require a higher switching frequency for the semiconductors and transformer (>1 kHz). And this can be achieved only through soft-switching to this point.

3

3. Basic circuit concepts from demonstrators

The main purpose of this chapter is to synthesize the topologies implemented in demonstrators. From a wide range of possible topologies, it turns out that only a few have been used on high power prototypes.

- Focus was on setups, prototypes and demonstrators with nominal power higher 100 kW or scalable prototypes
- Worth to mention demonstrators are divided in mainly three categories: traction, solid state transformers and medium voltage distribution
- From a whole range of possible topologies there is a clear trend on resonant or phase shift converters used in modular topologies, having cascaded configurations. This is the case for traction and SST.
- A lot of information was obtained from traction demonstrators: ABB, SIEMENS and Bombardier have some valuable work, mainly on medium frequency transformer design
- Some information was gathered from SST prototypes, but the power and voltage level are not high enough
- All demonstrators have bi-directionality, thus active switches on LV and MV side
- In all demonstrators, insulation and galvanic separation was realized with help of medium frequency transformers
- There are three principle topologies: Series Resonant r, LLC and Dual Active bridge (single and three phase)
- For medium voltage side, there were mainly two types of semiconductors used: IGBT and IGCT.
- For traction converter 1.7 kV, 3.3 kV and 6.5 kV IGBTs were mainly used

- For SST applications, SiC Mosfets were employed, having breakdown voltage up to 10 kV but very low current <30A.
- In medium voltage distribution, IGCT rated at 4.5 kV were used

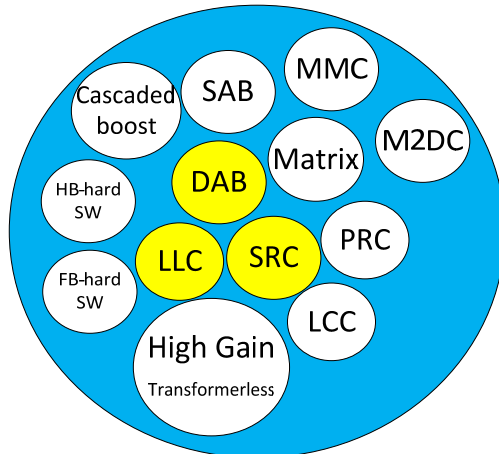


Fig. 11 Topologies implemented in demonstrators

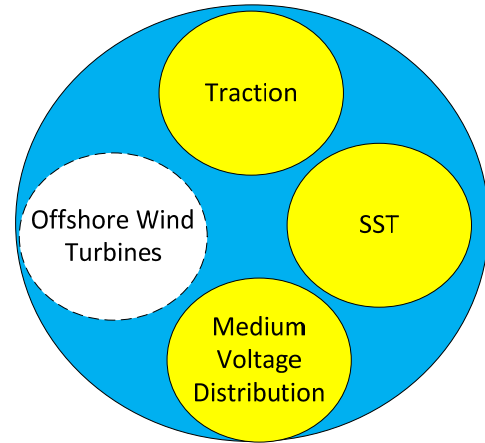


Fig. 12 Areas of applications for the demonstrators

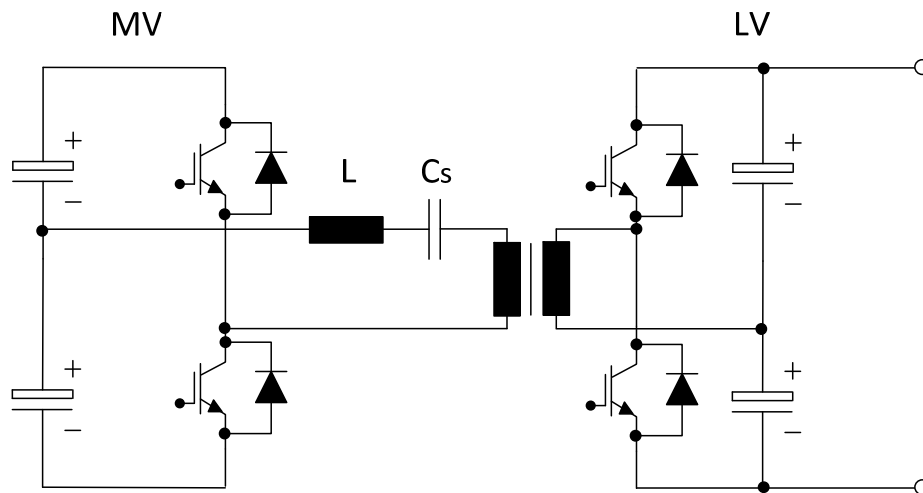


Fig. 13 Half-Bridge SRC

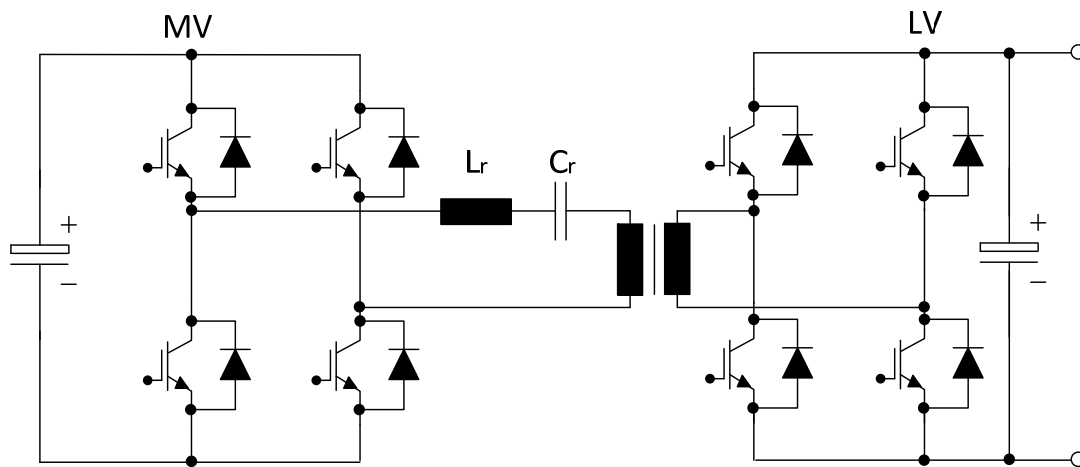


Fig. 14 Full Bridge SRC

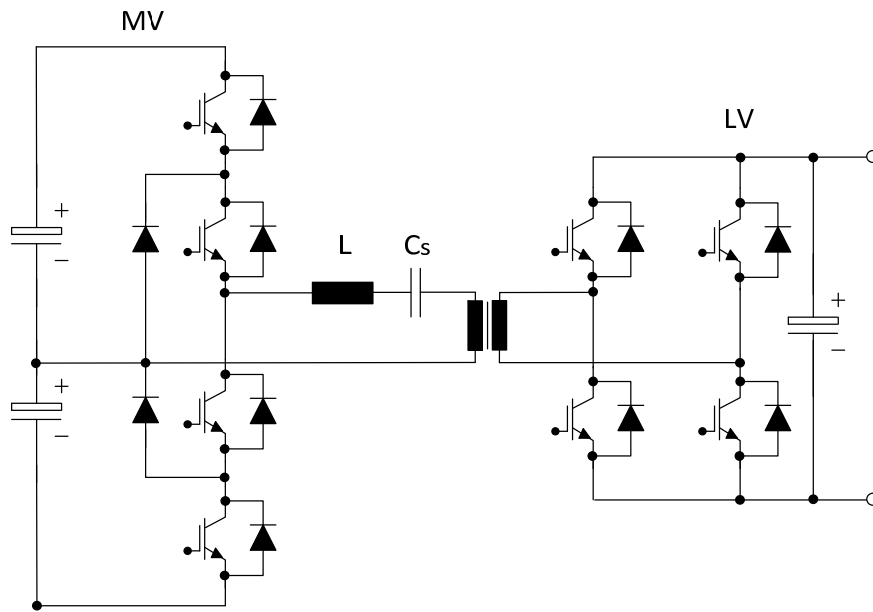


Fig. 15 NPC SRC

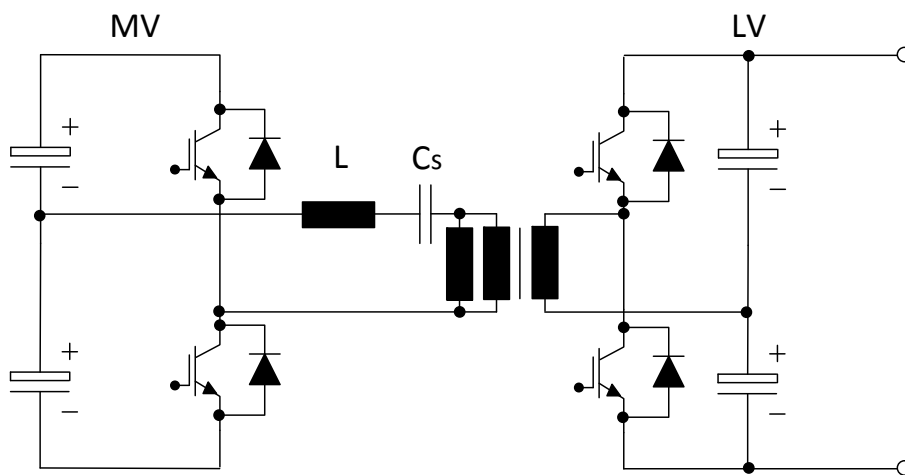


Fig. 16 Half-Bridge LLC

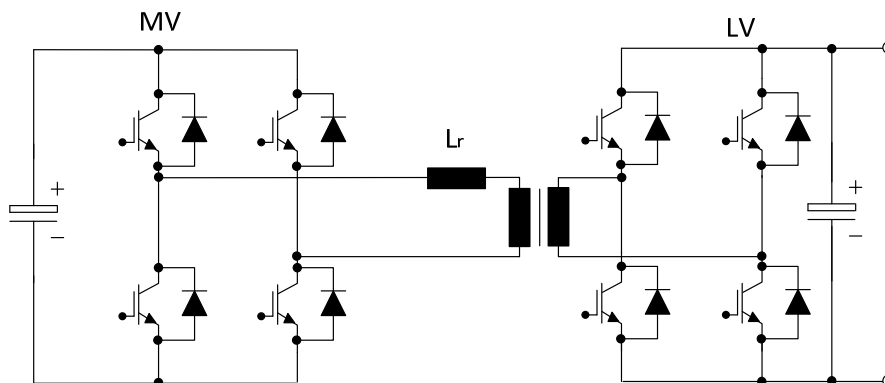


Fig. 17 Full-Bridge DAB

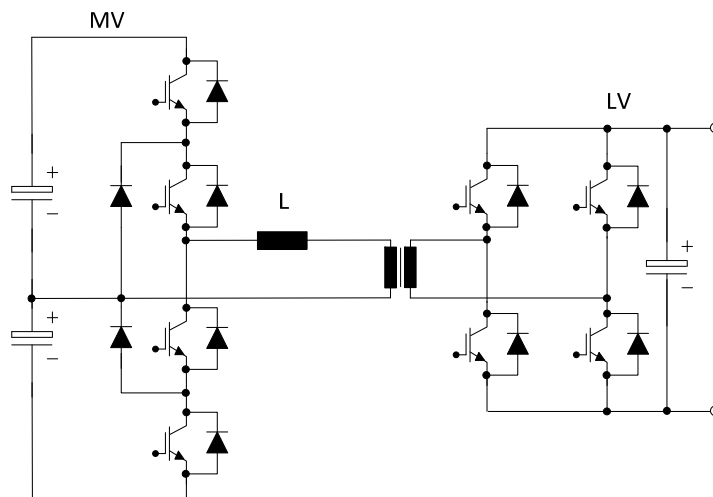


Fig. 18 NPC DAB

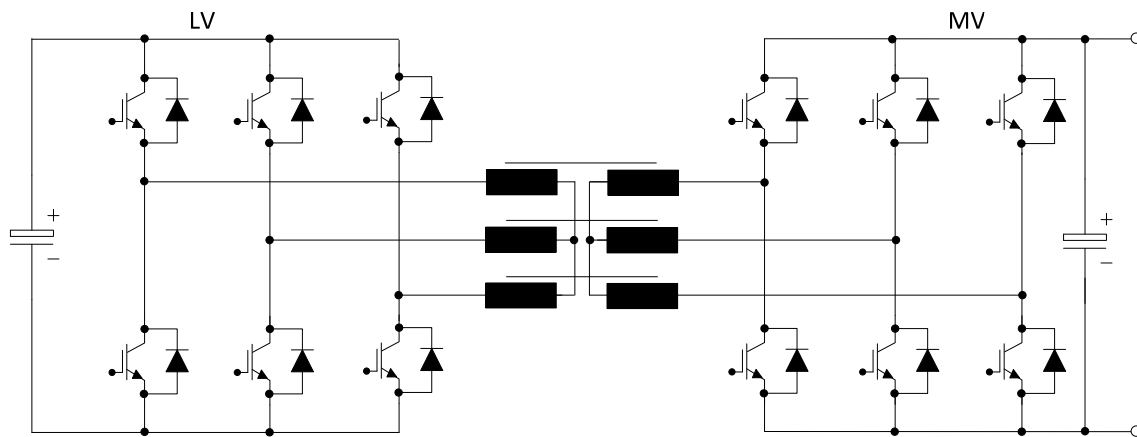


Fig. 19 Three phase Dual Active Bridge

- In traction converters, initial demonstrators were built on SRC topologies, but evolved to LLC
- The SRC is obtained by inserting a capacitor in series with the transformer, achieving protection against transformer saturation and allows reduced RMS transformer currents and switching losses.
- The SRC disadvantage is the control complexity and the resonant capacitor is subject to large current variations[20].
- Frequency control inspired the research of multi-resonant converters, with more than one resonant capacitor and/or inductor
- The introduction of the dual active bridge in single phase and three phase version represented a major step in the development of bi-directional isolated topologies.
- The simplest control of the DAB consists in producing a square wave voltage in each converter and varying the phase shift between them. The ZVS occurs naturally for the full power range only when the ratio of DC-voltages is unity, for the other cases advanced modulation scheme guarantees soft-switching for the MV-side.

- The three phase DAB results in lower device stress, better transformer utilization and lower filter requirements. On the other hand, the three phase transformer will require symmetrical leakage inductances, more complex manufacturing and additional power devices
- Research on multiphase series-resonant converters has been addressed in the literature only recently.
- In traction applications, the goal is to replace the conventional 16.7hz transformer saving mass and energy
- Each converter submodule consists of a Four Quadrant Converter and a MF dc/dc converter

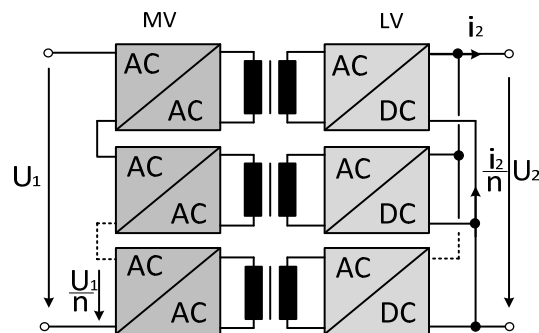


Fig. 20 Modular AC/DC converter with cycloconverter+rectifier

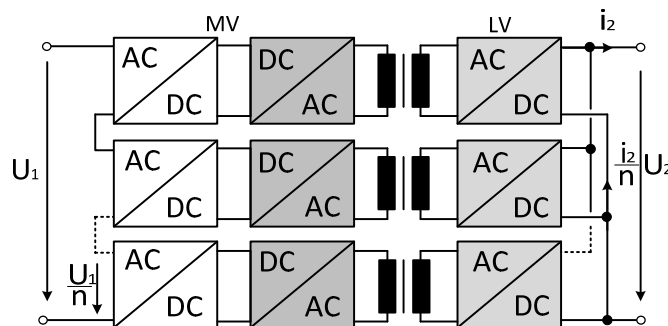


Fig. 21 Modular AC/DC converter with rectifier+inverter+rectifier

- The number N of cascaded converters submodules depends on the maximum line voltage, the individual dc-link voltage and the reserved voltage margin to control the line current as well as the order of redundancy
- Resonant topologies are mainly used so switching frequency can be increased and magnetics reduced
- Switching frequencies vary from 1 kHz to 20 kHz
- MV side input per module varies from 1.8 kV to 3.6 kV
- Module nominal power varies from 75 KW up to 450 KW

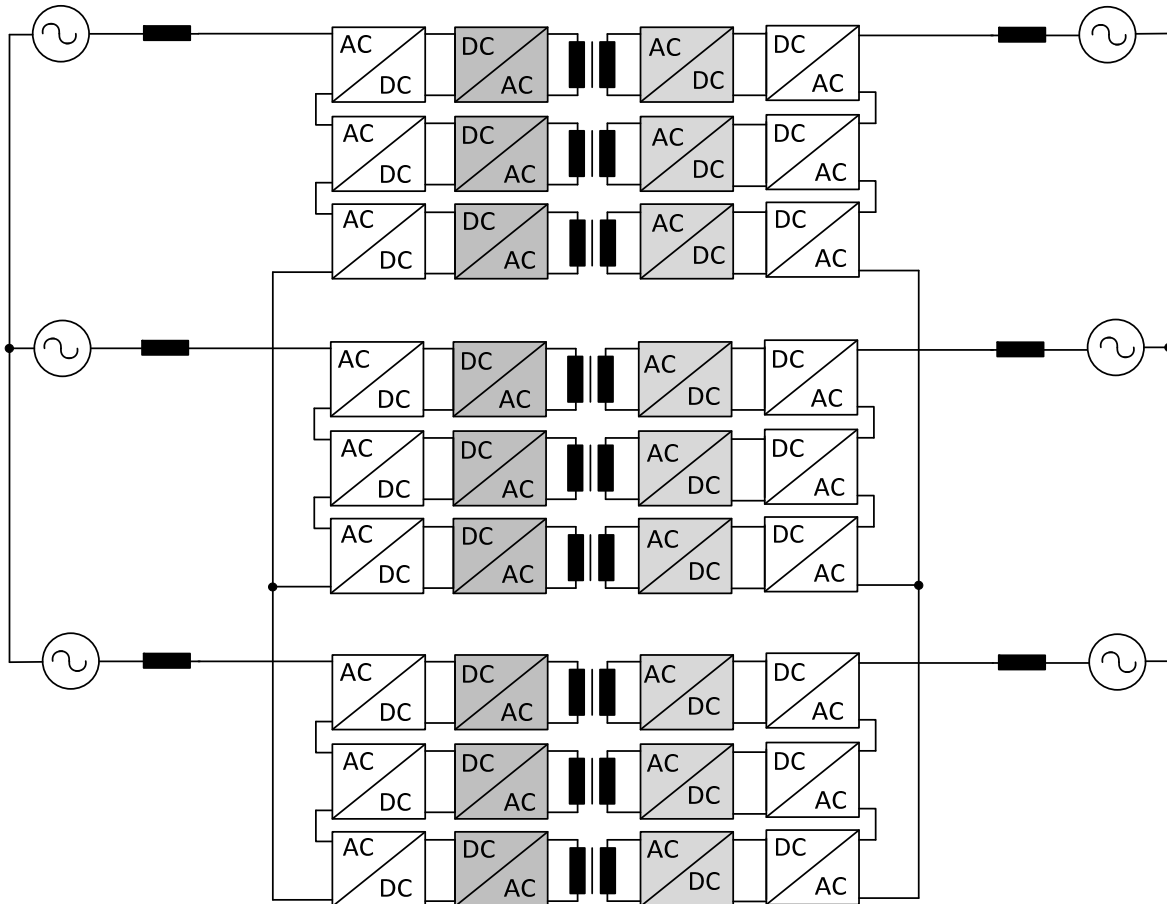


Fig. 22 Modular Three Phase SST

- Modular configuration, 3 stage SST: PWM Rectifier + DC-DC DAB + PWM Inverter
- This topology received the most interest due to superior controllability that enables several functionalities
- The AC-DC stage is based on full bridges which in modular configuration implement a cascaded multilevel rectifier
- The isolated DC-DC is based on on DAB modules that interface the MVDC link with LVDC link
- The main drawback of this topology is the large number of components which will mean lower efficiency and reliability.
- Multi-cellular, modular and scalable converter architecture
- Isolated modules can be connected in series/parallel
- Modular approach : Standardized building block, scalable, maintainability, economy of scale
- A modular approach can make the DC/DC converter robust and fault tolerant.
- On the other hand, the high number of modules will decrease it's reliability.
- Efficiency could be increased by disconnecting modules, and so cancelling their losses, during partial loading conditions.

4

4. Demonstrators for high power applications

a. Who has done what to solve functionalities?

- Several projects focusing on designing traction converters have been reported.
- This report is focusing on demonstrators.
- Until now there is a list with 17 relevant demonstrators
- It is possible to learn how following issues have been solved:
 - Transformer design at elevated frequency
 - Soft-switching of HV IGBT and IGCT
 - Cooling
 - Control of resonant converters
 - Compact design for high power density
 - Insulation coordination
 - Different manufacturers for transformers
 - Protection
 - Control at light load
 - How to commission a [MW] converter? Steps from prototype, lab setup to field application
- Traction literature presents different ways to construct a MF transformer. They describe the arrangement of the winding and core geometry and have been referred to a transformer with side by side windings, a transformer with coaxial windings or a transformer with planar windings.
- The simplest design of a coaxial transformer is achieved when a turns ratio of 1:1 is required.

- With respect to the topology structure in traction applications, typical solutions are phase controlled multilevel converters, multiphase modular multilevel and AC/DC converters including isolated resonant circuits.

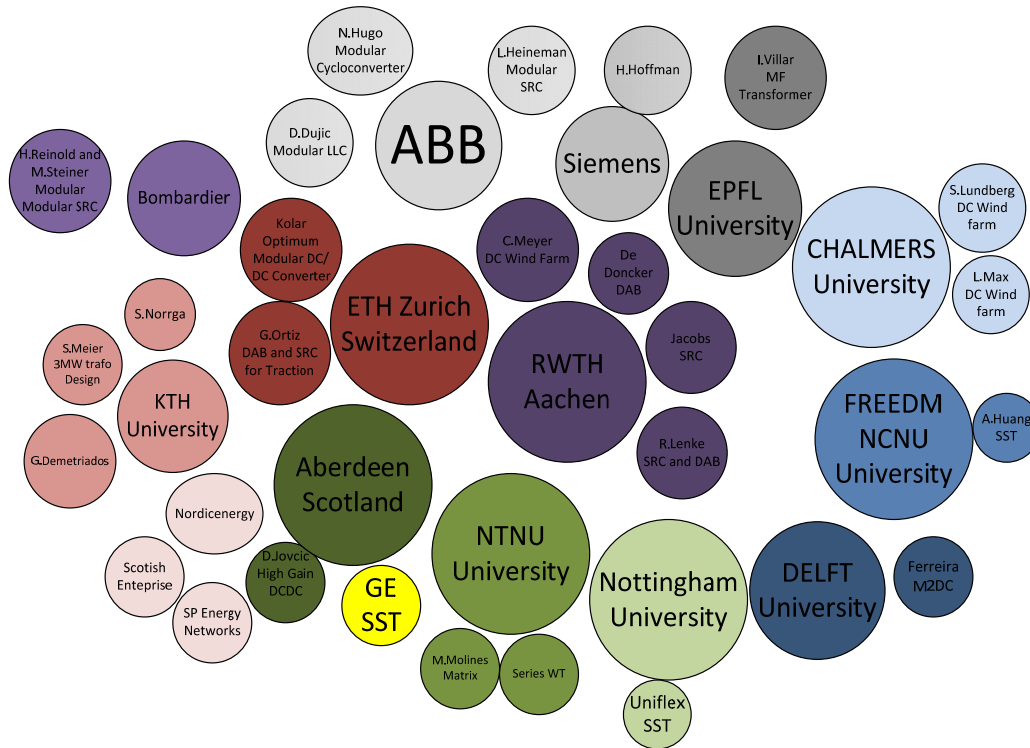


Fig. 23 Relevant research centers

Regarding traction:

The use of series resonant LC converters has been described in: [x],[y]. In [x], a full bridge series resonant dc-dc converter based on XX kV IGBTs with a unity transformer ratio and a switching frequency of X KHZ has been described. Standard 6.5 kV IGBTs and modified 6.5 kVIGBTs (irradiated in order to reduce carrier lifetime and thus lower turn-OFF losses) have been tested in XX. It was reported that with the use of modified IGBTs, the switching frequency could be increased by 30% compared to standard IGBTs (the frequency of interest was 5-8 kHz).

What is common in LC series resonant demonstrators, that the magnetizing inductance of the transformer is fairly large and thus does not participate as a part of the resonant circuit. The converter operates with ZVS, which may not be the most favorable choice due to the stored charges inside the device that are extracted when the complementary device is turned on.

No	Center	Pn [kW]	Vin [kV]	Vout [kV]	Fsw [kHz]	Application	Topology	Transformer type	Semiconductors	Cooling	Modules	Cite	Year
1.	ABB	75	1,8	1,8	0,4	Traction	Cycloconverter	Silicon Iron	3.3 kV IGBT	Oil immersion	16	[21]	2007
2.	ABB	350	3	3	10	Traction	SRC	Amorphous	Different modules	De-ionized water cooling	12	[13]	2002
3.	ABB	150	3,6	1,5	1,8	Traction	LLC	Nanocrystalline	6.5 kV IGBT on High Side 3.3 kV on LV side	Oil cooled trafo, water cooled PEBB	9	[12]	2014
4.	Siemens	450	3,6	3,6	5,6	Traction	SRC	Nanocrystalline VITROPERM 500F	6.5 kV IGBT	Internal cooled aluminium	8	[14]	2011
5.	ETH Zurich	166	2	0,4	20	Traction	DAB	N87 Ferrite	1,7 kV IGBT on High Side 600V on LV Side	Aircooled	6	[17]	2013
6.	ETH Zurich	166	2	0,4	20	Traction	SRC	Nanocrystalline	1,7 kV IGBT on High Side 600V on LV Side	Water cooled	6	[17]	2013
7.	Bombardier	400	3,6	2,8	8	Traction	SRC	Nanocrystalline	4.5 kV IGBT	De-ionized water cooling	8	[16]	2007
8.	Ikerlan	400	3	0,75	1	Traction	DAB	Silicon Iron	6.5 kV IGBT on High Side 1.7 kV on LV side	Aircooled	1	[22]	2012
9.	Ikerlan	400	3	0,75	5	Traction	LLC	Nanocrystalline	6.5 kV IGBT on High Side 1.7 kV on LV side	Aircooled	1	[22]	2012
10.	KTH	170	2,5	0,6	4	Traction	Cycloconverter	Amorphous METGLAS 2605SA1	Different modules	Oil immersion/Heatsinks Natural convection	1	[15]	2009
11.	GE	1000	13,8	0,4	20	SST	Soft-switching	Nanocrystalline	24 SiC Mosfets + 12 Schottky diodes assembled in one 10 kV half bridge and 120A	Aircooled	1	[23]	2011
12.	FREEDM NCNU	20	3,8	0,4	3	SST	DAB	Amorphous METGLAS 2605SA1	6.5 kV 25A SiC IGBT Powerex PM100CLA060	Heat sink-forced cooling	3	[24]	2011
13.	Uniflex	300	3,3	3,3	2	SST	DAB + Cycloconverter	Amorphous,designed by ABB Secheron	DYNEX 1700V, 200A	Oil immersion+ forced cooling	16	[25]	2010
14.	RWTH Aachen	5000	5	5	1	MVDC Distribution	DAB	Silicon Iron	IGCT (5SHY 3545L0001) antiparallel diode D1031SH45TS02	Water cooled	1	[2]	2014
15.	DELFT University	50	0,75	0,6	25	High power density	ZVS, Quasi-ZCS DC/DC	Amorphous core	Different modules	Water cooled	1	[26]	2009
16.	ETH Zurich	25	5	0,7	50	SST	DAB	N87 Ferrite	SiC JFET	Aircooled	1	[27]	2014
17.	Michigan Univ.	70	0,3	0,7	13	Metro Aux Supply	Full Bridge	Ferrite	Powerex CM600HU-24F	Aircooled	1	[28]	-
XTabel 3 List of demonstrators													

No.	Center	Pn[kW]	Fsw [kHz]	Application	Topology	Cite	Year
1.	Chalmers Univ.	5000	1	Offshore WT MVDC	SAB	[29]	2007
2.	RWTH Aachen	10000	2	Offshore WT MVDC	SRC and SAB	[3]	2007
3.	FREEDM NCNU	270	20	SST	DAB	[30]	2007
4.	FREEDM NCNU	5000	20	Offshore WT MVDC	Transformerless High Gain	[31]	2012
5.	KTH	3000	0,5	Offshore WT MVDC	Cyclo-converter	[6]	2004
6.	Jovcic	3000	2,8	Offshore WT MVDC	Transformerless High Gain	[32]	2009
7.	Jul-Ki Seok	10000	3	Offshore WT MVDC	Transformerless High Gain	[33]	2015
8.	Aalborg Univ.	5000	1	Offshore WT MVDC	SAB	[34]	2012
Tabel 4 List of concepts that were not demonstrated							

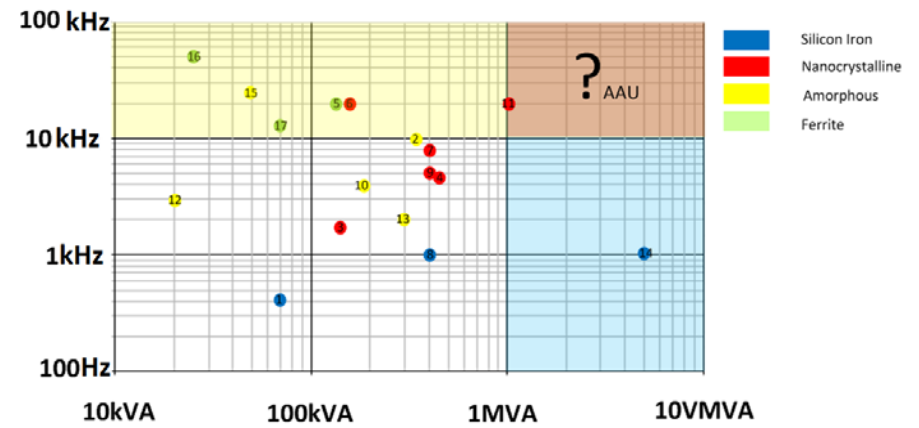
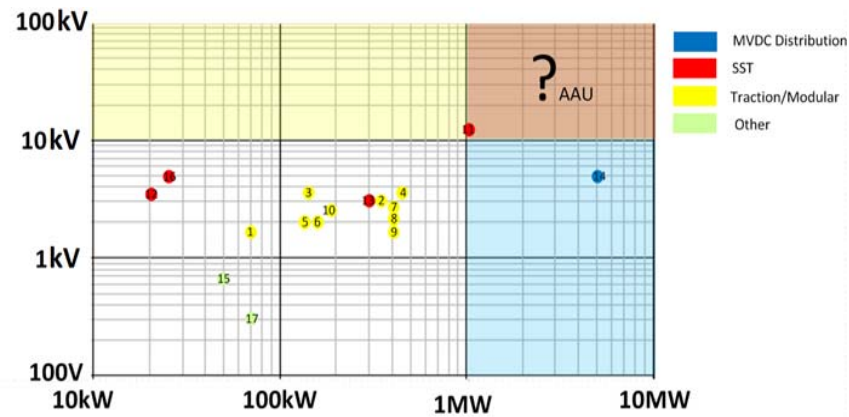


Fig. 24 Selected demonstrator projects

b. DC Turbine concepts

i. Dual active bridge and Series Resonant converter 2007

Concept

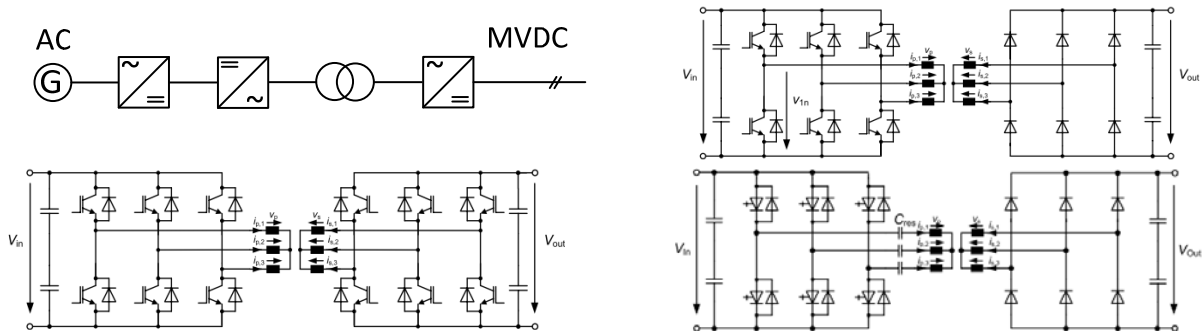
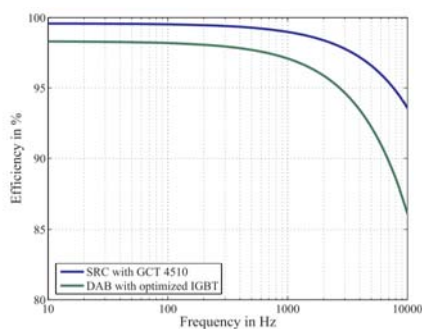


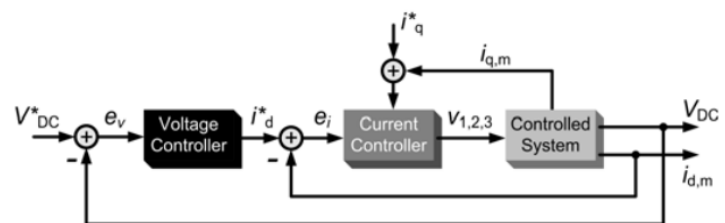
Fig. 25 Studied topologies in [3]

n [3], key components for offshore dc grids have been evaluated. High power dc-breakers, design of medium frequency transformers, dc/dc converters and possible configurations of grids were presented. A design tool for the transformer was developed, calculating losses and delivering a thermal model. For the turbine converter, a 4 stage topology was used as a benchmark and consists of: active rectifier, inverter, medium frequency transformer and grid rectifier. Following turbine converter topologies were investigated: single active bridge, dual active bridge and the series resonant converter. The conclusion is that the SRC offers superior efficiency (Fig. 26), but the DAB has advantages concerning controllability. In addition, a variation of the SRC has been developed, allowing an asymmetric bi-directional power flow.

Control



Efficiency of a 5 MVA SRC and a 5 MVA DAB for different frequencies



Basic schematic of control structure

Fig. 26 Efficiency and control diagram

Stability and controllability of the dc wind farm configuration were analyzed (Fig. 26). After presenting the modeling method of the components, the control system is designed. To prove the stability of the controller, simulations based on EMTP have been carried out. The results proved that the DC grid is stable and can be controlled at only one point. According to this work, all investigated DC configurations have let to lower costs compared to the AC grid if full scale converters are used. There were no experiments or practical implementations in this work.

ii. Full bridge 2009

Concept

In this thesis [7], a wind farm with an internal DC collection grid is investigated with focus on the design, the losses and the dynamical behavior of the DC grid. DC/DC converters are identified as key components and proposed topologies are composed from 4 stages. A suitable design of the converters is obtained including the choice of topology, the control of the converter and the choice of the switching frequency. It is found that for a frequency of 1 kHz, the weight of the medium frequency transformer is reduced by 90% compared to a 50Hz transformer. Three different topologies have been investigated in this work: a full bridge converter, single active bridge and a LCC resonant topology. From losses investigations, it turns out that the full bridge converter has better efficiency than the other two softswitching options, which makes the results questionable.

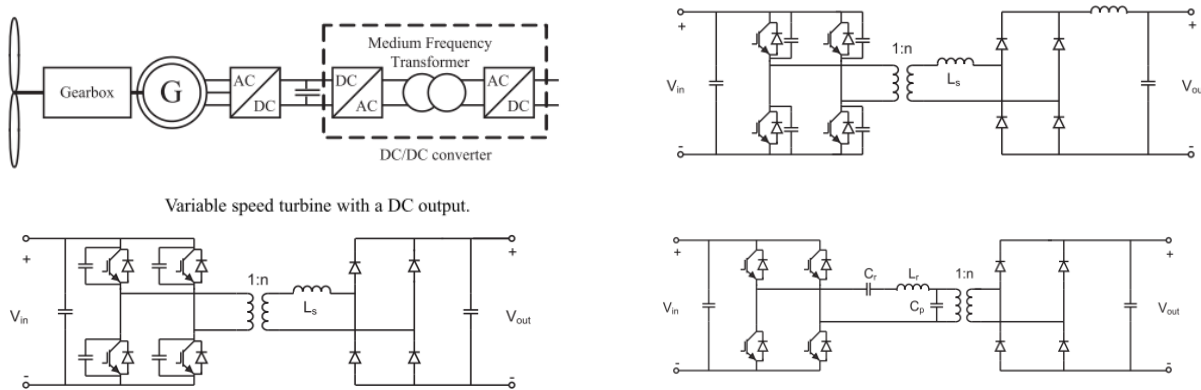


Fig. 27 Studied topologies in [7]

Control

Considering the dynamic operation of the internal DC collection grid in the wind farm, the DC/DC converters control the power flow and also the voltage levels for the DC Links. Voltage control is performed by substation converter, while wind turbine LVDC is controlled by turbine converter. The control method used for the control of the voltage is a droop control that works without communication within the wind farms. Further, the startup procedure of the wind farm has been developed and shown to be appropriate. Due to the unidirectional power flow in the turbine converters, the system must be energized from the wind turbines and it is shown that the wind farm can start up and the DC bus can be energized using 500V power sources in the wind turbine.

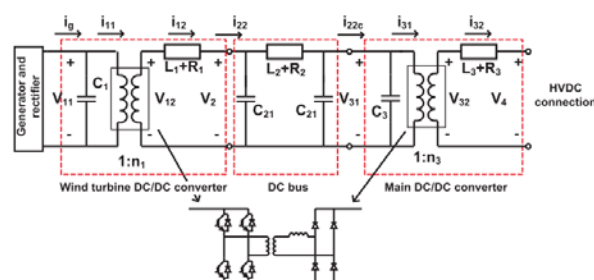


Fig. 28 Model of turbine converter

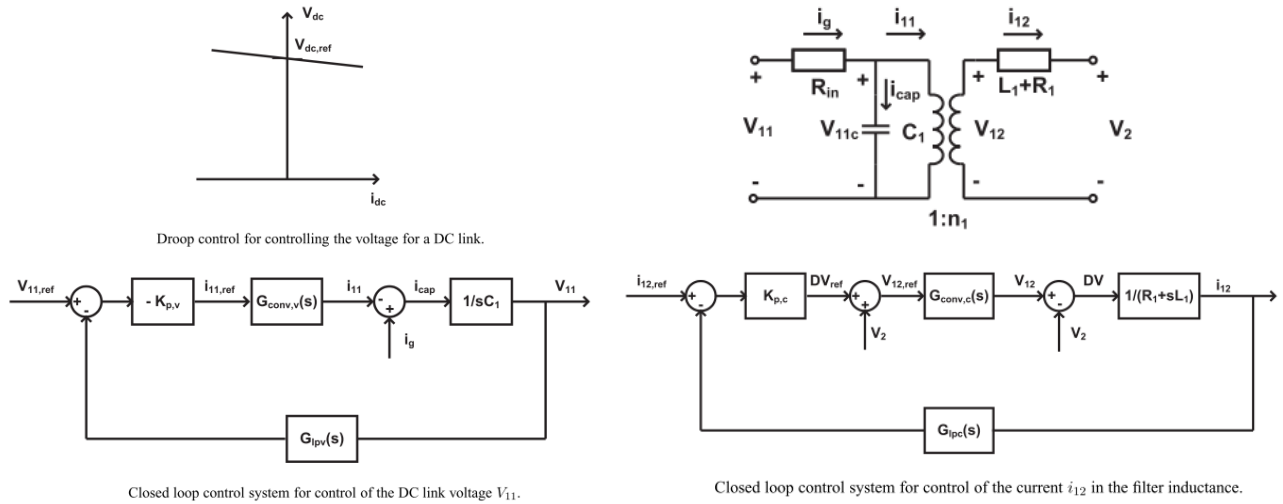


Fig. 29 Model of turbine control blocks

Fig. 29 shows the closed loop control system for DC link voltage and output current. Both controllers are designed in the same way.

Lab Setup

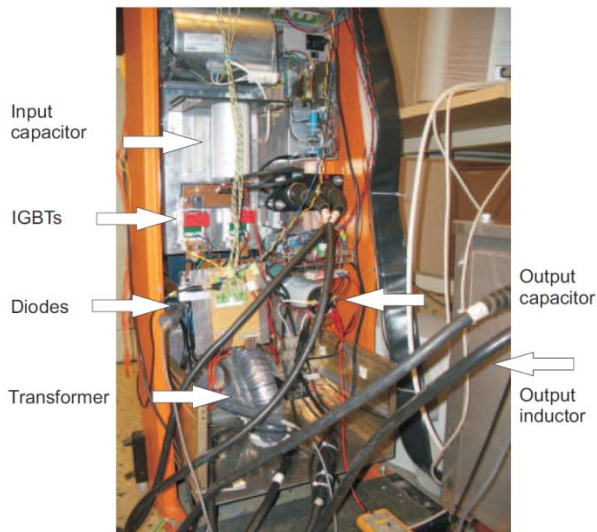


Fig. 30 Lab setup and transformer used in [7]

A scaled down setup was implemented to validate simulation waveforms and loss calculation. The power rating of the converter is 9 kW, with an input voltage of 300V and an input current of 30A. The transformer of the converter has a ratio of 1:1. The main components of the setup are the IGBT modules, diode modules, the transformer, the filter inductance and capacitance. There are auxiliary components such as the driver circuits, measuring system, cooling and power supply to the auxiliary components. Semikron power modules rated at 1200V and 320 A were used, while for the rectifying bridge, modules rated at 1000V and 30A are employed. Transformer core material is iron alloy 2605SA1 from Metglas. For the control system, a dSpace DS1103 is used. Input and output currents are measured with LEM modules

iii. Single active bridge 2012

Concept

In [35], a DC grid for offshore wind farms is investigated with focus on the design and control. A parallel connected SAB dc/dc converter is used in the turbines (see Fig. 31). By paralleling lower power converters, the current rating of the power switches can be lowered and by interleaving the output currents, the total output current ripple can be reduced significantly without increasing the switching losses or device stresses. Analysis of both the input and output current characteristic and design aspects of the transformers, the filter inductor were presented.

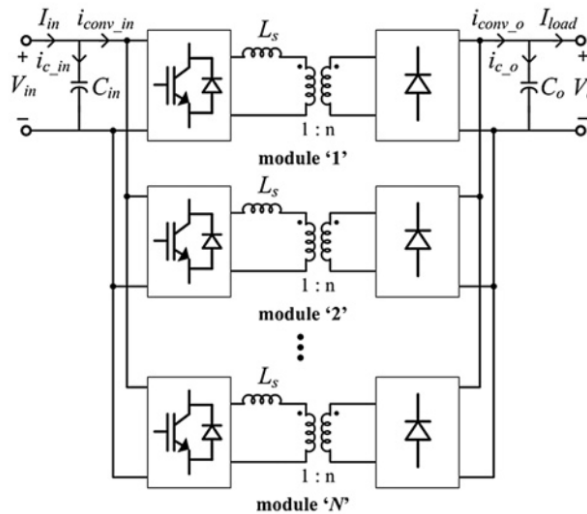


Fig. 31 N-parallel connected SAB dc-dc converters from [35]

Control and lab setup

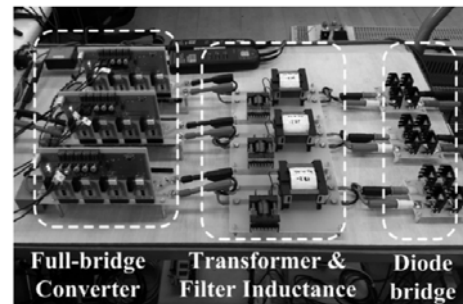
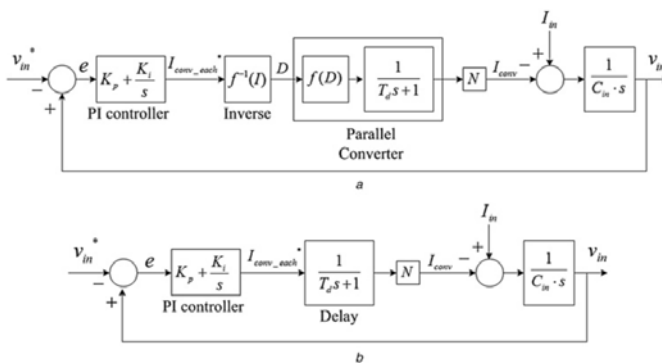


Fig. 32 Control and lab setup from [36]

The control block diagram and lab setup are shown above. The converter is represented with the non linear function of the actuator and a first order low pass filter which represents the time delay of the converter system. The prototype rated power is 1 kVA, input voltage is 120V, output voltage is set to 600V, while switching frequency is around 10 kHz. 3 parallel converter are connected.

iv. Full bridge 2006

Concept

In [37], aspects regarding wind park design and grid connection were treated. Various wind turbines were investigated and selected topology is based on a 4 stage concept. In this work, the turbines are connected in series. The main part of the thesis dealt with the dynamic investigation of the series connected wind park concept. The wind turbine controller needs a control structure that can handle the operation of the turbine when the input power to the turbine varies strongly. In order to avoid too high energy production loss, the output voltage rating of the wind turbine must be at least 35% higher than the nominal output voltage. Two DC/DC candidates were investigated. The full bridge isolated boost converter and a full bridge converter.

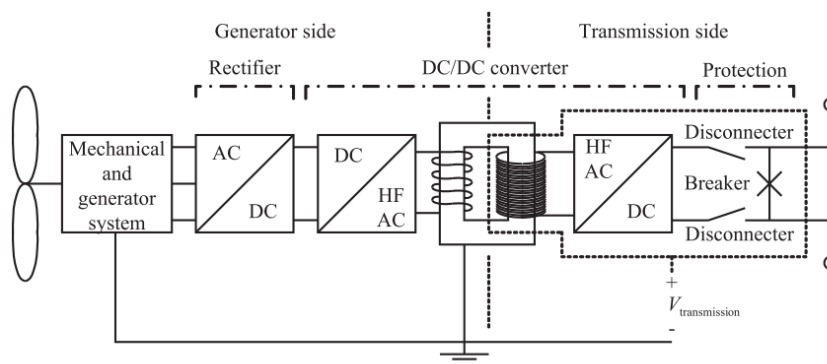
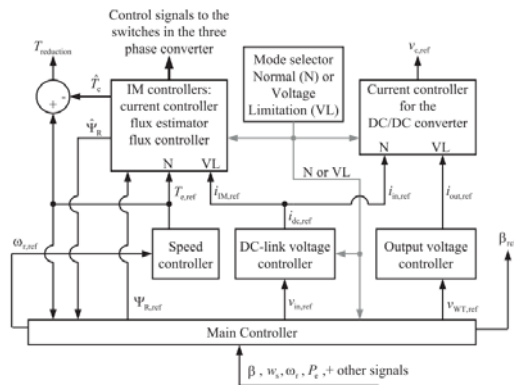


Fig. 33 Selected topology in [37]

Control and lab setup



Principle controller structure for a wind turbine with additions for controlling the series-connected wind turbine. Inputs marked with N are used in normal mode and inputs marked with VL are used in voltage limitation mode.

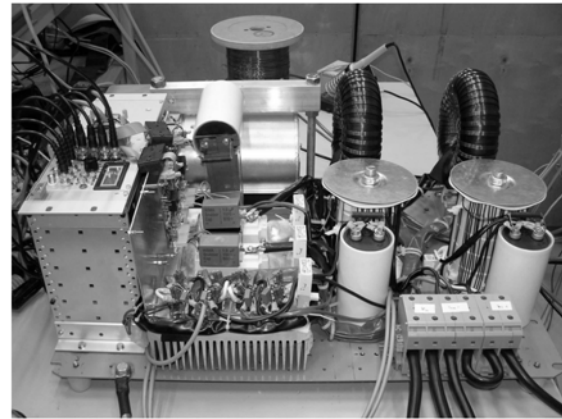


Fig. 34 Control and lab setup used in [37]

Main controller and lab setup are shown above. The down scaled converter is rated at 5.8kW, 300V input voltage and output voltage. The ratings of the IGBT are 1200V and 400A, while the output diodes are rated at 1000V and 70A rms. The currents are measured with LEM LA-100s current transducers. To control the converter, dSPACE DS1103 is used. The material for the transformer core was Metglas alloy 2605SA1, with a width of 30mm.

v. Matrix 2012

Concept

In [8], HVDC based on a series connection of an offshore wind farm are researched. The thesis demonstrates the advantages of this type but also new challenges which were not studied before. Turbine converter is based on matrix topology connected to multiple drive train generators. The matrix converter was selected because it reduced the stages of conversion (Fig. 35). Simulation and experimental results demonstrate the efficiency and feasibility of the converter.

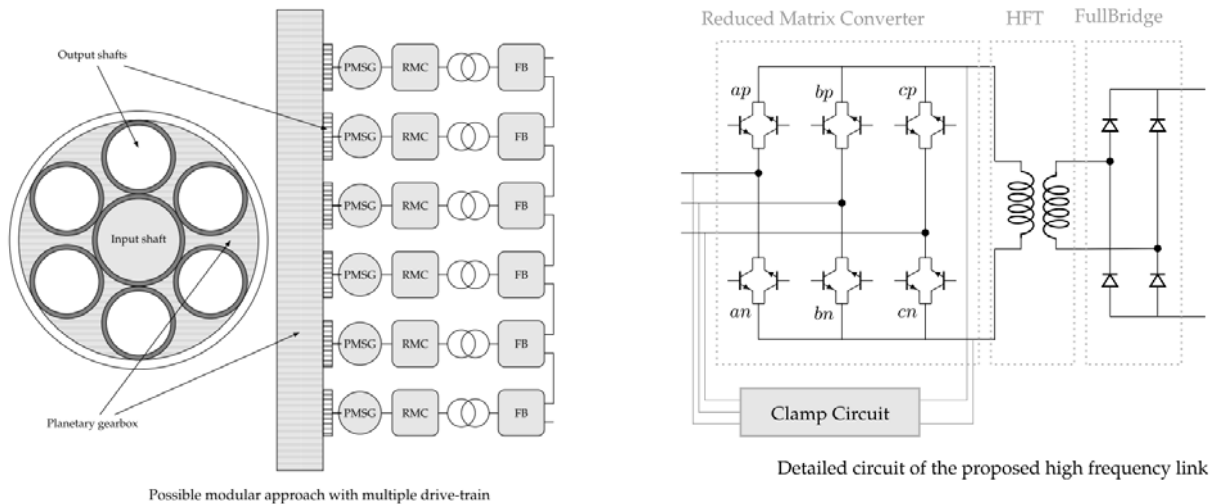


Fig. 35 Selected topology in [8]

Control and lab setup

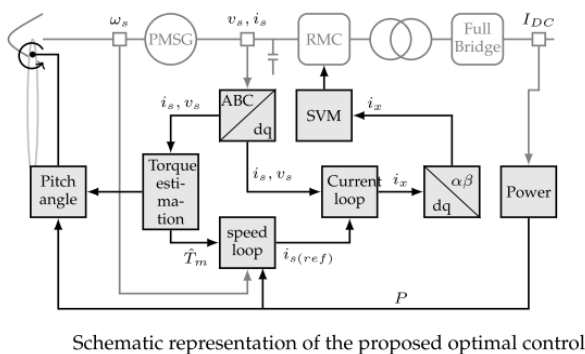


Fig. 36 Control and lab setup used in [8]

Experimental studies proved the concept of the reduced matrix converter. High frequency operation was achieved with a 10 kW converter@10kHz, 200 Vrms input and 326Vdc output voltage. . The control of the converter was studied only through simulations. Controlling current source converters is a complex task and problems appeared due to resonance of filter capacitors with the grid. A proportional plus estimation strategy was used for controlling the wind turbines. Output voltages and currents have a very low harmonic distortion.

vi. Modular transformer less 2013

Concept

In [38], a modular series connected converter suitable for transformerless offshore wind turbine is analyzed (Fig. 37). The main objective was to verify the proposed converter as a suitable interface between a modular axial flux ironless stator PMSG and a high voltage DC link. The modular converter topology consists of N 3-phase VSC units. Each unit is connected to an independent 3-phase winding output from the modular generator. The high output voltage is obtained by connecting the converter unit DC buses in series. This converter topology provides the necessary interface to a high voltage grid for a generator insulation system which makes a compact, high voltage machine feasible.

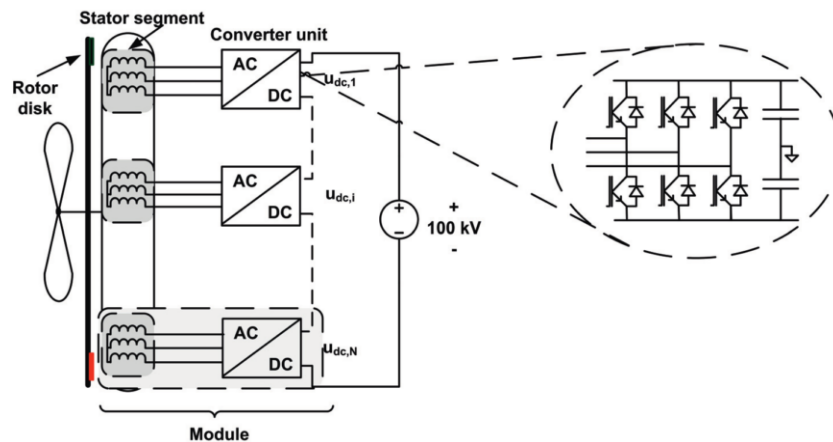
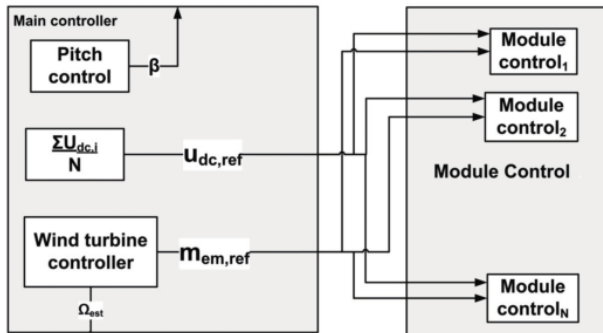


Fig. 37 Proposed topology in [38]

Control and lab setup



Overview of the control system for Concept 4. The turbine controller units are in the main control, and the converter unit control blocks in the modules.



Laboratory setup: Input induction machine, gearbox and low speed shaft connection to the large diameter modular generator in the back. Modular series connected converter with the FPGA-control cards in the rack.

Fig. 38 Control and lab setup in [38]

The concept is verified experimentally based on a 45 kW prototype. Implementation of the control system is done as an embedded control, using FPGA/processor based control card for each module. The feasibility of the system, theoretical models, modular control synthesis approach for the series connected converter and the DC-droop control functionality are all verified by the experimental results.

vii. High gain transformer less 2009

In [39], demonstration of 30 kW IGBT LCL DC/DC converter as proof of concept for interconnecting HVDC systems is performed. According to this paper, the LCL DC/DC converter, comprises two active full bridges and can achieve high stepping ratios with no internal ac transformer. This work details the control design and closed loop testing on a 200V/900V specification. Four PI controllers are implemented for each VSC bridge to fulfill the control objectives of active power flow control and zero reactive power circulation. Switching frequency is set to 5.1 kHz. The closed loop testing demonstrate good stability, tracking and accurate reactive current regulation.

Concept and lab setup

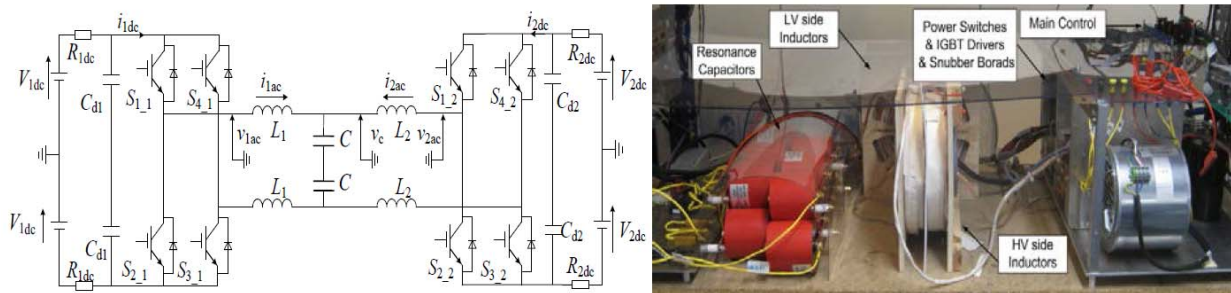


Fig. 1 IGBT based LCL DC/DC converter, topology and prototype picture (1-LV side, 2-HV side).

Fig. 39 Topology and lab setup

viii. High gain transformerless 2012

A high efficiency, high power step up resonant switched capacitor converter for offshore wind energy systems is proposed in [31]. This work presents a converter, which is characterized by soft switching condition for all switches and diodes. The experimental results of a 24 kW/17levels prototype are presented to verify the proposed converter. The switching frequency and resonant frequency are 7.5kHz and 8kHz, respectively. All the resonant inductors are air core inductors. Input voltage is 600V, while output voltage is 10.2 kV.

Concept and lab setup

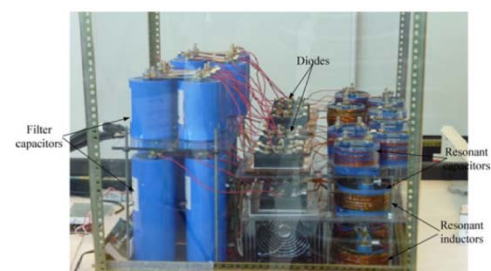
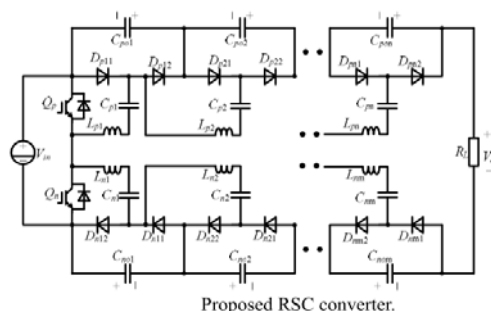


Fig. 16. Prototype of 600 V/10.2 kV, 24-kW 17-level ZCS RSC converter.

Fig. 40 Topology and lab setup

ix. High gain transformerless 2015

In [33], another high gain transformerless converter, based on resonant switched capacitor cell is developed. The proposed converter is characterized by the resonant switching transitions to achieve minimal switching losses and maximum system efficiency. A 5kW prototypes is evaluated, with switching frequency set at 4.5kHz. Input voltage is 100V, while output voltage is 500V. Maximum efficiency of 97% is reached at 2kW.

Concept and lab setup

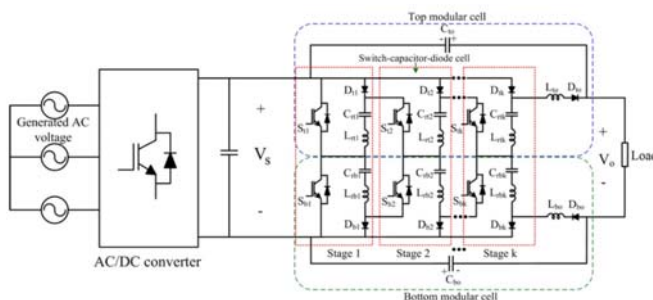


TABLE IV
PROTOTYPE COMPONENTS

Parameter	Value
Resonant inductor	20 μ H with powder core
Resonant capacitor	2 \times 25 μ F/450 V – Film capacitor connected in parallel
Output capacitor	2 \times 130 μ F/450 V – Film capacitor connected in parallel
IGBT module	600 V-SKM200GB063D from SEMIKRON
Diode	DSEP2X91-06A

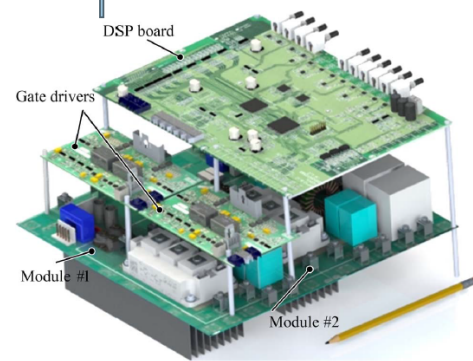


Fig. 20. 5-kW DS-based prototype converter.

Fig. 41 Topology and lab setup

c. Traction demonstrators

i. Traction Cycloconverter 2007



Fig. 42 Photo of demonstrator [21]

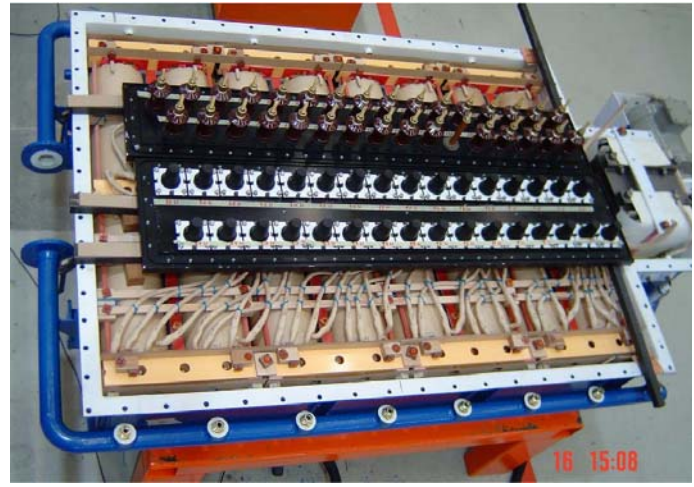


Fig. 43 Photo of the sixteen medium frequency transformers [21]

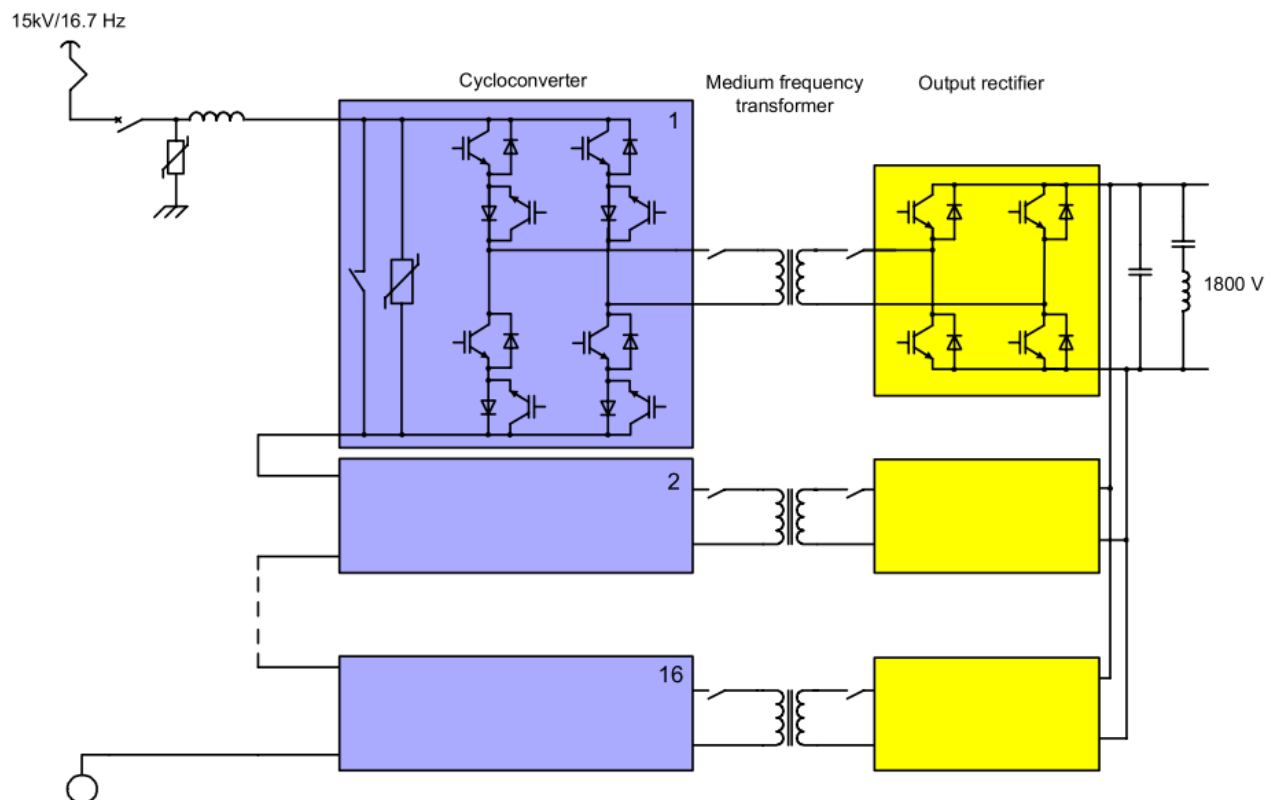


Fig. 44 Converter circuit used in [21]

Topology

The system is designed to meet railway specifications. It has bi-directional power flow. On MV side there are 16 bidirectional cycloconverters, connected in series to the catenary 15 kV, 16.7hz through a chock inductor. On LV side, there are 16 four quadrant converters connected in parallel to a 1.8 kVDC link. The system frequency comes from a

technical and economical compromise. On one hand, increasing the frequency will decrease the transformer size, but it will increase losses. On rectifier side, capacitors and converters have been arranged to reduce stray inductance and the turn off overvoltage. A current sensor is present on each transformer to protect the power electronics from an over current. The losses of the converter at rated power are 3%. The authors conclusion is that the weight is reduced with 50% and the volume by 20%, compared to a classic 16Hz transformer.

Transformer

16 medium frequency transformers, running at 400hz. The MF transformers are using silicon iron sheets and bar conductors. Specific design rules were used to obtain a very low short-circuit impedance required by the topology. If a fault is detected, a stop sequence is launched and the faulty module is isolated from the rest of the system using static contactors. The main characteristics of the transformers are: very low short circuit impedance ($>2\%$), insulation for the 15 kV network, 400hz and 1:1 turn ratio. Mechanical design is like a conventional traction transformer.

Semiconductors

On both MV and LV side, 3.3 kV/2 x 400A IGBTs are used, for volume and cost purpose. The gate drivers are using a high voltage insulated power supply based on a high frequency current source feeding current transformers. All firing signals are done with optical fiber to be free from any potential and also to keep a high level of immunity against EMC. All switching are made in a ZCS mode.

Cooling

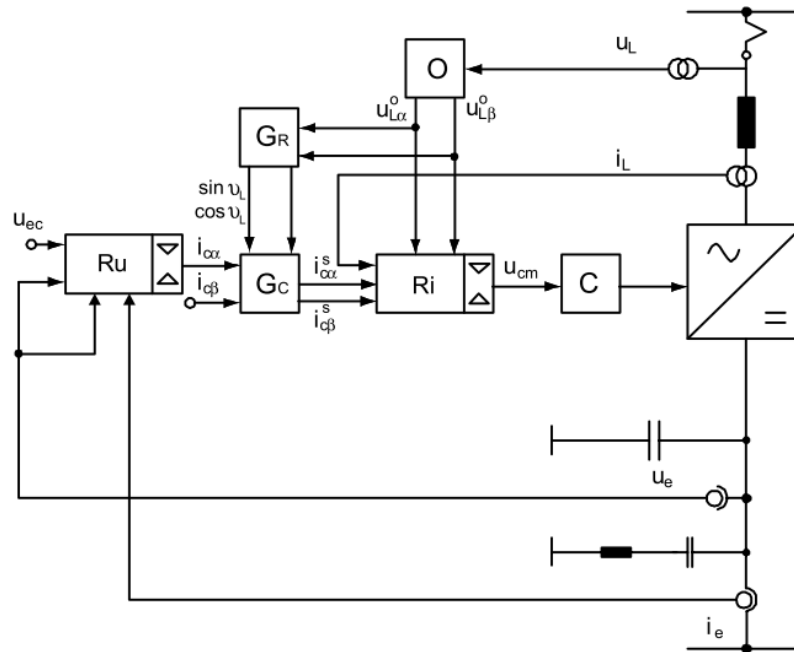
In order to reduce costs, maintenance and size, oil cooling is used for the converters and transformers. Oil is used because it has natural capabilities.

Challenges

Cooling, grounding, auxiliary power supply, design of medium frequency transformers, insulation and failure modes

Control

Fig. 45 shows the control principle. It has been implemented with a high performance controller (ABB AC800PEC). The control of the test bench is based on a separate PLC unit (ABB 800xA). The aim is to obtain a stabilized intermediate DC voltage regardless of the motor drive power consumption. This has to be done while keeping the input current sinusoidal, with a power factor close to one. The converter is connected to the grid through an inductance which enables to control the current. An observer, fed by the catenary voltage, provides two signals in quadrature that are synchronous to the grid. These signals are normalized and used to produce the sinusoidal current set points as well as direct intervention for the state space current controller. The amplitude of the active current set point is given by a superposed state space voltage regulator. The magnitude of the reactive current set point is usually set to zero.



Protection

Valve complexity

cgd@et.aau.dk
www.dcc.et.aau.dk

ii. Traction SRC 2002

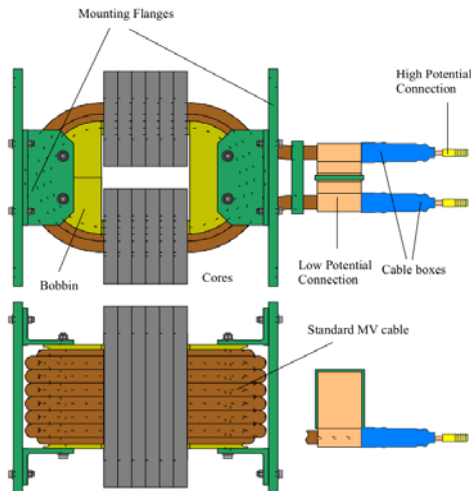


Fig. 46 Basic configuration of coaxial transformer [13]

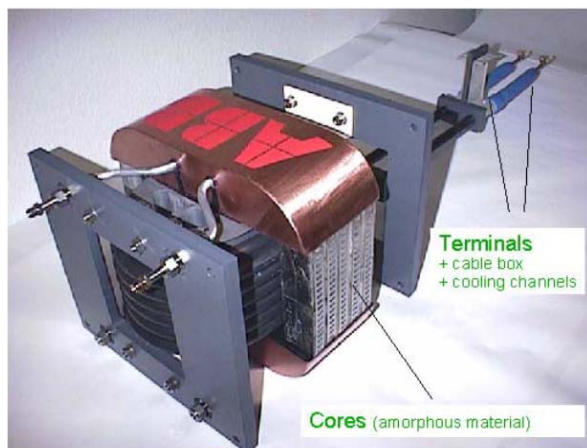


Fig. 47 Physical arrangement of transformer [13]

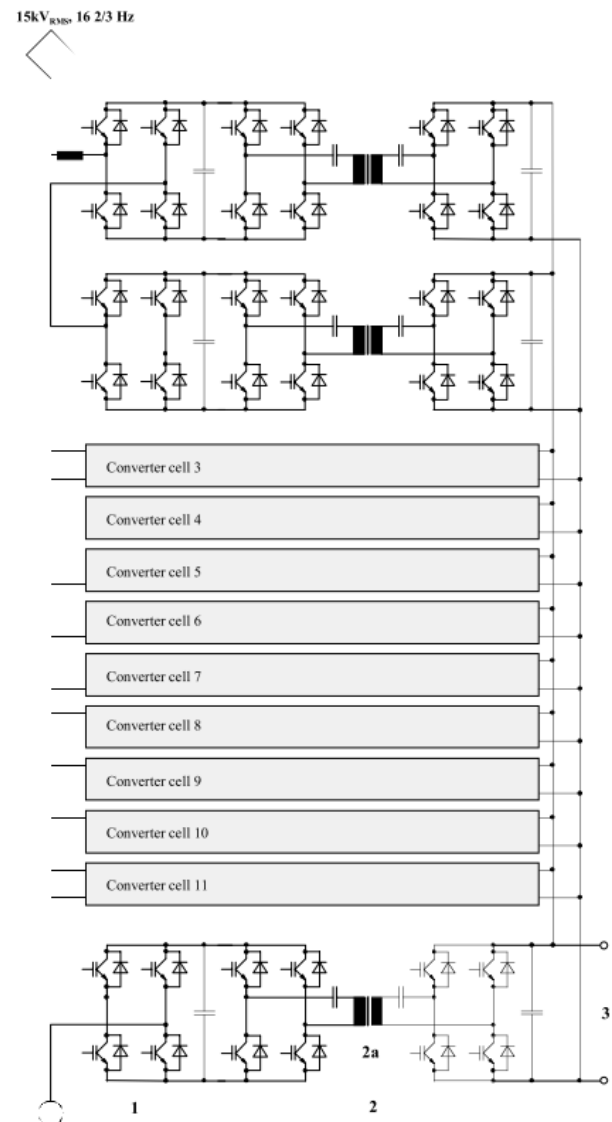


Fig. 48 Converter circuit used in [13]

Topology

Cascaded series resonant converter, used for high speed train application, for a line voltage of 15 kV, 16.7hz. The Converter is designed for bi-directional power flow and has 12 individual converter cells, connected in series on the primary side and in parallel on the secondary side. Each converter has a standard AC-DC chopper, a resonant SRC DC-DC converter on MV and LV side. The primary side is at high potential and the parts are mounted in a special compartment to form a dielectric barrier against secondary sided ground. The multilevel converter concepts help to reduce the HF stress of the insulation material

Transformer

350 KW transformed, built with amorphous core material and coaxial windings. Special attention was paid on the insulation problem, since dielectric losses and the influence of the voltage waveform with very steep edges had to be investigated in detail to guarantee a long life time of the device. Primary and secondary voltages are 3 kV. The insulation level is set to 38 kV. The weight of the transformer is less than 50[kG]. To minimize the amount of copper the use of a hollow inner winding in the form of a tube with wall thickness in the region of the expected skin depth is recommended, having the advantage of cooling the inner winding with water or forced air cooling.

Cooling

The transformer and the converter are both cooled with de-ionized water

Challenges

Transformer design was the main challenge of this demonstrator. In order to meet basic requirements like low weight, low loss and low volume on the transformer, some characteristics had to be achieved:

- Low loss and solid high voltage isolation between primary and secondary side windings.
- Selection of right core material with low losses and high saturation induction
- Minimization of copper losses due to skin and proximity effect
- Low and controllable leakage inductance
- Efficient cooling of windings and core
- Influence of voltage waveform with a magnitude of more than 20 kV with very steep edges or aging of insulation was investigated.

For this demonstrator it was not possible to find information regarding Control, Protection or Valve Complexity.

iii. Traction LLC 2014



Fig. 49 Photo of HV PEBB

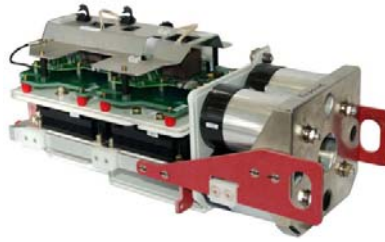


Fig. 50 Photo of LV PEBB

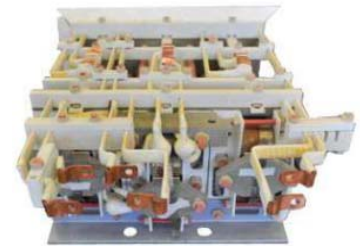


Fig. 51 MF Transformer

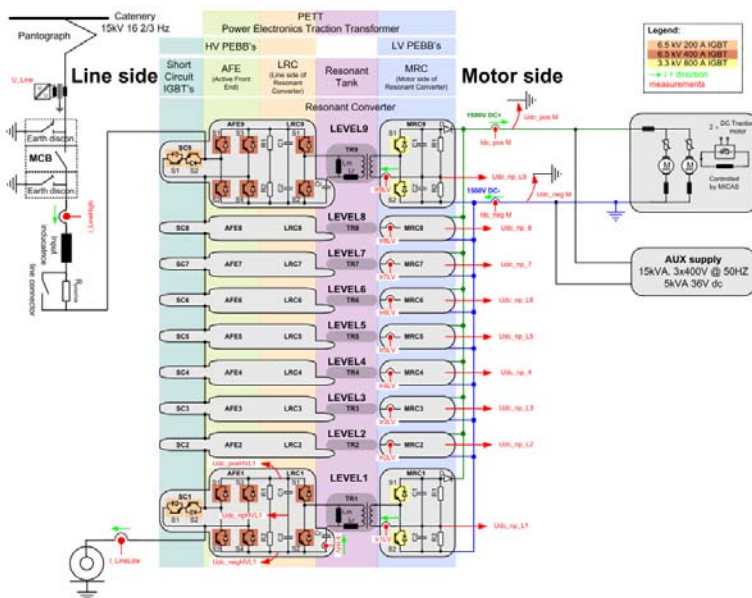


Fig. 52 Photo of developed PET demonstrator

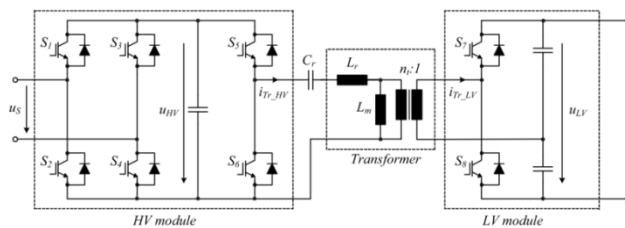


Fig. 2 Detail topology of one level of the PET demonstrator composed of a full-bridge circuit and a half-bridge LLC resonant circuit.

Fig. 53 Converter circuit used in [12]



Fig. 54 Photo of the tank, including 9 MF transformers

Topology

This is one of the few modular demonstrators implemented on a field locomotive. The world's first ever locomotive which is powered by the *Power Electronic Transformer*, has been put into service from February 2012. The PET demonstrator is developed for the AC single phase 15 kV, 16 2/3 Hz and has a nominal power of 1.2[MW] and 1.8[MW] peak output power for a short time duration. The DC/DC converter is controlled by means of variable frequency, fixed duty cycle PWM. The demonstrator is composed of cascaded multilevel front end circuit and N parallel-output DC/DC circuits with galvanic isolation provided by the medium frequency transformers. The output voltage of the demonstrator is 1.5 kVDC. One cell is composed of an AC-DC full bridge + a DC/DC stage realized by a half bridge LLC isolated converter. The resonant frequency is set to 2005 Hz, coming from $L_r=350\mu\text{H}$ and $C_r=18\mu\text{F}$. The demonstrator has an efficiency of around 96% in a wide range of output power. At low ratios of the two resonant inductors a narrow variation of switching frequency is enough to control a wide range of power. The DC/DC converter is driven in open loop, so the PET converter can be simplified to an H-bridge used to control a DC Link voltage, while the PET under consideration serves to provide constant dc output voltage. In contrast to the LC resonant tank, the LLC resonant tank employs the magnetizing inductance not only to maintain ZVS during turn-ON but also to provide low current during turn-OFF. Considering the LLC dc-dc converter, main emphasis has been placed on the turn-OFF losses, identified as the main contributor to the overall losses in the system. The LLC resonant converter seems to be a promising solution for high power MV applications as an interface converter between two different dc links. The low number of required semiconductors, soft switching properties, simple control, load independent operating point and easy integration of the resonant elements within the transformer. The main advantages of the LLC topology are:

- Wider output regulation range
- Reduction of switching losses on the primary side through ZVS over the entire load range
- Low turn-off current controlled by the design (not really ZCS)
- Low voltage stress and ZCS on the secondary side diode rectifier
- Load independent operation at resonant frequency

Transformer

The transformer in this case has 3 roles: galvanic separation, adaptation from 3.6 kV down to 1.5 kV and to help the IGBT modules in the LLC circuit to commute in the soft switching mode. The target value for the magnetizing inductance is achieved by air gapping the core.

Semiconductors

6.5 kV IGBT modules are employed on the medium voltage side, in order to obtain a low number of cells. In this case 8+1 cells are implemented, with one extra cell for redundancy. In case of failure, the demonstrator can operate with 8 modules. The intermediate DC-Link voltage is set to 3.6 kV. Due to the presence of the LLC, soft switching commutation of the IGBT modules is achieved, by the involvement of the magnetizing and leakage inductance of the transformer into the resonance. This means, the IGBTs are turned on with ZVS and are turned off with significantly smaller current. Soft switching allows for increasing the switching frequency to 1.8 kHz. On the secondary side, 3.3 kV ABB HiPak modules are used. To reduce the ripple on the output capacitors, interleaving of the PWM carriers is applied. Depending on the power flow, either the 3.6 kV or the 1.5 kV side of the DC/DC converter is PWM controlled, while the other side acts like a diode rectifier, respectively.

Because the switching frequency (1750 Hz) is smaller than resonant tank frequency, the IGBT modules are turned on with ZVS and turned off with almost zero current switching. Therefore, the IGBT modules in the LLC resonant circuit

can be switched with a higher frequency than those switched in the hard switching commutation mode, which enables the employment of medium frequency transformers in the PET demonstrator

Cooling

Oil cooled trafo, water cooled PEBB

Challenges

Challenges are related to the selection of IGBT power modules and transformer design, especially the mechanical arrangement to achieve high voltage insulation between grid voltage and ground potential.

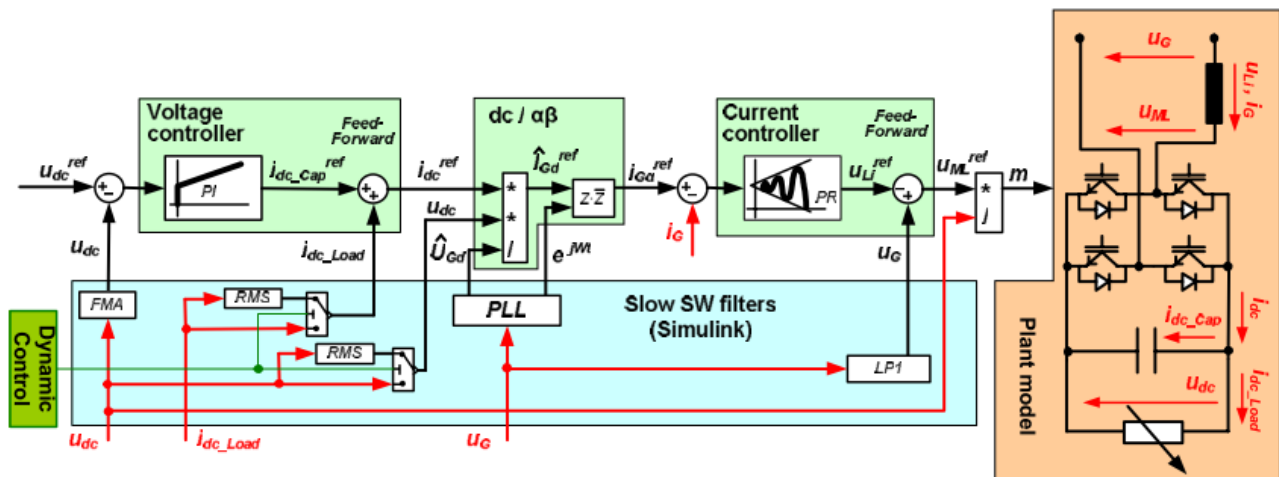
There is a high focus to avoid partial discharges in the insulation material, ionization of air and flashovers. The mechanical arrangement to achieve high voltage insulation includes an insulating support structure and a number of conducting enclosure or shields. The enclosures have geometrical features like rounded corners and edges, as well as flat and even faces, to homogenize the electric fields around them, thus reducing partial discharges and the minimum clearance distances around the enclosures

Control

Control targets are: sinusoidal input current, near unity power factor, constant average DC link voltage and grid harmonic rejection. Fig. 55 shows the implemented control structure. Because the DC/DC converter is driven in open loop, the PET converter is simplified to an H-bridge used to control a DC link voltage from the controller point of view. The controller features two main loops on the ARU side, an inner line current control loop and an outer DC link voltage control loop. The current controller is implemented with a proportional resonant PR controller operating in the stationary reference frame. The DC link voltage controller is based on a standard proportional integral PI controller. It takes into account the 2nd harmonic ripple due to the power fluctuation (characteristic for a single phase system). This is done by filtering the DC link voltage u_{dc} with a fast moving average filter FMA, that has a time window with the length of the 2nd harmonic ripple.

In order to reach a power factor unity value at the input side, synchronization with the railway grid voltage u_G is required which is done using a standard PLL for a single phase system. An other interesting feature is the dynamic controller, which depending on the required system dynamics changes the filtering of u_{DC} and the load current i_{DC_Load} . When high dynamics are required the values are not filtered, but during slow dynamic changes the rms values are used.

The PR controller enables a simpler implementation than a PI controller working in the dq frame. It also provides a better dynamic response and enables a simple harmonic cancelation for low frequency harmonics. The entire control structure was build on the AC800PEC platform of ABB.



Protection

Valve complexity

iv. Traction SRC 2011



Fig. 56 Prototype of MF transformer



Fig. 57 Winding arrangement of MF transformer

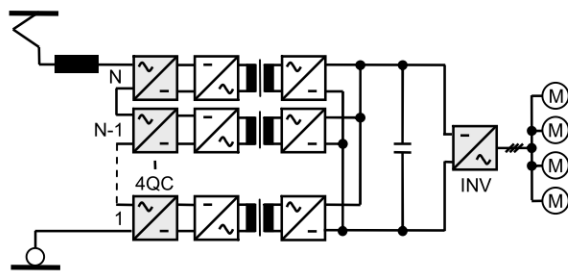
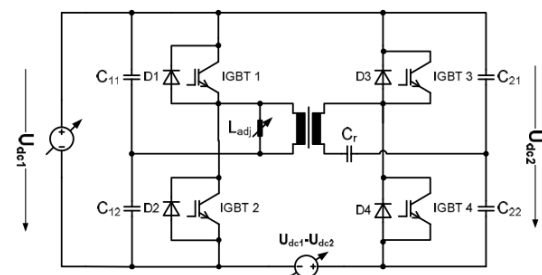


Fig. 58 Converter circuit used in demonstrator [14]

**Topology**

This is also a demonstrator for traction application, connected at 16.7Hz, 15 kV, built with series connected converter submodules, based on MF-DC/DC Converters. Each converter submodule consists of a four Quadrant Converter and a MF transformer. The considered number of sub modules is 7. For connection to 25 kV, at least 12 modules should be used. The introduced topology is based on a bidirectional medium frequency series resonant converter. The inverter and rectifier are each equipped with a half bridge to keep the currents and power low while power throughput is preset. In this way, the IGBTs can easily be pushed to their limit, while the component count and the complexity are kept low.

Transformer

An electromagnetic, thermal and hydraulic model for the transformer was built. The optimum switching frequency was found by optimizing the MF transformer and the inverter/rectifier together. The investigated transformer was designed with interleaved windings. Isolation between primary and secondary winding is achieved by oil and between the conductors inside of the layers with NOMEX isolation material. The conductors are designed as hollow profile type in aluminum. Heat removal is provided by deionized water flow through the conductor profiles. For the core, nanocrystalline material VITROPERM 500F was used. Different core materials (like VITROVAC 6030F-amorphous and Ferrite K 2006) were compared to nanocrystalline core and it was discovered that the lowest mass is achieved only with the previous material. The highest transformer mass resulted with ferrite material, due to low saturation flux density, leading to a high core dimension and losses. The isolation thickness between adjacent conductors inside the layers results for a defined isolation material from the maximum dclink voltage, the converter topology and the chosen winding number. Optimum value of MF transformer's efficiency was achieved at 5.8 kHz switching frequencies. Optimum value of MF transformer's efficiency was achieved at 5.8 kHz switching frequencies. A coupled thermal, hydraulic and electromagnetic analysis of the transformer with internal liquid cooled conductors shows that both conductor geometry and switching frequency have a significant influence on the resulting transformer efficiency and transformer mass.

Semiconductors

6.6 kV IGBTs were employed and characterized in resonant mode. In typical application for HV-IGBTs in the fields of traction converters can be characterized by high currents at a comparably low switching frequency without any soft switching. Therefore, the IGBTs are designed to have a minimum conduction loss. In this demonstrator two different types of IGBTs have been tested: The first one is a standard IGBT used in traction, while the second one has been irradiated with electron doses in order to shift the balance towards reduced E_{off} loss, accepting increased static conduction loss. Comparing both IGBTs, with regard to achievable switching frequency, the benefit of the modified IGBT is an increase of 30% transferred power

Control

To be investigated further.

Protection

To be investigated further.

Valve complexity

To be investigated further.

v. Traction DAB and SRC 2013

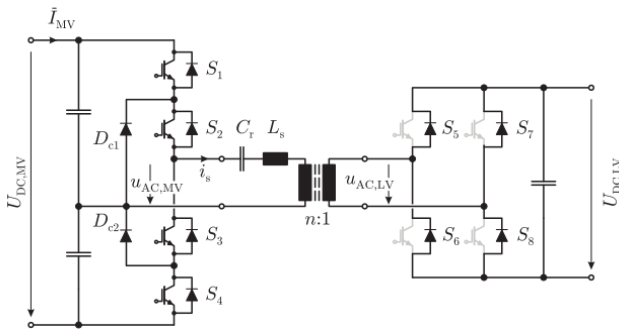


Fig. 59 3L NPC Series Resonant [17]

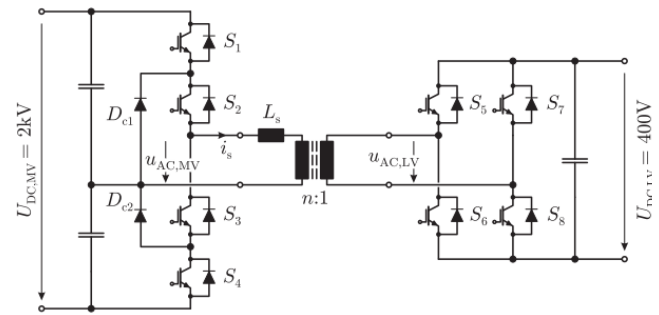


Fig. 60 3L NPC Dual Active Bridge [17]

Topology

Demonstrator built in modular fashion, with three stages: inversion, isolated dc-dc conversion and inversion. Aimed power for a full demonstrator is 1[MW], 12 kV input and 1.2 kV output, with an operating frequency of 20 kHz and it's composed of 6 modules. One module has 166 KW nominal power, 2 kV input and 400V output. Each converter module can be subdivided into three main parts: the MV side with NPC half-bridge, the LV side full bridge and the MF transformer. The MV side is built around a NPC half bridge leg while LV side has a full bridge. 1.7 kV power semiconductors are selected for the MV side. For LV side, 600V class semiconductors are considered since switch technologies in this voltage level are characterized by outstanding conduction and switching capabilities, whereby majority and minority carrier-based semiconductor technologies (MOSFET and IGBT) coexist in this range, widening the range of available switch options. NPC half bridge was favored for the MV side, given it's capability of dealing with higher DC voltages while still utilizing relatively LV-rated devices. In addition, the NPC half-bridge arrangement is able to generate three output voltage levels. The work is mainly focused on finding soft-switching strategies, for reducing the IGBTs turn off losses, finally resulting in a ZCS transition.

Two topologies which allow ZCS modulation are considered:

- Half-Cycle Discontinuous Conduction Mode Series Resonant Converter (HC-DCM-SRC)
- Triangular current Mode Dual Active Bridge (TCM-DAB)

The main drawback of the HC-DCM-SRC is its incapability of controlling the power throughput since, in order to operate in DCM while achieving ZCS, the active bridge must be operated without duty cycle control. This disadvantage restricts the utilization of the HC-DCM-SRC to application where tight in/out voltage ranges are required or where the voltage regulation can be done by other stages of the SST.

In case power transfer control is required while still keeping ZCS (zero current switching) transitions at least for the MV side of the converter, the DAB is an interesting solution.

Transformer

For the HC-DCM-SRC, the turns ratio is defined to 5:2, while for the TCM-DAB the turns ratio is 3:1. A fluid-dynamic/thermal simulation was performed with COMSOL Multiphysics in order to estimate the temperature rise of

the designed cooling system. Regarding MF transformers, two different concepts were proposed for the two topologies. An optimized procedure which outputs the optimum transformer design for a given set of constant parameters is also proposed, leading to the construction of these two transformer prototypes, whereby their mechanical assembly is extensively covered. Shell type transformers were considered for both HC-DCM-SRC and the TCM-DAB. However, both trafo differ in core material, isolation medium and cooling concept. For the HC-DCM-SRC system, a compact high power density design is aimed. Nanocrystalline core material and water cooling are selected. A layer of isolation based on mica tape is placed between the LV winding and the MV winding. This material can isolate up to 13.8 kV and is originally designed for isolation of medium voltage electrical machines. In addition to this isolation layer, the windings are initially covered with a semi-conductive tape in order to even out the electric field within the isolation. The cooling concept is based on aluminum pieces conducting the heat to top/bottom water-cooled heat sinks.

In case of the TCM-DAB transformer, a ferrite-based construction was preferred in order to achieve a comparatively lower cost solution. The isolation concept is based on a PTFE(Teflon) bobbin where the windings are placed. The cooling concept is forced air-cooling for both the winding and the cores. Top and bottom heat sinks are utilized in order to cool the ferrite cores.

Semiconductors

The losses associated with ZCS transitions are related to the dynamic behavior of the semiconductor switching device. During its conduction phase, a bipolar power switch builds up a large amount of charge in order to become conductive and hence to reduce the associated conduction losses. The instantaneous value of this charge is dynamically related to the current conducted through the semiconductor device during its conduction phase and is responsible for the switching losses encountered when the device transitions from conducting to blocking state, as this charge must be evacuated when the semiconductor device enters the blocking state (tail current of IGBTs). FF450R17ME4 1700V/450A EconoDUAL IGBT module was used for MV side. Regarding cooling of the device, the MQT1914 water cooled heat sink from MaxQ Technology was considered. For LV side, the 600A Infineon FF600R06ME3 power module was considered, while for MOSFET, STY112N65M5 650V/96A was taken in consideration. A theoretical basis for getting data required to estimate the dynamic behavior of this charge for arbitrary current shapes was laid out. With an understanding of the internal dynamic processes taking place in the semiconductor device, several improvements were proposed to the standard modulation schemes

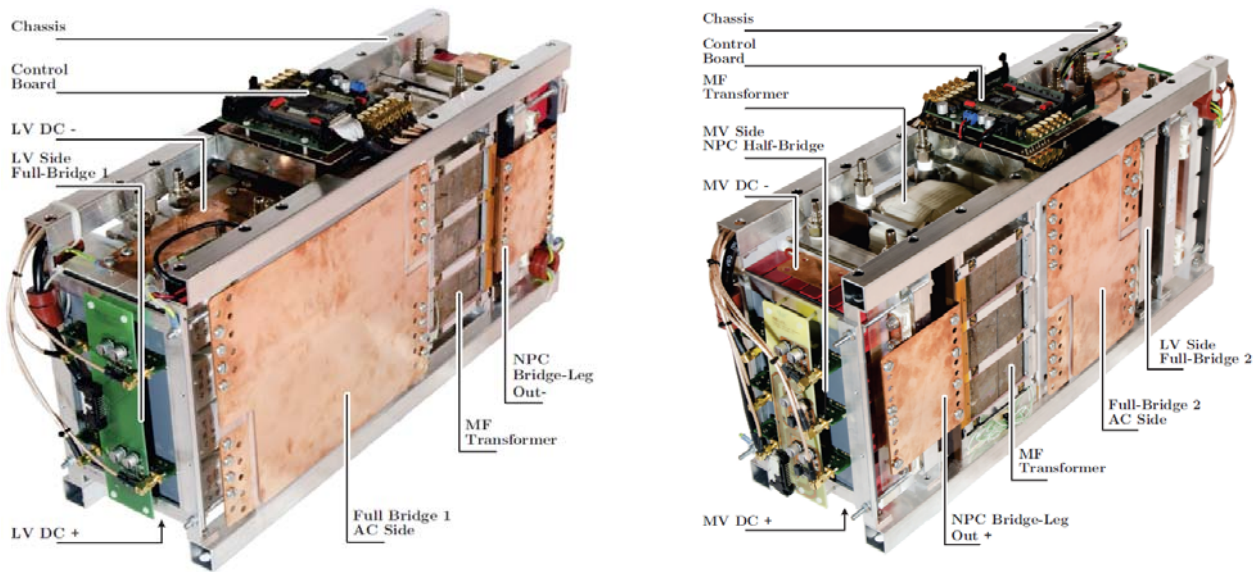


Fig. 61 Assembly of SRC Module (front and back view) [17]

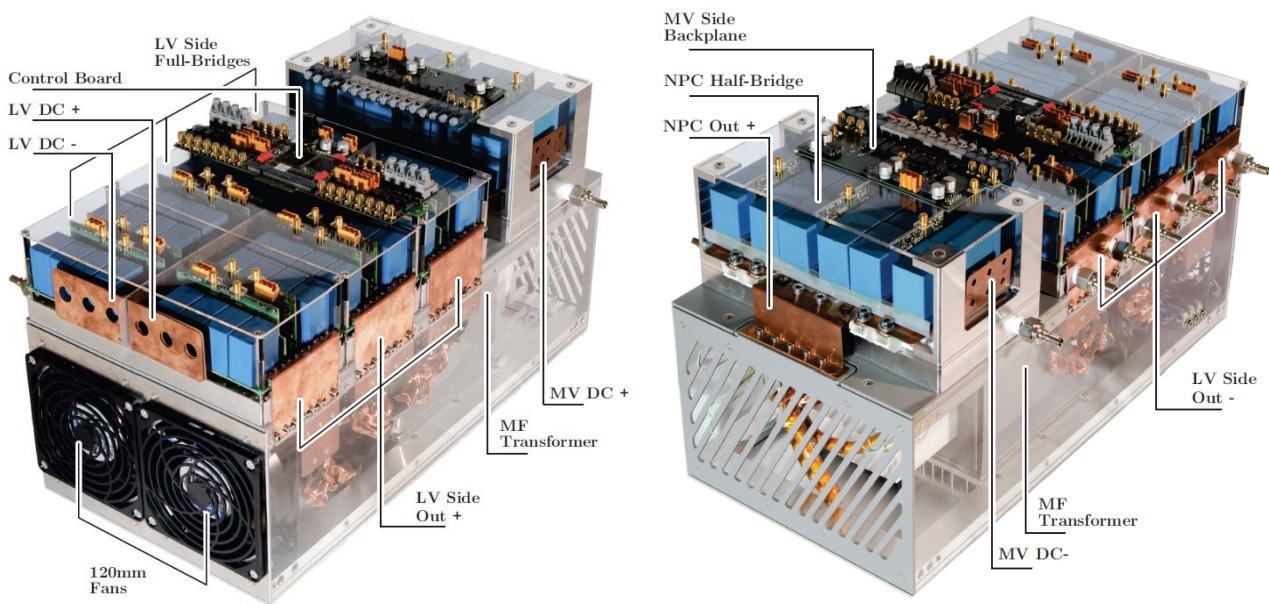


Fig. 62 Assembly of DAB module (Front and back view) [17]

The final construction of the HC-DCM-SRC is arranged with two LV bridges in the front, followed by the MF transformers and the MV bridge in the rear. Since all bridges and the MF transformer were designed with equal height and depth, they can all be fitted within an aluminum frame serving also as chassis in order to achieve a high mechanical stability. The DC-link connections are placed on the top and bottom for both MV and LV side bridges. All water cooling connections are accessible from the top, leading to an easy connection of the hoses carrying the cooling fluid. All gates and feedback signals are routed through the hollow aluminum bars in order to shield them from external disturbances. These signals are routed to the control board, which is placed on the top of the assembly. The final

construction of the TCM-DAB has the ferrite transformer on the bottom, whereby the top cover serves as mounting plate for the water cooled heat sinks of the power electronic bridges. The three LV side full-bridges are placed next to each other and their connection to the MF transformer is done through independent copper plates. The DC Link connection of these bridges is done from the front with two copper busbars which then connect to all LV side bridges. Behind the LV side bridges, the MV side NPC half bridge is placed. The MV side backplane is placed on the top contacting the respective gate drivers. The MV side DC-Link connections are placed on each side of the bridge, while the AC connections are done from the front and the back side of the bridge. An aluminum frame provides the mechanical stability of the converter. Considering power density, the HC-DCM-SRC system achieves the highest value, due to the different cooling concept and core material. Regarding efficiency, the calculated efficiencies show a better performance for the resonant converter, while for the DAB converter, the switching losses on the LV side represent a large contribution to the overall losses, despite the utilization of MOSFETs in these bridges.

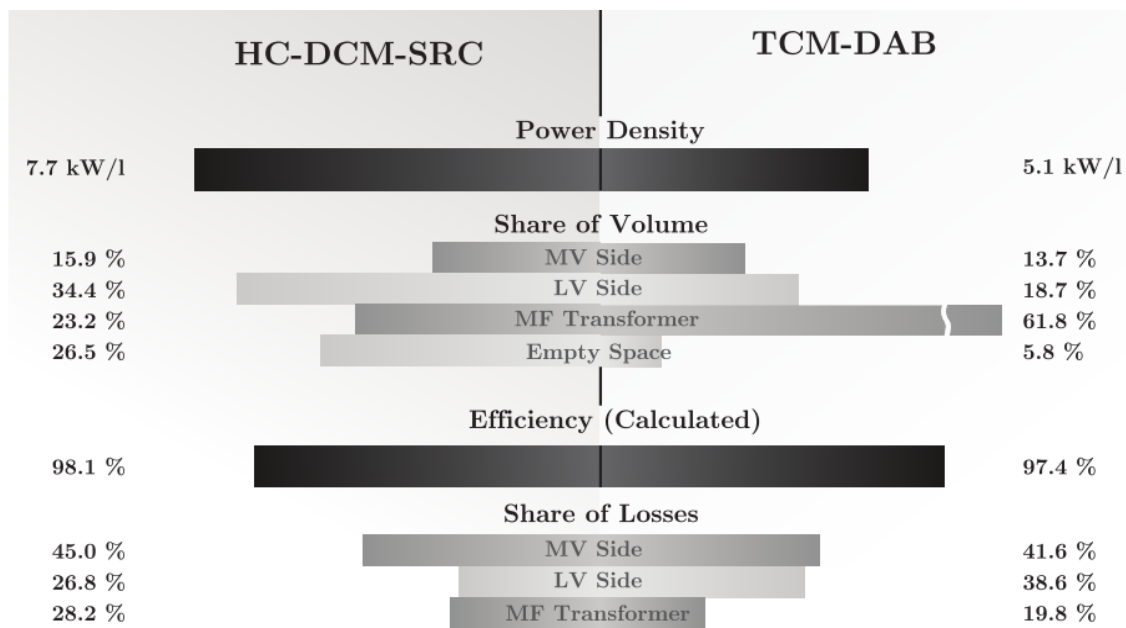


Fig. 63 Summary of power densities and efficiencies at rated power of both designed converters and the respective volume and loss shares [17]

Control

The main control units are based on a DSP/FPGA platform integrating various functionalities such as 12 PWM channels, 32 general purpose input/output signals such as 12 PWM channels, 32 general purpose input/output signals, 16 ADC channels and trip zone circuitry. The control platform are TMS320F28335 floating point DSP from TI and the LFXP2-5E-T144/TNN144 FPGA from Latiice. This control unit is built on a PCB which additionally contains all voltage regulators and circuitry for all analog inputs. An interface board is required in order to link the control board with the respective gate signals, feedback signals and analog inputs.

The software programmed in these platforms allows to independently adjust the three TCM-DAB control signals: the phase shift, the MV side and LV side duty cycle. Other functionality such as burst or continuous operation are also supported in order to safely test the converter. In case of the HC-DCM-SRC, only duty cycle control is provided. According to the described operation of this bridge, one side of the converter is left uncontrolled.

Protection

To be investigated further.

Valve complexity

To be investigated further.

vi. Traction SRC 2007

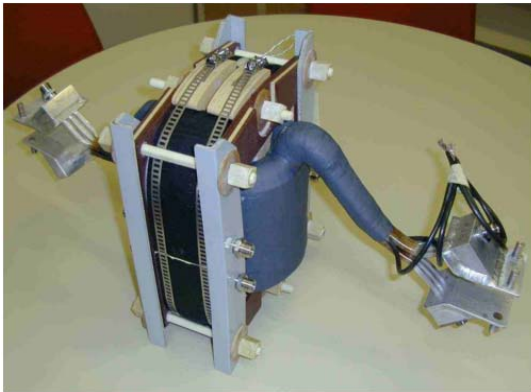


Fig. 64 Photo of MF prototype [16]

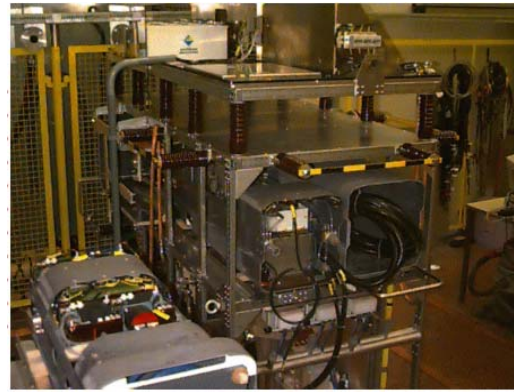


Fig. 65 Lab setup [16]

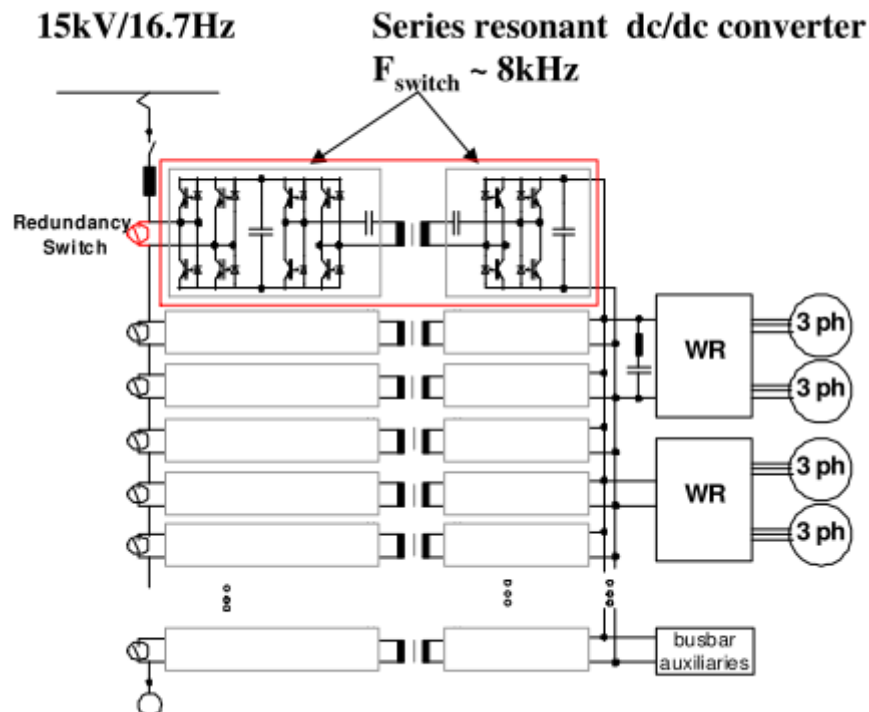


Fig. 66 Converter circuit used in demonstrator [16]

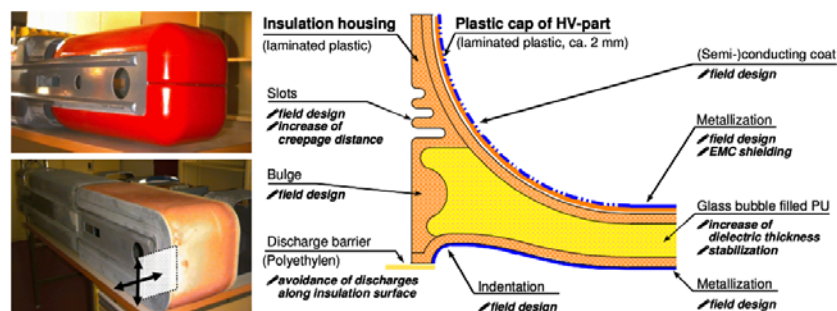


Fig. 67 Insulation system, the right side is a schematic cut through the housing section marked with white arrows in the bottom picture of the left side

Topology

This medium frequency topology is connected to a 15 kV Catenary voltage and it consists of modular system with 8 subsystems and a total power of 3[MW]. The topology is based on dual active series resonant converters switching at 8 KHZ. MV and LV sides have both 3.6 kV. Compared to a classic converter, the quantity of IGBTs and Gate Drive Units is significantly increased by a factor of 2.6 or even 4.5 in case of a redundant system. Due to the increased number of components the reliability is expected to decrease. The DC/DC converter in combination with a low transformer stray inductance and operating in series resonant mode guarantess a fast and hard coupling of the primary and the secondary dc link without any close loop control. Neither current nor voltage sensors need to be used for controlling the power flow. Regarding dimensions, the 3[MW] MF system consisting of 8 subconverter/4 double subconverter leads to dimensions of 180cm width, 40cm height and 240 length.

Transformer

A transformer ratio of 1:1 offers the possibility to use the same IGBT technology for the primary and the secondary bridge. The los transformer stray inductance in combination with the small losses in the dc/dc converter leads to a well damped resonance with limited over-currents. The resonance capacitors become very small and have similar specifications like GTO snubber capacitors. Nano-crystalline core is used. The low leakage inductance is realized by an encapsulated, coaxial winding arrangement with the primary winding between two layers of the secondary windings. That arrangement realized a homogenous electrical field distribution between the primary and the secondary windings. This insulation, which has to withstand the full line voltage, is based on an insulation system known from medium voltage motors. An 8 kHz prototype transformer was successfully tested concerning insulation test, partial discharge test and power transmission up to 500 KW. The weight of the prototype is 18 [kG] only .Special terminals realized combined water and electrical connections of the windings. The two cutted cores are colled by flat water coolers from both sides. The main inductance of the transformer which guaranties the ZVS of the converter can be designed by a defined air gap between the cutted cores.

To avoid partial discharge through the field between components and ground a conducting/semiconducting housing covering the standard components on the HV side is introduced. Since the cover does not have sharp edges but rounding, the field does not have local peaks. To reduce the necessary clearance between cover on HV potential and housing ground, an insulation material is introduced. Glass bubble filled PU with a thickness of a few cm was the choice, allowing an increase of dielectric strength.

Semiconductors

Different lab prototypes have been realized in order to investigate semiconductor losses of 3.3 kV, 4.5 kV and 6.5 kV IGBTs, the steady state and the dynamic performance of the converter. A compromise between noise, transformer size and semiconductor losses lead to an operational frequency of 9 kHz.

Cooling

Direct water cooling of the transformer winding by using deionized water and rectangular aluminium profiled tubes was realized. Nearly all components are directly cooled with deionized water, the semiconductors having their water cooler on the potential of their dc-link.

Control

To be investigated further.

Protection

To be investigated further.

Valve complexity

To be investigated further.

vii. Traction DAB and LLC 2012



Fig. 68 Photo of SRC MF prototype

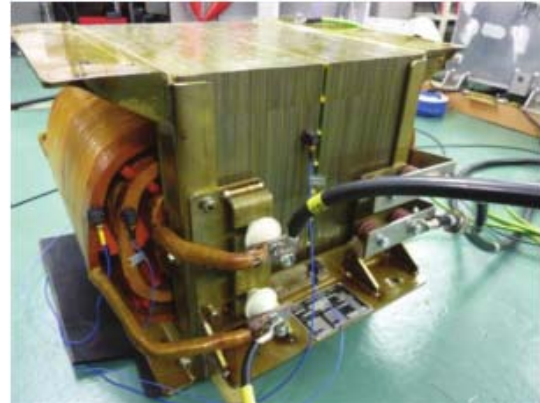
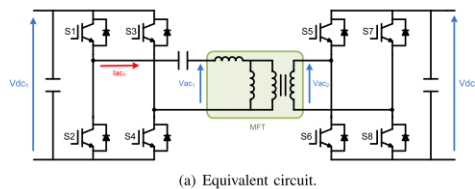


Fig. 69 Photo of DAB MF prototype

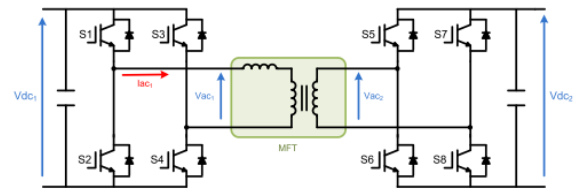


Fig. 70 Converter circuit used in [22]

Topology

This work presents the application of a MF transformer design methodology applied to a 400 kVA transformer, intended for railway application. In order to validate the proposed MF transformer design methodology in a full scale application, a 400 KW isolated dc dc conversion system intended for multi voltage traction application has been defined. In both conversion systems the same converter hardware has been used. The only difference lies on the control strategy and on the passive elements. Input voltages was set to 3 kV and the load consisted on an inverter supplying a motor. It has been pointed out the need to evolve from a SRC topology to a LLC one in order to avoid ZCS losses in the IGBT

Transformer

Two prototypes have been developed: a 1 KHZ silicon steel transformer and a Dual Active Bridge , and 5 KHZ with a nanocrystalline core and a Series Resonant Converter, which later evolved towards a LLC topology. The second prototype has weight reduction of 85% compared to the first one. Initially for the DAB transformer, iron-based amorphous allow was the choice. But, due to its high magnetostriction value and therefore unacceptable acoustic noise for this frequency range it was not the option.

Semiconductors

The power semiconductors on both HV and LV sides of the MF transformer are used in a full bridge configuration. In the HV side 6.5 kV IGBTs are used, while in the LV side 1.7 kV one

Control

To be investigated further.

Protection

To be investigated further.

Valve complexity

To be investigated further.

viii. Traction Cycloconverter 2009

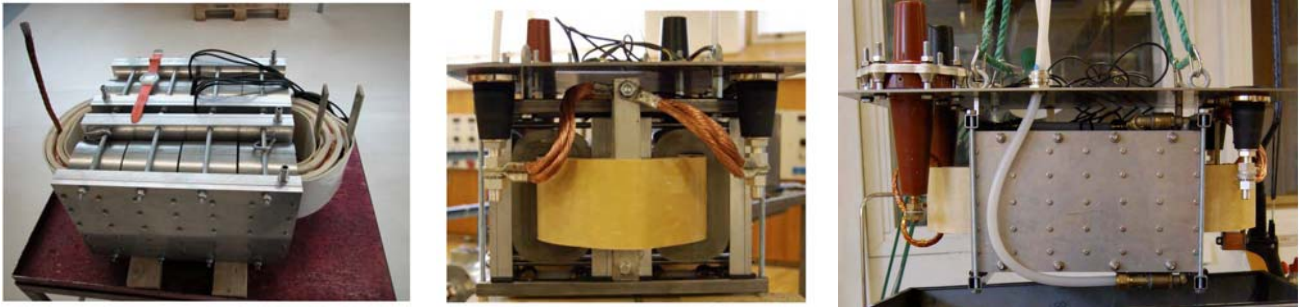


Fig. 71 Photo of MF transformer prototype

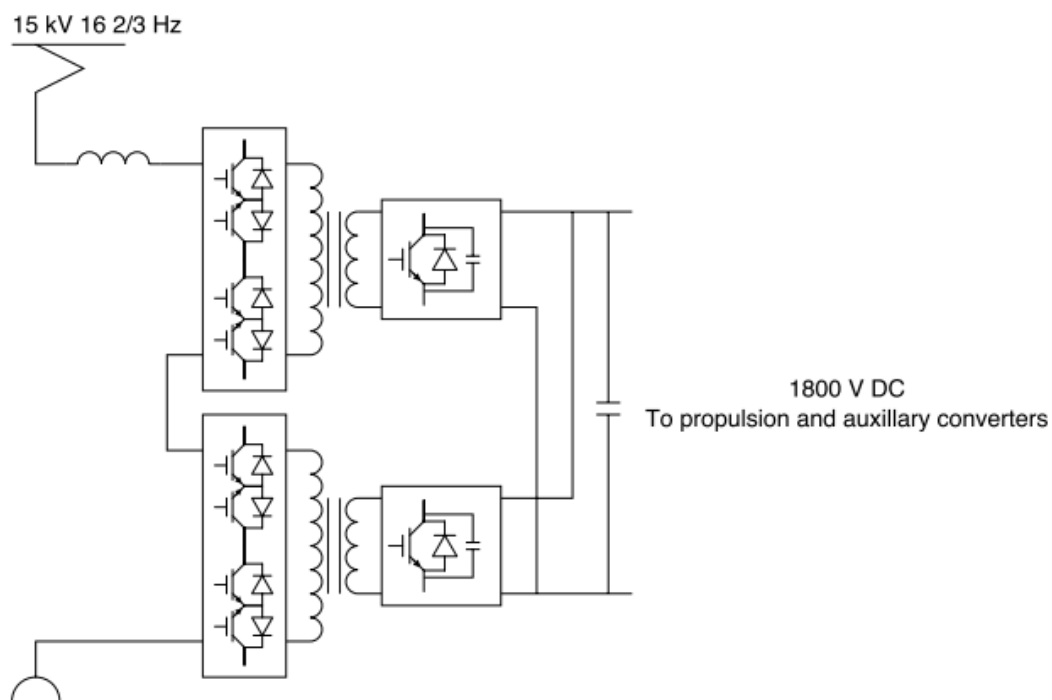


Fig. 72 Converter circuit used in [15]

Topology

In this work a 170 kVA transformer prototype operated at 4 kHz has been developed and tested. A transient thermal model was developed and verified experimentally. Simulations indicate that the overloading capability of the transformer is comparable to a conventional traction transformer. During optimization of the prototype, a full scale transformer for a 1MVA converter system was considered. The design was then scaled down to be suitable for laboratory work. The voltage rating was reduced to one third by reducing the number of turns and height of the transformer. The current loading was slightly increased to fit the design to commercially available standard cores. The transformer prototype maintains approximately the same electrical per unit properties and thermal properties as the full scale transformer.

Transformer

Regarding transformer requirements, high voltage slope stress the inter-turn insulation and the insulation system in the transformer has to be adapted accordingly. Depending on the structure of the converter cell, the voltage stress of the high voltage insulation may be beyond 30 kV with voltage slopes around 50 kV/us. The voltage slope is a compromise between switching losses in the converter and the stress on the transformer insulation as well as EMC issues. Stranded wires can be used to reduce proximity and skin effects in transformers. Litz conductors were used.

The insulating material needs to have good dielectric properties as heat transfer properties. It can be flowing like liquid mineral oil or synthetic oil, paper and pressboard impregnated with oil or dry insulating materials like epoxy.

If no cooling ducts are arranged, heat must be transported from the inside of the transformer windings and core by conduction of the heat. Regarding transformer geometry, the size of the MF transformer becomes very small compared to the voltage level. Therefore, it is important to design the layout of the HV winding and insulation as simple as possible.

High flux density in the cores results in very high loss density in cores. Therefore, the cores are clamped together using water cooled plates.

The windings were prefabricated using Litz wire for the primary winding and a two turn foil winding for the secondary winding. The cores, which are made from an amorphous material are clamped around the windings by water cooled heat sinks. Oil impregnated paper was chosen for the prototype due to its low dielectric losses and high insulation capabilities.

Control

To be investigated further.

Protection

To be investigated further.

Valve complexity

To be investigated further.

d. Solid State Transformers

I. SST SiC 2011



Fig. 73 SiC Enabled SST Prototype

Topology

In this work, the main focus was on 10 kV SiC Mosfets and Schottky diodes, with application on solid state transformer. A custom designed SST (13.8 kV to 465V) was demonstrated with the state of the art SiC modules up to 855 kVA operation and 97% efficiency. Softswitching at 20 kHz, the SiC enabled SST represents a 70% reduction in weight and 50% reduction in size, compared to a 60hz conventional transformer.

Semiconductors

The Mosfet device exhibit excellent static and dynamic properties with encouraging preliminary reliability. 24 MOSFETs and 12 Schottky diodes have been assembled in a 10 kV half H-bridge power modules to increase the current handling capability to 120A per switch. In addition to performance, the 10 kV devices seem to be robust too. At 150deg for 1000hrs, both devices demonstrate excellent 10 kV blocking and forward conduction stability. The 10 kV half H-bridge module is based on a commercial 140x190 mm² Si IGBT module footprint with low inductance bus-work and appropriate creep/strike distances and encapsulation to permit 10 kV operation. The half H-bridge configuration has an upper and lower switch, each capable of 120A operation in the on-state. In order to suppress the device degradation due to the turn-on of the body diode, low voltage Si Schottky diodes are placed in series with the SiC Mosfets to prevent reverse conduction.

Transformer

The transformer is built around a nanocrystalline core.

Cooling

Proper cooling is achieved via commercial of the shelf liquid cooled chill plates.

Control

To be investigated further.

Protection

To be investigated further.

Valve complexity

To be investigated further.

II. SST DAB 2011

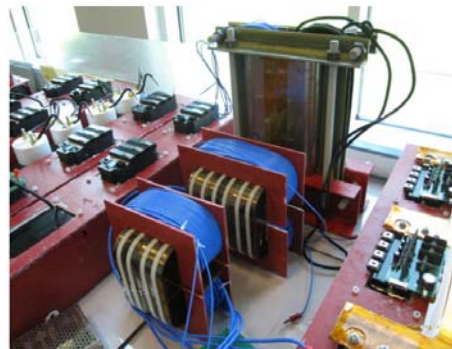


Fig. 74 SST Prototype

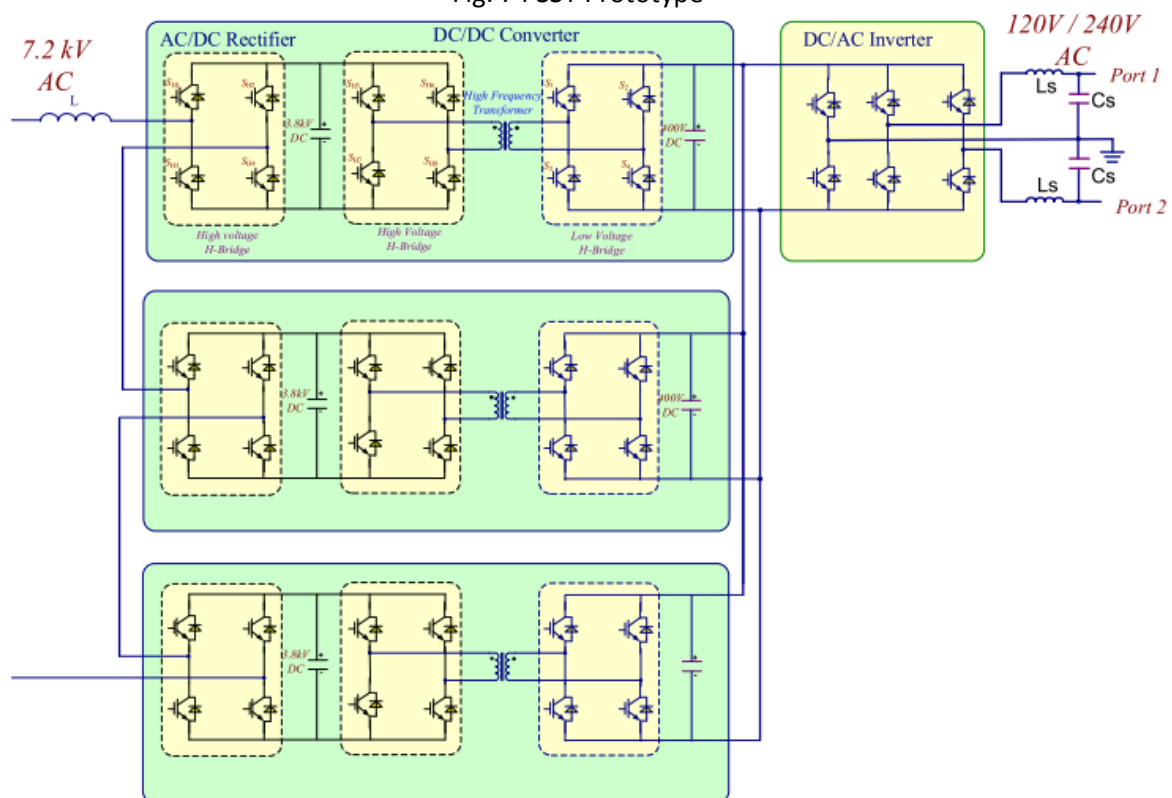


Fig. 75 Converter circuit used in demonstrator [24]

Topology

This work presents the design and hardware implementation of a 20 kVA silicon based SST. A topology of 7 level cascaded H bridges is deployed for the high voltage rectifier stage. A new compact voltage sensors with high voltage isolation capability was designed. 1080 hz is the switching frequency for the rectifier stage, 3 kHz for the DAB stage.

Transformer

The transformer has a turn ratio of 9 to 1. 3 versions of 7 kVA HV-HF transformers were built and tested. The transformer in each stage provides voltage transfer between 3.8 kV in primary side and 400V in secondary side DC link. Metglas, amorphous alloy cores were used.

Semiconductors

A 6.5 kV 25A dual IGBT module has been customized packaged specially for this high voltage low current application. The proposed 20 kVA SST is designed to convert 7.2 kV primary AC voltage to 120/240AC for utility applications and 400V DC for connecting renewable sources and batteries

Control

To be investigated further.

Protection

To be investigated further.

Valve complexity

To be investigated further.

III. SST DAB 2010

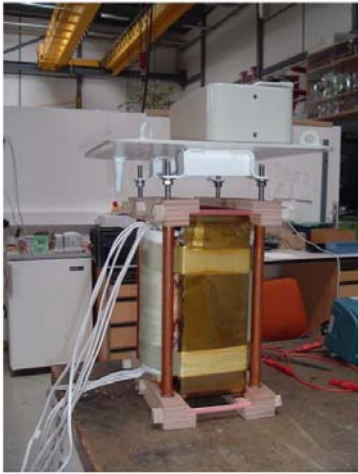


Fig. 76 Uniflex - Photo MF Transformer

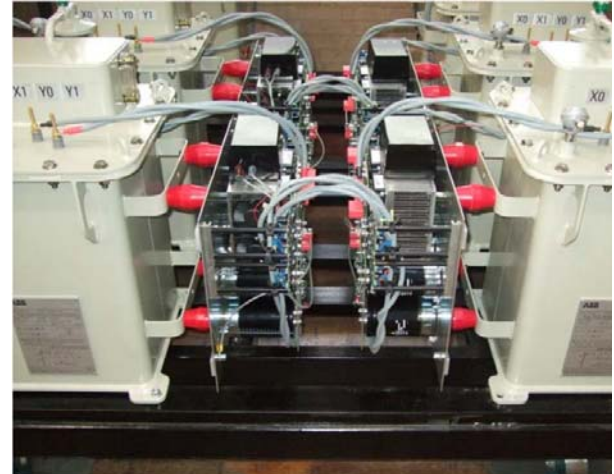


Fig. 77 Photograph of 25 kVA transformers with the power electronics in place on the converter baseplate

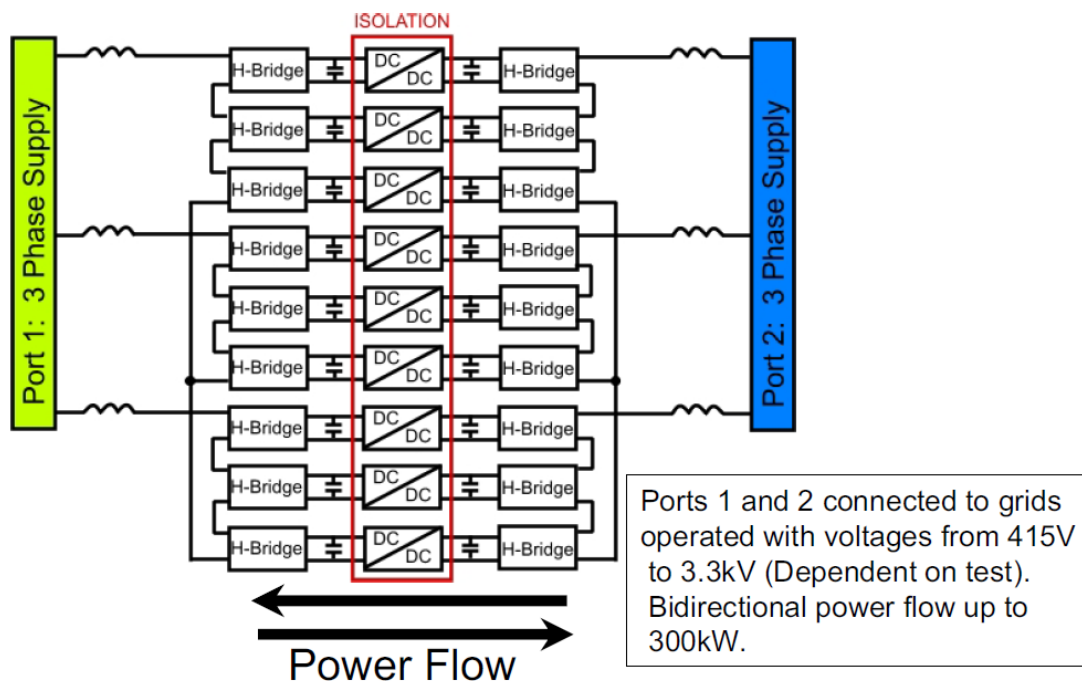


Fig. 78 Converter circuit used Uniflex demonstrator [25]

Topology

Modular DAB CONVERTERS with medium frequency isolation were used. Structure allow the converter to be arranged in parallel and series combinations to meet application power levels. Bidirectional power flow up to 300 KW, with voltages up to 3.3 kV. The work was focused more on functionality and not hardware design.

Transformer

MF transformer is designed by ABB Secheron, Switzerland. It operates at 2 kHz, uses an amorphous core and litz wires.

Cooling

Oil immersion for the transformer and forced air cooling used on H-bridges.

Control

Following control strategies were investigated:

- Synchronous reference frame dq control
- Predictive Control
- Stationary reference frame control
- Natural reference frame control

Protection

To be investigated further.

Valve complexity

To be investigated further.

e. Medium Voltage Distribution

I. SST DAB 2014

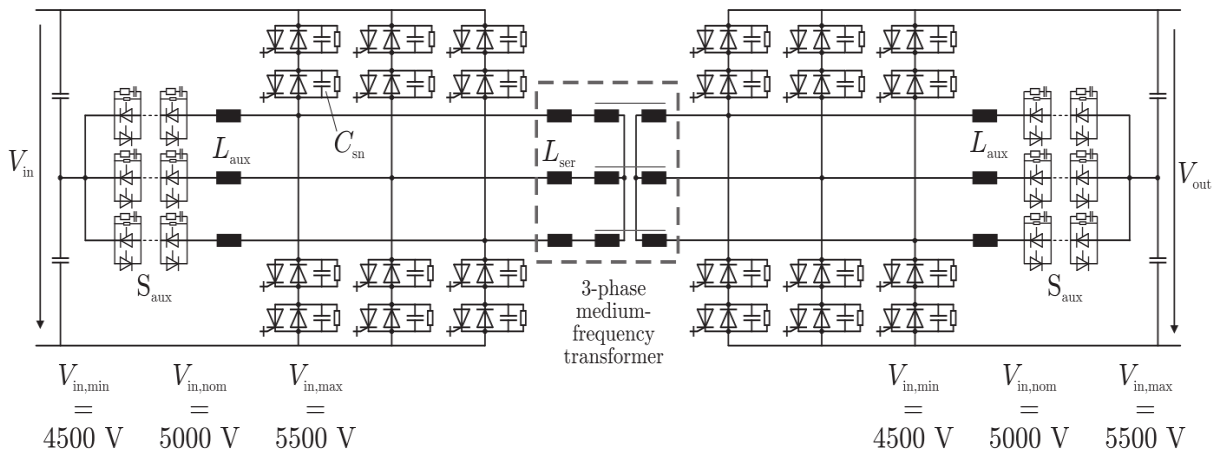


Fig. 79 Converter circuit used in RWTH Aachen [2]

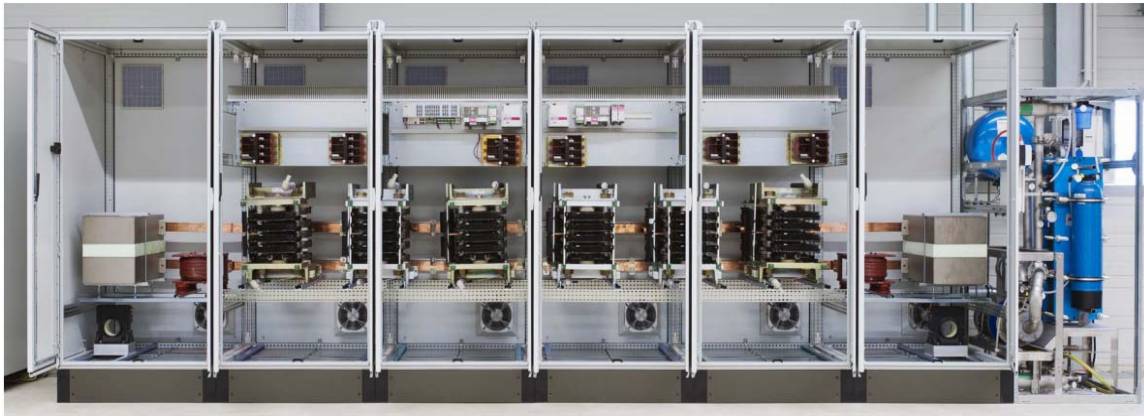


Fig. 80 RWTH-Photo of MV DC/DC Demonstrator

Topology

At the E.ON Energy Research of the RWTH Aachen University a demonstrator for a 5[MW] medium voltage dc dc converter is constructed. A three phase dual active bridge is used as main topology. In this work, it is discussed which are the optimal switching devices, whether IGBTs or IGCTs and a further improvement using a Dual ICT is evaluated. Soft switching operation using lossless snubbers is employed. The DAB3 has been presented first in 1991. It consists of two three phase bridges interconnected with a three phase transformer. Both bridges are operated in fundamental frequency modulation. A six step voltage waveform is applied to the transformer. Power is transferred by setting a load angle α between the primary and secondary bridge. Switching frequency of power electronic switches is around 1 kHz. In a large operation range, the DAB3 features soft-switching operation. The nominal input voltage of the demonstrator is 5 kV. To prove the concept and to ease the commissioning, the nominal output voltage is also 5 kV. Therefore, the input and output dc link can be connected together to circulate the energy. Therefore, an expensive high power load is unnecessary and the dc power supply only needs to compensate the losses. The demonstrator is commissioned in three stages. First, the converter is operated with a single phase transformer as single phase DAB. Afterwards, the series connection of two IGCTs and the voltage balancing are implemented. Finally the converter is operated with two additional transformers as three phase DAB. The commissioning of the 5[MW] demonstrator

results in a comparison of a single phase and a three phase dual active bridge. Transformer saturation, lower dc link currents and decreased turn off losses are important reasons, making the three phase dual active bridge superior in high power medium voltage applications.

Transformer

There is a high focus on the suitable transformer core materials. Regarding the medium frequency transformer, for the considered power rating and operation frequency, silicon steel and amorphous iron are suitable core materials. To apply nanocrystalline or ferrite core materials economically, the operation frequency is too low, being limited by the power electronic devices, is too low. Constructing the MVA transformer for the demonstrator, a single phase transformer has been build first due to the novelty of the design. The transformer is made of silicon steel with a sheet thickness of 0.18mm. ThyssenKrupp Electricl Steel provides sheets down to 0.18mm. The core material is well known, comparatively cheap, offers low magnetostriction and acceptable core losses at the given frequency. The casted windings are made of litz wire. The weight of the transformer is 600[kG] and the dimensions are 0.72 x 0.65m x 0.48m.

Semiconductors

Turn on losses of the switches are eliminated due to ZV/ZC switching, while the turn off losses can be reduced by snubbers. For this application, IGBT and IGCT are considered. In general, one could suggest that thyristor based devices are advantageous in soft switched converter as they offer lower conduction losses than IGBTs. By simulation, the semiconductor losses are compared in a DAB3 application, with PLECS.

4.5 kV IGCT are used, with two devices per inverter arm connected in series. The IGCTs offer lower forward voltage drop as well as lower switching losses than the StakPak IGBTs. Efficiency increases slightly with the use of IGCTs. The power electronic switches are “5SHY 3545L0001” IGCTs provided by ABB Switzerland. Apart from slight modifications, the same PEBBs are applied in commercial ABB ACS 6000 inverters.

Cooling

The IGCT and diode stacks are all water cooled.

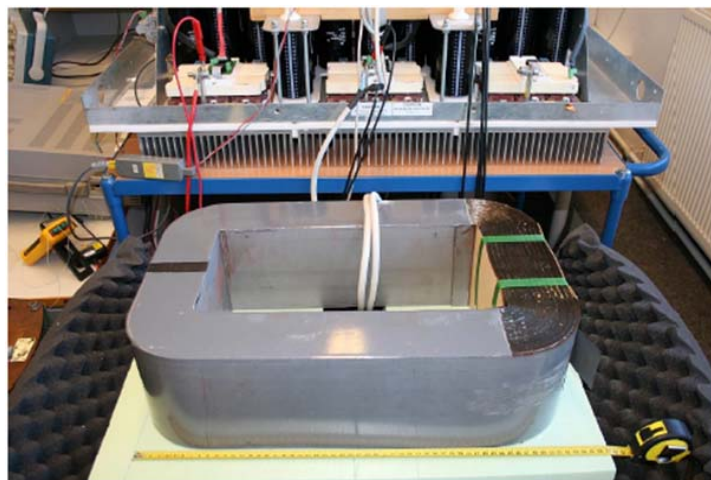
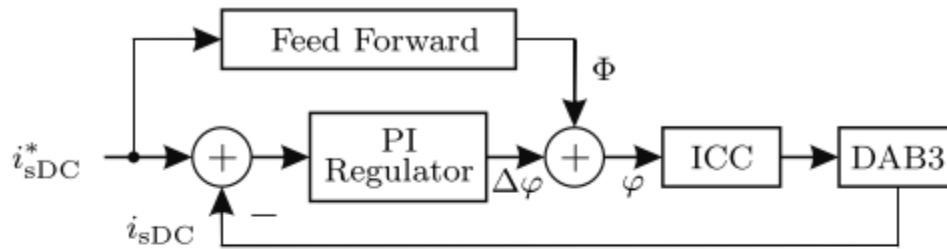


Fig. 81 Amorphous Iron Core [5]

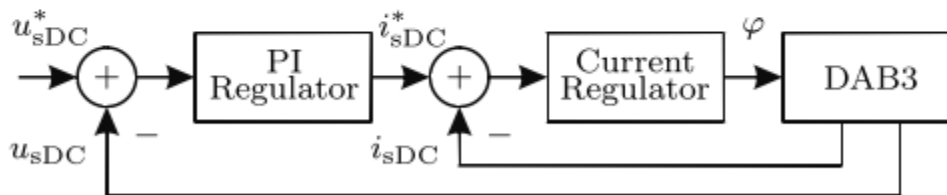
Control

The control of a DAB3 is implemented on a control hardware provided by ABB, on a unit with the model number PC D247. The control unit features a PowerPC intended for tasks with a cycle time in the range of 100 to 1000us. The build-in Xilinx Spartan3 FPGA performs quicker tasks at time frames down to 25ns. The power PC and the FPGA exchange data through a dual ported RAM.

Considering the DAB3 application, the voltage and current control is implemented on the Power PC. The FPGA performs the gate driving of the IGCTs, implementation of dead time and load angle regulation.

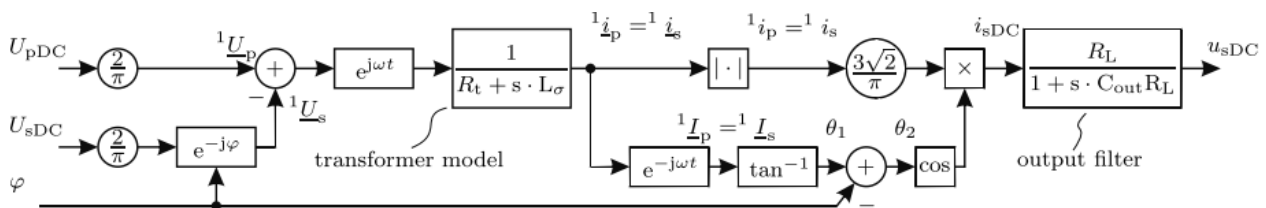


Closed-loop current control



Closed-loop voltage control

Fig. 82 DAB Closed loop control



Dynamic FHA model

Fig. 83 DAB First Harmonic Aproximation Model

- The three phase DAB is model using two different approaches: a state space averaging approach and the first harmonic approximation (Fig. 83)
- From the modelling work the instantaneous current control ICC was developed
- Based on the ICC, a voltage controller is presented.
- The ICC sets an arbitrary reference current within one third of switching period. Consequently, when the parameters of the transformer are known, the current control can be made very fast

- A feed-forward controller translates a new reference current directly into the corresponding load angle. The controller applies according to the power equation of a DAB3, the control angle. A feedback control is mandatory to provide high precision. This can be for an example a PI regulator
- Applying the fast current regulator achieved through the ICC, a closed loop voltage control can be implemented in a cascaded manner. With the cascaded control structure, a robust voltage controller is achieved (Fig. 82)

Protection

To be investigated further.

Valve complexity

To be investigated further.

5

5. Medium Frequency Transformers

A transformer is mainly composed of winding and core parts. The characterization of both parts is widely analyzed in the literature. However, usually there is a lack of global comparison and validity studies, mostly in medium/high frequency applications, finding hard to compile information from widely scattered data.[40]

The transformer is ideal if the magnetic coupling is perfect and the energy transfer lossless, fulfilling the following suppositions:

- The resistance of the winding is zero, there are no losses in the windings
- The coupling factor is 1, there is no leakage inductance in the transformer
- The permeability and the resistivity of the core are infinite, there are no losses and there is no energy stored in the core

Transformer characterization is essential to create optimal energy transfer devices, both in electromagnetic and thermal fields. In medium frequency dc-dc converters the isolation transformer is excited with non-sinusoidal current and voltage waveforms, requiring more complex expressions. The frequency dependent behavior of magnetic material and the redistribution of magnetic fields with frequency, as well as, the utilization of different conductor types to face detrimental frequency effects, has to be correctly characterized to create optimized medium-frequency transformers. Besides power loss characterization, an optimized transformer design requires specific thermal characteristics in order to develop an efficient cooling system.[40]

a. Core

In conventional 50/60hz transformers, typical used core materials are silicon or nickel-steel. The losses of these materials drastically increase at high frequencies. Before the use of amorphous and nanocrystalline, ferrite dominated the market of magnetic cores for power electronics, showing high electrical resistivity and low eddy currents. The application of ferrite is limited to low power and voltage because of small

saturation flux density (B_{sat}). The main material requirements for transformers at high frequency and power are low core loss, high saturation flux density and high continuous operating temperature.[41]

Nanocrystalline and amorphous are the most well-known materials in this case. As, it can be seen in Tabel 5 nanocrystalline is the best choice for high frequency and power applications due to high B_{sat} and low losses.

Magnetic material		$B_{sat}(T)@25^{\circ}C$	KW/m^3 0.1T,100 kHz	Continuous Oper.Temp.
Ferrite Ferrixcube	3C93	0.52	49	140
Nanocrystalline Vacuumschmelse	Vitroperm500F	1.2	73	120
Fe-Amorphous Metglas	2605SA1	1.56	1377	150
Silicon steel JFE	10JNHF600	1.87	1757	150
Tabel 5 Properties of magnetic materials				

Beside the materials, core configuration is an important issue in medium frequency transformer design. In literature, there are mainly four concepts: core type, shell type, matrix and coaxial winding transformer. Core type is constructed by single magnetic core with windings wound on both legs. Generally, two LV windings are in parallel and HV windings are around LVs and series. In shell type, two magnetic cores encircle one single winding. Matrix transformer topology is a combination of shell and core types and is based on several parallel magnetic cores with LV windings on the outer legs of the core and one central HV winding around the middle legs. The main advantage of core type is the two parallel LV windings resulting in reduction of the height of transformer. Nonetheless, core material is surrounded by the windings and due to poor thermal conductivity of insulating materials and also higher sensitivity of magnetic materials, shell type has better performance in thermal point of view.

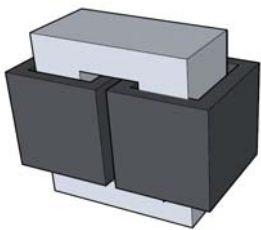


Fig. 84 Core type transformer

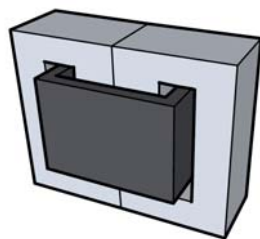


Fig. 85 Shell type transformer

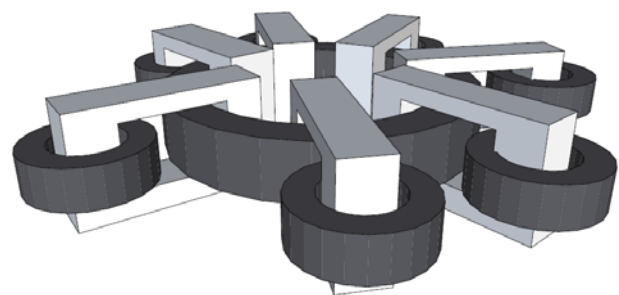


Fig. 86 Matrix type transformer

Matrix transformer seems to have both advantages of shell and core types, but two main drawbacks restrict its applications. Firstly, using separated core units results in higher volume and weight and increases the total loss and cost. Secondly, primary and secondary windings are separated and wound on different legs leading to higher leakage inductance.

Demonstrator	Core		Windings	Isolation	Power [[kW]]	Fswitching [KHZ]	Cooling	Weight [[KG]]	Turns ratio	Voltages
	Material	Type								
ABB1	Si-Fe	C-core		For 15 kV	75	0,4	Oil	50%ofPT	1:1	1.8 kV-1.8 kV
ABB2	Nanocrystalline	Co-axial	Lm=25mh, Lstray=3uh Al and Copper	38 kV	350	10	De-ionized water	<50	1:1	3 kV-3VK
ABB3	Nanocrystalline	C-core	Litz wires	For 15 kV	150	1,8	Oil ODAF	-		3,6 kV-1.5 kV
Siemens	Nanocrystalline	C-core	8<Nt<16 Aluminium	Nomex, oil 25 kV	450	5,6	Core-oil De-ionized water for AL conductors	<60		
ETH1	Ferrite	Shell	Litz wires	PTFE	166	20	Air cooled	-	3:1	
ETH2	Nanocrystalline	Shell	Litz wires	Mica Tape	166	20	Water	-	5:2	
Bombardier	Nanocrystalline	Co-axial	Lstray=2,3uh	Full line MV motors Glass bubble filled PV	400	8	Water	<20		
Ikerlan 1	Si-Fe	Shell	Ls=390uh	18 kV	400	1	Dry	<460	4:1	
Ikerlan 2	Nanocrystalline	C-core	Ls=10uh	18 kV	400	5	Dry	<60	4:1	
KTH	Amorphous	Shell	Litz wires	Epoxy 30 kV Oil paper	170	4	Oil	<150	15:1	
GE-SST	Amorphous	-	-		1000	20	-	-	-	
FREEDM SST	Amorphous	C-core	Lm=235mh Litz wires	15 kV pfa	20	3	Dry	<13	9.5:1	3.8 kV-0.4 kV
Uniflex SST	Amorphous	-	-	-	300	2	Oil	-	-	
RWTH Aachen	Si-Fe	C-core	Litz wires	BIL of 12 kV	2200	1	-	600	1:1	

Tabel 6 List of medium frequency transformers

b. Windings

There are important parameters needed to be taken in consideration when designing the windings: utilization of winding area, low loss, good thermal behavior and proper electrical isolation. The conductor type is of important relevance too. Large currents will lead to big conductor cross section. Eddy currents at high frequencies will force smaller diameters. Therefore, Litz wires are used, containing separately insulated wire strands twisted or braided together. To equalize the flux linkage of all strands and have the same current through them, these isolated strands take all the possible positions in the cross section of the conductor. Different topologies of Litz wires are presented in Fig. 87. The use of such conductors results in better utilization of winding space and greater copper density.

Thin foil conductors are used to reduce the eddy currents in low voltage winding and to have maximum filling factor. Each turn of the foil conductor forms an entire winding layer.

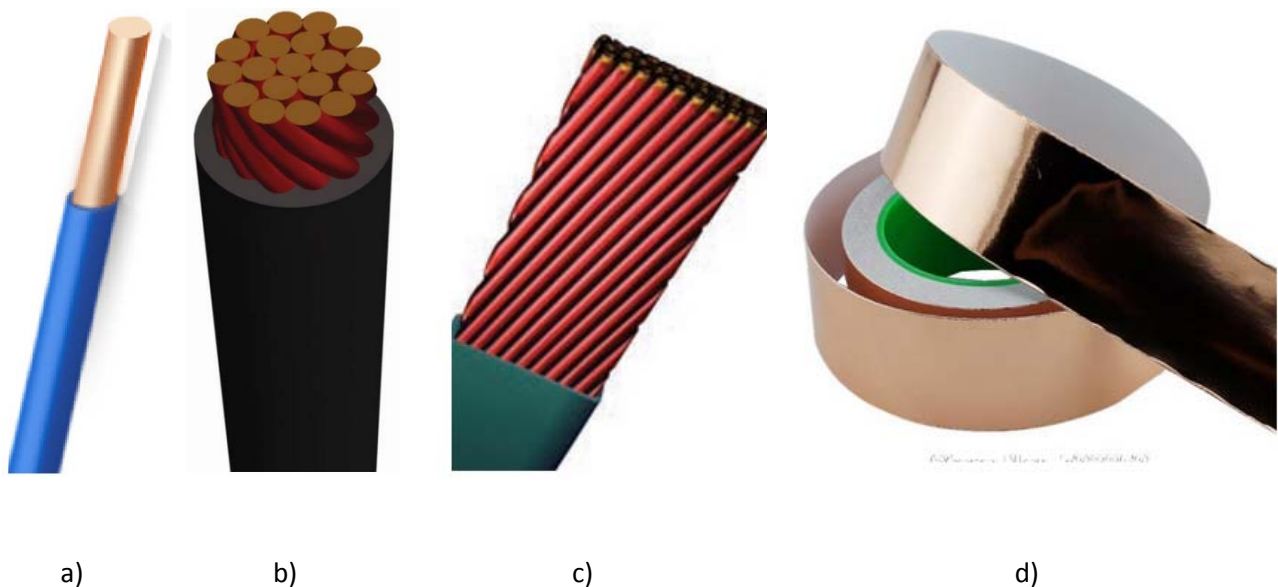


Fig. 87 Conductor topologies a) Solid and b) Circular Litz, c) Rectangular Litz and d) foil

c. Insulating Material

Insulation is another important element in winding construction and the main role is to provide high voltage insulation between the high and low voltage windings and to transfer heat dissipated in the windings and the core. The insulation should have three main properties: high dielectric strength, low loss and high maximum operating temperature. High dielectric strength is required to have smaller isolating distance and makes the transformer more compact. The dielectric losses of the insulation should be as low as possible. Common insulating materials are : epoxy, micares , pvc[41]

d. Design considerations

- In low power applications, transformer design is done using look-up tables,
- When designing high power medium voltage transformers, focus has to be on : selection of magnetic material, windings, conductors size
- Design criteria is based on weight, efficiency, cost, isolation and temperature rise
- The final temperature rise is the final design criteria and it will decide maximum allowed losses.
- There are three main areas of losses: core, windings and dielectric loss.
- The operating temperature will be an important design parameter. Thus, it's necessary to calculate and implement thermal models. Basically, there are three different categories for thermal modeling network.
- The first group works with analytical approaches considering the flow of heat inside each element and solves differential equations in each direction to find unidirectional steady-state heat conduction.[40]
- The second group deals with an equivalent nodal network which describes the thermal behavior by a circuit including linear elements. In this group, each part of the transformer is modeled as one single node and all the generated losses will be concentrated at that point.
- The last category is related to FEM based approaches which calculate spatial loss dissipation and resulted temperature using finite element software and approaches. This method is rarely used by designers due to its high complexity, long simulation time and large amount of required data [41],[42].

e. ETH Zurich transformer prototypes

Interesting work and research has been done at ETH Zurich, where three concepts for transformers (with different constructions and isolation mechanisms) have been investigated and compared in terms of power density, losses and volume. The core material in all cases is the VITROPERM 500F. [18]

The design of U-core, shell-type and matrix transformer was presented with different isolation mechanisms. For the winding losses, HF skin and proximity effects were included and in the case of the core losses, non-sinusoidal effects of the applied voltage were also included [43].

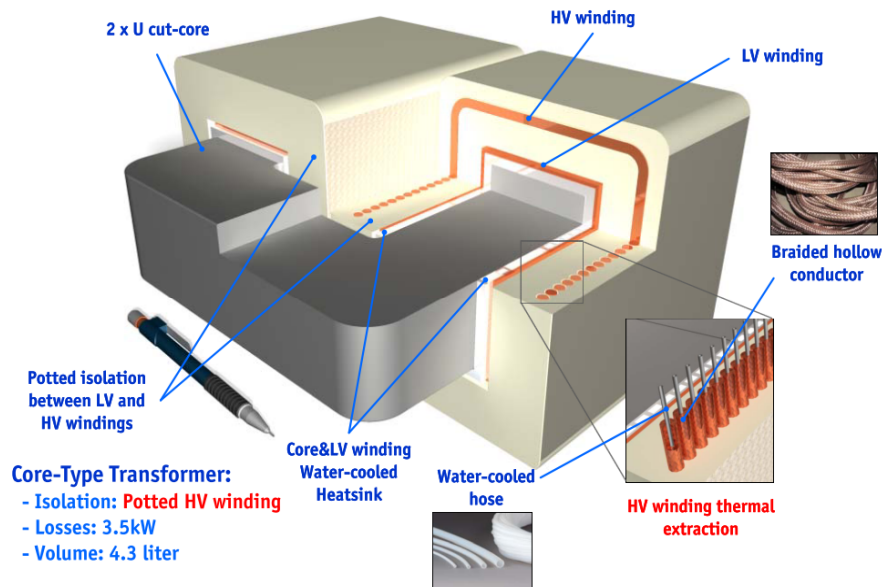
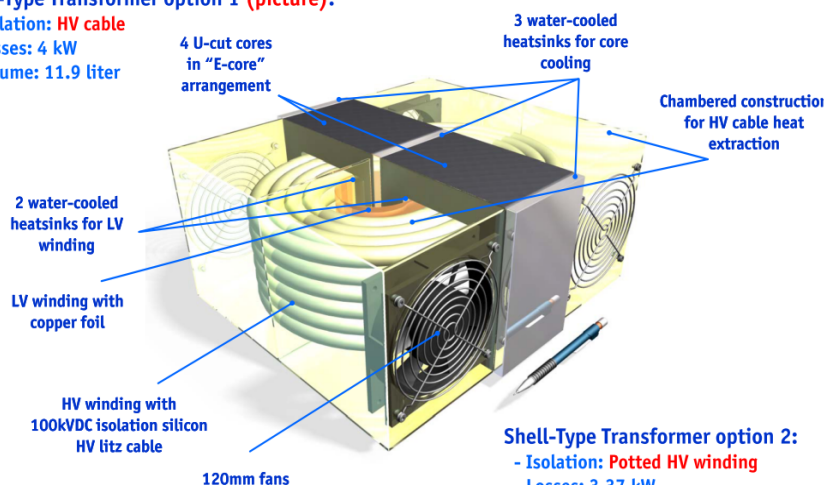


Fig. 88 ETH Zurich U-Core type transformer

- The U core transformer is based on a single magnetic core with windings in both legs of the core. A 3d CAD design of the transformer is presented in Fig. 88.
- Regarding winding arrangement, the LV winding is built with two HF optimized copper foils of 0.3mm. Each leg of the core has one of these 4-turn LV windings which are then parallel connected. The HV winding is built with a litz wire of 840 strands of 0.1mm each. Two windings of 26 turns each are wound around the LV windings and then series connected.
- Regarding isolation, a 20mm dry isolation layer is placed between primary and secondary. The distance is required to integrate the series inductance within the transformer's leakage inductance. A 300 kV isolation is achieved using the Micares material. The use of a litz wire optimized for HF operation further reduces the transformer losses which are 3.5 KW at 1[MW].
- Regarding thermal management, water cooled heat sinks are placed on one side against the core surface and on the other side on the LV winding surface. For the HV winding, water cooled heat sinks are placed on the outer face of the cast isolation where the heat is transferred through the outer isolation layer.

Shell-Type Transformer option 1 (picture):

- Isolation: **HV cable**
- Losses: 4 kW
- Volume: 11.9 liter

**Shell-Type Transformer option 2:**

- Isolation: **Potted HV winding**
- Losses: 3.37 kW
- Volume: 3.5 liter

Fig. 89 ETH Zurich Shell type transformer concept

- The shell type transformer consists of two pairs of U cores arranged in E-core configuration as seen in Fig. 89.
- For winding arrangement, the LV winding is built using an HF optimized 0.5mm thick copper foil wound around the middle leg formed by the two pairs of U cores. The HV winding is then placed around the LV winding using a 133 strand HV cable.
- For isolation, the HV cable is able to withstand 100 kVDC isolation, using a silicon based material [44]. The use of this isolation mechanism significantly reduces the complexity of the construction.
- Because of the HV isolation requirements, the volume of the transformer increases radically.
- For thermal management, water cooled heat sinks are placed between the core and the windings for the heat extraction of the core and LV windings. Additional heat sinks are placed in the outer face of the core to extract the core heat. Two chambers are created by an additional enclosure to create independent ventilation ducts through which respective 120mm fans blow to cool the HV winding. The distance between each HV winding turn must be adjusted to enable the required heat extraction.
- Another shell type transformer was designed considering a litz wire for the HV side winding with a potted isolation as with the U-core transformer. The volume is reduced from 11Liters to 3.5liters and the losses to 3.37 KW with this isolation type.

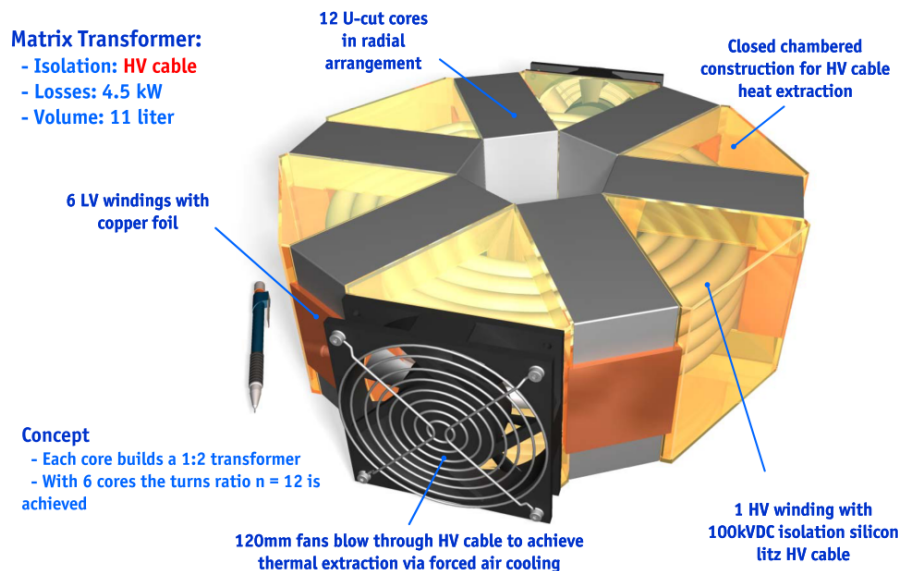


Fig. 90 ETH Zurich Matrix type transformer concept

- A matrix transformer arrangement is presented in Fig. 90, where several magnetic cores are interwired with series/parallel conductors.
- There are 6 magnetic cores; each with a LV winding of 8 turns of a HF optimized 0.3 mm copper foil. Through all 6 cores, 16 turns of a HV cable are wound.
- The main advantage of this transformer construction is the requirement of less HV cable turn in comparison to the core and shell type transformer.
- By using separated magnetic core units, a magnetic paralleling of semiconductors is possible, enabling a better current distribution among the devices.
- For isolation, the HV cable reaches an isolation level of 100 kVDC using a silicon based isolation material.
- Regarding thermal management, water cooled heat sinks for each magnetic core is used.
- On each side of the transformer, 120mm fans are used to blow air through the HV cable.

Transformer Design Summary [45]

	Core-type	Shell-type 1	Shell-type 2	Matrix
Losses	3.5 KW	4 KW	3.37 KW	4.5 KW
Volume	4.3Liter	11.9Liter	3.5Liter	11 Liter
Isolation	Potted	HV cable	Potted	HV Cable

- The isolation type has a strong impact over the efficiency and volume of the MF transformer
- Potted isolation enables high power density and efficiency with a high mechanical construction complexity, but increases the dielectric losses and partial discharges
- Achieving isolation with a HV litz cable enables a reduced complexity in the mechanical construction of the transformer with the price of lower efficiency and power density
- The high insulation requirements introduces considerable challenges in the transformer's thermal management
- Among the studied transformer concepts, the core type transformer reaches the highest efficiency and power density with a potted 100 kVDC isolation, which increases considerably the transformer mechanical construction
- The matrix and Shell-type transformers with isolation provided by a HV cable present a considerably easier mechanical construction, with reduced overall efficiency.
- As a conclusion, a clear trade-off between mechanical construction complexity and power density needs to be performed.

6

6. Semiconductor Overview

This chapter is showing some available fast rectifying diodes, IGCTs, IGBTs and IEGT. A short comparison between press-pack and power module packages is given and finally a list of commercial MV valves is presented.

A method of selecting the proper device should be evaluated. For example, in [5], Lenke has an interesting method of comparison and device selection for MVDC converters, in that case for Dual-Active Bridge topology. According to it, the following combination of properties would be attractive for the device of choice:

- As high as possible voltage ratings at acceptable conduction and switching properties
- Current ratings of several KA
- Low conduction losses
- Low switching losses in ZVS operation
- Low integration effort for series connection of multiple devices
- Active fault protection without additional components, including large maximum turn-off current capability
- Low gate drive power demand

Now, there are no devices at the present that meet all above features. So, a trade-off between device ratings and efforts of integrations should be performed to select the proper device.



Fig. 91 Different packages

a. Line Frequency Diode

Rectifier diodes are split into two sub-classes: Normal recovery diodes and avalanche diodes. Rectifier diodes are generally used for conversion of AC to DC and are optimized for low conduction losses and high currents, while avalanche diodes are self protected against transient over-voltages.

Manufacturer	Package	Switch	V_{RRM} (V)	I_{FAVM} (A)
ABB	Press-pack	5SDD 06D6000	6000	662
ABB	Press-pack	5SDD 09D6000	6000	845
Infineon	Press-pack	D471N90T	9000	565
Infineon	Press-pack	D471N85T	8500	565
Infineon	Press-pack	D471N80T	8000	565
Infineon	Press-pack	D270N36T	3600	270

b. Fast Rectifying Diode

Tabel 7 gives an overview of press pack and power modules for fast rectifying diodes. Standard recovery diodes where not interesting to evaluate, because even if they have low conduction losses, they can withstand only moderate dynamic stress in transition from conduction to blocking state. On the other hand, fast diodes, which are normally used as companion devices to switches in DC to AC conversion. Fast diodes are optimized to accept high dynamic stress, but have higher conduction losses compared to standard diodes.

Manufacturer	Package	Switch	V_{RRM} (V)	I_{FAVM} (A)
ABB	Press-pack	5SDF 10H6004	6000	1100
ABB	Press-pack	5SDF 13H4501	4500	1200
ABB	Press-pack	5SDF 08T4505	4500	767
ABB	Press-pack	5SDF 04T4504	4500	361
ABB	Press-pack	5SDF 02D6002	6000	250
ABB	Module	5SLD 0600J650100	6500	2 x 600
ABB	Module	5SLD 1200J450350	4500	2 x 1200
ABB	Module	5SLD 0650J450300	4500	2 x 650
Infineon	Press-pack	D901S45T	4500	900

Infineon	Press-pack	<u>D371S45T</u>	4500	330
Infineon	Press-pack	<u>D291S45T</u>	4500	290
Infineon	Module	<u>DZ950N44K</u>	4400	850
Infineon	Module	<u>DZ435N40K</u>	4000	435
IXYS Westcode	Press-pack	<u>M0588LC450</u>	4500	588
IXYS Westcode	Press-pack	<u>M1010NC450</u>	4500	1010
IXYS Westcode	Press-pack	<u>E0170YH45C</u>	4500	208
IXYS Westcode	Press-pack	F0900VC520	5200	816
IXYS Westcode	Module	MDK630-36N2	3600	632
Mitsubishi	Module	<u>RM1200DG-90F</u>	4500	1200
Mitsubishi	Module	<u>RM300DG-90S</u>	4500	300
Mitsubishi	Module	<u>RM600HE-90S</u>	4500	600
Semikron	Module	<u>SKKE 1200</u>	2200	1180
Semikron	Module	<u>SKKD 260</u>	2200	260
Tabel 7 List of fast rectifying diodes				

Some conclusions:

- Only a few manufacturers of press-pack diodes are on the market. This can be a disadvantage for costs and sourcing for a commercial product
- Also, not so many manufacturers for power modules with break down voltages above 4.5 kV
- The selected diodes are normally used as freewheeling using GTOs, IGCT, IGBTs or snubbers
- Suitable diodes for our application should have high blocking voltage (> 4.5 kV) and relative small average current (< 400 A) so high utilization is achieved. An example could be 5SDF 02D6002 from ABB, D291S45T from Infineon or E0170YH45C from West code.
- Press pack diodes with diameters of 60 or 75mm could be a choice as they will require smaller cooling effort and plates.
- Smaller diameter will impact valve mechanical complexity and integration

				
Φ	60mm	75mm	100mm	120mm
$I_{FAVM}(A)$ range	175 : 615	380 : 1256	585 : 1200	1950 : 2620
Tabel 8 ABB press pack diodes				

c. IGCT

Commercially available IGCT have current ratings between 520A and 5000A and blocking voltage capabilities from 4.5 kV to 6.5 kV. Beside 91mm and 152 wafer devices (85mm and 130mm pole-to face diameter), also 51 and 68mm devices are commercially available for smaller power demands. Asymmetric GCTs are only available for the larger wafer sized (to be used with external diodes in voltage-source converters). The maximum turn-off capability of the highest rated GCT device amounts to approx $I_{max} * V_{DC} \approx 30$ [MW]. For the class of 91mm 4.5 kV devices, the figure is limited to about 15[MW].[5]

For ex, ABB PCS 6000 system can reach power levels up to 9MVA without device paralleling. Compared to power modules, IGCTs can offer superior robustness to thermal cycling. This superior characteristic results from soldering and internal bonding based design. Another advantage characteristic, the device does in fault conditions not show any desaturation effects and can then handle almost any system fault currents in a safe operating mode. [19]

Also, short circuit operation will not lead to the damage of neighboring components. This could be an advantage for high power density converters.

The dc/dc converter has to operate at high ambient temperatures without power derating. Therefore, it must be ensured that all system components are operating below their rated temperature.

Switch	$V_{DRM}(V)$	$I_{TAVM}(A)$	Package(mm)
<u>5SHY 42L6500</u>	6500	1290	85
<u>5SHY 50L5500</u>	5500	1290	85
<u>5SHY 35L4522</u>	4500	2100	85
Tabel 9 List of ABB IGCT			

In [5], a list of semiconductors with their switching losses and on-state voltage was arranged. This was then visualized in a technology map of state-of the art high voltage semiconductors. According to [5], all GCTs feature a significantly lower on-state voltage drop V_{on} , than the IGBT peers, so that both groups of devices form two well separated clusters in the diagram. In both groups, the higher voltage rating is in tendency worse than that of lower voltage devices. This is intuitive, since higher voltage ratings require increased device thickness resulting in higher conduction and switching losses.

d. IGBT

Tabel 10 is showing a list of commercial IGBTs with in the range of 1.7 up to 6.5 kV in press pack and power module packages.

IGBTs for medium voltage applications are currently offered with standard voltage ratings of 2.5, 3.3, 4.5 and 6.5 kV. The largest available standard modules (footprint 140mm x 190mm) integrate up to 24 parallel connected IGBT dies and their free-wheeling diodes, yielding maximum turn-off currents I_{max} 2400A for 4.5 kV devices and 1500A in case of 6.5 kV devices. 4.5 kV press pack IGBT devices in 125 mm pole face disc housing sport turn-off current limits up to 5.8KA at a continuous operating current capability of 2100A. With the specified dc voltage of 2700V, this yields a maximum SOA product of 15.7[MW], corresponding closely to that found for 91mm IGCTs.

Manufacturer	Package	Switch	$V_{CES}(V)$	$I_C(A)$	Type
ABB	Module	<u>5SNA 0750G650300</u>	6500	750	Single IGBT
ABB	Module	<u>5SNA 1200G450350</u>	4500	1200	Single IGBT
ABB	Module	<u>5SNA 1500E330305</u>	3300	1500	Single IGBT
ABB	Module	<u>5SNA 3600E170300</u>	1700	3600	Single IGBT
ABB	Module	<u>5SND 0800M170100</u>	1700	2x800	Dual IGBT

Infineon	Module	FZ750R65KE3	6500	750	Single IGBT
Infineon	Module	FD500R65KE3-K	6500	500	Chopper
Infineon	Module	FZ1200R45KL3_B5	4500	1200	Single IGBT
Infineon	Module	FZ1500R33HL3	3300	1500	Single IGBT
Infineon	Module	FZ3600R17HE4	1700	3600	Single IGBT
Infineon	Module	FS500R17OE4D	1700	500	Six pack
Infineon	Module	FF1400R17IP4	1700	1400	Dual
IXYS Westcode	PressPack	T0258HF65G	6500	258	Single IGBT
IXYS Westcode	PressPack	T0900DF65A	6500	900	Single IGBT
IXYS Westcode	PressPack	T2400GB45E	4500	2400	Single IGBT
Mitsubishi	Module	CM750HG-130R	6500	750	Single IGBT
Mitsubishi	Module	CM1200HG-90R	4500	1200	Single IGBT
Mitsubishi	Module	CM1500HG-66R	3300	1500	Single IGBT
Mitsubishi	Module	CM1200HC-50H	2500	1200	Single IGBT
Mitsubishi	Module	CM2400HC-34H	1700	2400	Single IGBT
Semikron	Module	SKM600GA17E4	1700	600	Single Switch
Semikron	Module	SEMIX653GD176HDc	1700	450	Six Pack
Fuji Electric	Module	2MBI400VE-170-50	1700	400	Dual IGBT
Fuji Electric	Module	1MBI1500UE-330	3300	1500	Single IGBT

Tabel 10 List of IGBTs

According to [5], GCT technology currently allows to build more efficient devices as compared to IGBT technology at voltages higher than 4.5 kV, provided that the loss optimization toward conduction losses is acceptable with respect to the target switching frequency. Studying the distribution of IGBT devices, one finds in analogy to GCTs that devices optimized toward low switching losses tend to have better efficiency ratings.

e. IEGT (Injection Enhanced Gate Transistors)

Manufacturer	Package	Switch	$V_{DRM}(V)$	$I_{TAVM}(A)$	Package(mm)
Toshiba	PressPack	ST2100GXH24A	4500	2100	Single IEGT
Toshiba	PressPack	ST1500GXH24	4500	1500	Single IEGT
Toshiba	Module	MG900GXH1US53	4500	900	Dual IEGT
Toshiba	Module	MG1200GXH1US61	4500	1200	Dual IEGT

Tabel 11 List of IEGTs

f. Press pack vs. power modules

Due to the high costs of maintenance in offshore wind farm applications, the reliability of the system is important. The IGBT and GCT are both capable of handling Mega-Watt power levels in a DC/DC converter, but from the reliability aspect, the IGCT is preferred for following reasons:

In terms of mechanical structure, an IGCT generally consists of a single wafer whereas an IGBT typically consists of multiple parallel chips interconnected by wire bonds. The IGCT is mechanically much less complicated than a flat pack IGBT and is less likely to suffer from thermal cycling issues than an IGBT in

which many different interconnections and materials are required in order to attach the silicon to the base plate, while maintaining isolation

Device	IGCT press-pack	IGBT press-pack
Benefits	Possibility of series connection of more than 20 switches	Easier to achieve homogenous voltage sharing Low power consumption gate driver
Deficits	High power consumption gate driver Required di/dt snubber	Maximum 20 series connected switches

In terms of behavior after failure, the IGCT normally fails to a short circuit whereas a flat pack IGBT becomes an open circuit. This behavior of the IGCT makes a system with series connected devices more reliable. For example, additional series IGCTs can be connected, so that if one device fails, the circuit will continue to function (N+1 redundancy). [46]

Moderate levels of power density and reliability can be sufficient for a general cost-effective MV AC drive operating with mild mission profiles. Applied to large wind turbines, MV-VSCs are required to have high power density due to the space and weight limitation in wind turbine nacelle, but the first priority needs to be design for reliability. This is due to severe mission profiles under harsh operating conditions of temperature, humidity, vibration and the maintenance of remotely located wind turbines is quite costly. Therefore, first, the converter topologies and switch technologies should be selected among the state of the art converter topologies and switch technologies such that the highest reliability are to be attained and then power density. The converter power density is determined by the power rating and volume of the full scale MV-VSC.[47]

	IGCT press pack	IGBT module	IEGT press pack	IGBT press pack	Impact
Cooling side	Double	Single	Double	Double	Power density
Snubber need	Yes	No	Yes	No	Power density
On-state voltage	Low	Moderate	Low	Moderate	Power density
Current density	High	Low	Moderate	Moderate	Power density
Gate driver volume	Moderate	Small	Small	Small	Power density
Switching frequency	<500HZ	<2000HZ	<1000HZ	<1000HZ	Power density
Semiconductor contact	Pressure Contact	Bond wires	Pressure Contact	Pressure Contact	Reliability
Failure mode	Short	Open	Short	Short	Reliability
Short-circuit current	Snubber limited	Gate driver limited	Gate driver limited	Gate driver limited	Reliability
Series connection	Moderate	Easier	Easier	Easier	Reliability
Parallel connection	Difficult	Easier	Easier	Easier	Reliability
Thermal cycling tolerance	High	Moderate	High	High	Reliability

g. Converter integration aspects

One issue of integrating devices into the medium voltage converter would be the effort of series connection of a large number of semiconductors to reach the desired voltage levels. Considering the assumption that power modules housing are not an efficient solution for series connection, only devices in pressure contact housings can be considered an applicable solution. According to [5], the choice of press-

pack IGBTs would currently be limited to 4.5 kV devices or below. On the other hand, 6.5 kV IGCTs have also a poor efficiency compared to the 4.5 kV class.

Press pack IGBTs were used with success in HVDC converters up to 150 kV with several dozen devices connected in series. But, stacking this large number of devices will rely on expensive spring contact housings that decouple the contact pressure of the IGBT dies from the mounting force of the stack to avoid damaging the fine cell structures due to an inhomogeneous pressure distribution [5]. However, even the spring contact housing does not permit to connect more than about 20 IGBTs in one stack. So, several stacks have to be series connected to reach the HVDC voltage levels.





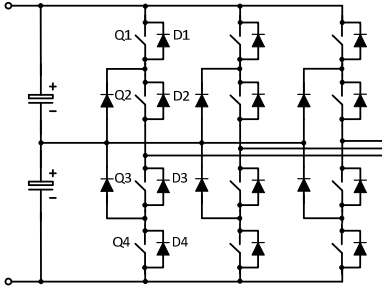
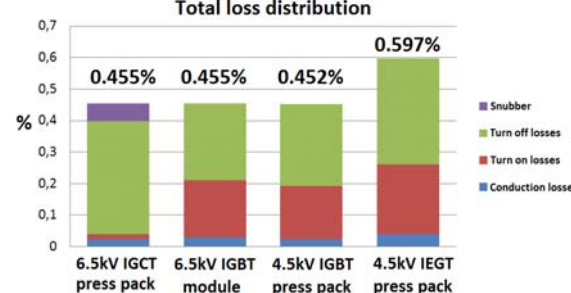
Now, on the other hand, the absence of a sensitive cell structure makes the mechanical integration of series connected IGCTs easier. In classical current source converter HVDC systems, more than ten single wafer thyristors are regularly mounted in a single stack in standard disc type housings. This number of devices does not represent a mechanical limit, but results rather from the desire to design conveniently sized sub stacks, since a low inductive device integration is not required in these converters. It is therefore reasonable to assume that also higher number of thyristor devices can be series connected in stacks with moderate mechanical effort [5].

The main reason why series connected IGCTs have not been used in HVDC converters or alike despite the easier mechanical series connection is the higher difficulty of homogenizing the transient voltage stresses on single devices compared to IGBTs. An additional clamp circuit required for di/dt limitation of IGCTs would be expensive in both terms of component cost and additional losses.

When stacking many devices in order to reach high voltage levels, a potential advantage for IGBTs is the very low power consumption on the gate drive units, which limits the effort for the insulated gate drive power supply. On the other hand, modern IGCT gate drive units may consume up to 100W, a demand that will increase the cost.

h. Loss comparison of different semiconductors based on a 5[MW] 3L-NPC inverter

In [48], loss analysis of 6.5 kV/3800A IGCT, 4.5 kV/2400A press pack type IGBT, 4.5 kV/2100A press pack type IEGT and 6.5 kV/750A module type IGBT for 5[MW] PMSG MV wind turbine employing a back to back 3L NPC voltage source converter is presented (see Fig. 92). The switching frequency is set to 1020HZ and grid side input voltage is 4.16 kV. The loss analysis is confirmed through PLECS simulations. The simulation results show that press-pack type IGBT and IGCT semiconductor device have the highest efficiency (see Fig. 93).

<div></div>																			
	IGCT	Press-pack IEGT	Press-pack IGBT	Module type IGBT															
Device	Press Pack IGCT	Press Pack IEGT	Press Pack IGBT	Module IGBT															
Manufacturer	ABB	Toshiba	Westcode, IXYS	ABB															
Code	5SHY 42L6500	ST2 100 GXH22A	T2400 GB45E	5SNA 0750G650300															
Blocking Voltage [V]	6500	4500	4500	6500															
Turn-off current [A]	3800	2100/5500	2400/4800A	750/1500															
Part	GCT-part	-	IGBT	IGBT	Diode														
$V_{TO}(\text{MAX})$ [V]	1.88	3	1.49	2	2.5														
$R_T(\text{MAX})[\text{m}\Omega]$	0.56	1	1.05	2.5	1.3														
$E_{ON}(\text{MAX})[\text{J}]$	3.1	18.4	15	6.4	-														
$E_{OFF}(\text{MAX})[\text{J}]$	44	17	14	5.3	2.7														
Meas.condition	4 kV/3800A	3 kV/2100A	2.8 kV/2400	3.6 kV/750A															
T_{vj_max} [°C]	125	125	125	125															
$R_{th(j-c)}$ [K/[kW]]	8.5	5.25	5.2	11	21														
$R_{th(c-h)}$ [K/[kW]]	3	3	3	9	18														
$R_{th(h-a)}$ [K/[kW]]	6	6	6	10	10														
					<table><tr><td>Parameter</td><td>Value</td></tr><tr><td>Output power</td><td>5 [MW]</td></tr><tr><td>Grid frequency</td><td>60 HZ</td></tr><tr><td>Grid side input voltage</td><td>4.16 kV</td></tr><tr><td>Grid side input current</td><td>708A</td></tr><tr><td>Switching frequency</td><td>1020HZ</td></tr><tr><td>DC Link voltage</td><td>7 kV</td></tr></table>	Parameter	Value	Output power	5 [MW]	Grid frequency	60 HZ	Grid side input voltage	4.16 kV	Grid side input current	708A	Switching frequency	1020HZ	DC Link voltage	7 kV
Parameter	Value																		
Output power	5 [MW]																		
Grid frequency	60 HZ																		
Grid side input voltage	4.16 kV																		
Grid side input current	708A																		
Switching frequency	1020HZ																		
DC Link voltage	7 kV																		
Fig. 92 3L-NPC VSC			Fig. 93 Total loss distribution		VSC parameters														

According to [48] and Fig. 93, the 6.5 kV IGCT has the highest turn off losses among the four kinds of power devices, while the IGCT turn-on loss is relatively smaller than the other devices.

Press pack IEGT has the highest loss value (0.87%) while module type IGBT exhibits the loss value of 0.74%, which is close to those of IGCT and press pack type IGBT. Loss data of module type IGBT corresponds to the case of two devices in parallel. In this paralleling of devices or converters, the equal sharing of current becomes a quite important design task. It may further complicate a control algorithm or mechanical concept as compared to the single device approach such as IGCT, press-pack IGBT and press-pack IEGT.

i. Recent advances in power electronic semiconductors

SiC insulated-gate bipolar transistor and thyristors technology becomes attractive for high voltage (15 kV to 25 kV) due to their superior on state characteristics, fast switching speed, low loss and wide reverse biased safe operating area. Silicon power devices are reaching their physical limits for power handling and switching frequency speed. They have achieved very large power handling capability by increasing current handling to more than 1500A per device, their frequency capability is typically below 4.5 kHz and their frequency capability is below 1 KHz. These devices normally cannot be used at temperatures higher than 125deg in power electronics systems.

The continuous demand for power electronics systems with smaller size and higher power density requires the development of power semiconductor devices capable of even higher frequencies, higher voltages and higher temperatures. Using higher voltage power devices can effectively lower the current hence reducing the copper conductor requirement, part count and cooling requirement in high power applications.

Wide bandgap silicon carbide material is the most promising post silicon alternative to achieve these goals because of its superior properties (ten times higher breakdown electric field, higher thermal conductivity and much lower intrinsic carrier concentration when compared with silicon). Following SiC devices are underdevelopment at the moment: 10 kV SiC MOSFETs, 7 kV SiC GTO, 15 kV SiC IGBTs and the world's first SiC ETO.

Among the high voltage SiC devices whose properties have been experimentally verified, the on-state resistance of the SiC MOSFET increases significantly as the blocking voltage (>10 kV) and operating temperature increase, which make it unacceptable for applications where high DC supply voltage (up to 25 kV) are used. For this range, SiC IGBT and thyristor technology becomes attractive due to their superior on state characteristics, reasonable switching speed and excellent safe-operating area. By integrating the high-voltage SiC GTO with the mature silicon power MOSFET technology, the SiC ETO is expected not only to simplify the user interface, but also to improve the speed and dynamic performance of the device [49].

j. Valve mechanical concepts

Following sub chapter is focusing on different commercial semiconductor valves used in medium voltage applications.

➤ ABB ACS6000

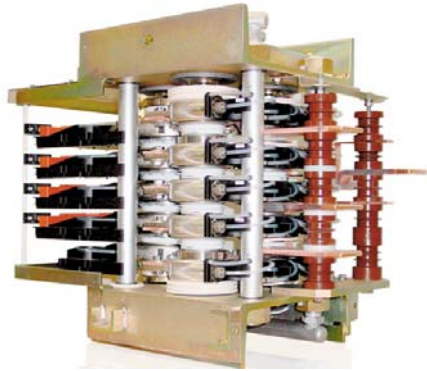


Fig. 94 ABB One phase leg of a 3-level VSI

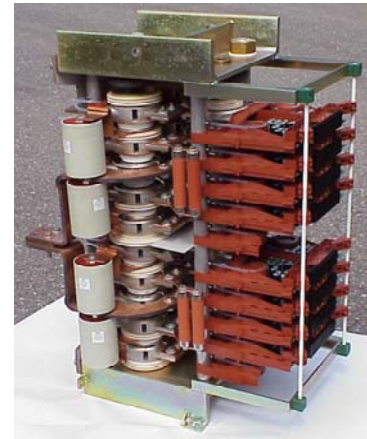


Fig. 95 ABB Phase leg with 8 IGBTs

- ABB ACS6000 is mainly used in medium voltage drives for marine, mining and metals
- Power ranges from 315 KW up to 72[MW] and line voltages from 2.1 kV to 13.8 kV
- Well proven modules, possibilities for redundancy and a compact footprint

➤ Siemens SILCOVERT

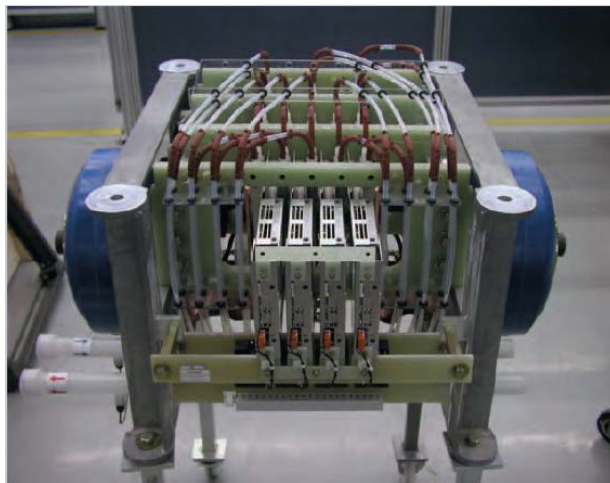


Fig. 96 Siemens IGCT Phase module in SINAMICS GM/SM150 drives

- Water cooled valve with power range on 20 to 24 MVA
- Limited output frequency ($f_m < 250\text{Hz}$) due to low switching frequency of high blocking semiconductors
- Output voltage limited to 7.2 kV
- 4.5 kV Blocking Voltage and 5KA turn-off current

➤ IXYS Westcode

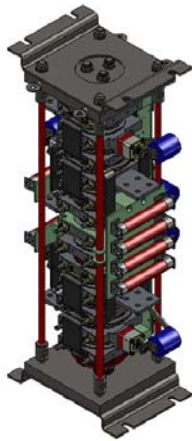


Fig. 97 Westcode NPC phase leg

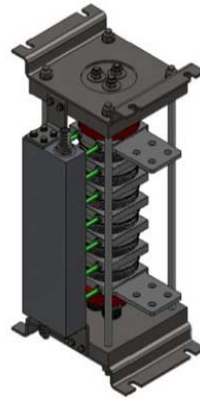


Fig. 98 Westcode Diode Valve

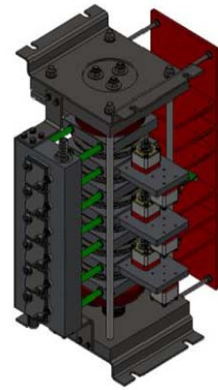


Fig. 99 Westcode IGBT valve

- A range of 3-level topology assemblies using press pack IGBTs or diodes developed for 3.3 kV, 6.6 kV and 10 kV systems
- The 6.6 kV and 10 kV systems are based on the combination of 2 IGBT stacks and 1 diode stack
- Each system benefits from direct water cooling to provide highly effective heat dissipation away from the devices and pre-loaded disc spring clamping to evenly distribute the applied force across the entire surface area of the device

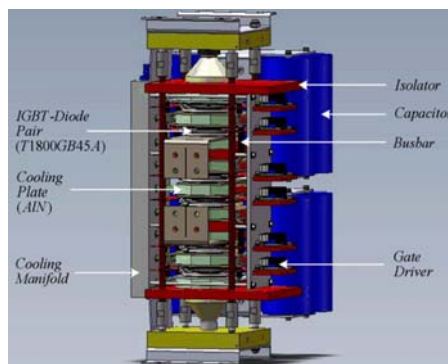


Fig. 100 Single leg structure of 3L-NPC-VSC and 3L-ANPC-VSC

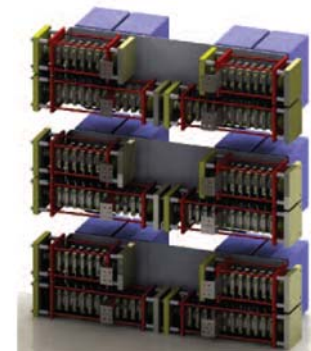


Fig. 101 Possible configuration of an 18[MW], 6.6 kV variable speed drive

- Also, designed into each system is an integrated snubber circuit design and an isolated clamping rod system to limit the occurrence of eddy currents within the unit
- Single unit mechanical configuration: short inductance paths for relative size of unit to avoid high stray inductance
- Advanced optically fired gate trigger circuits

➤ GVA Thyristor valves

- The thyristor pulser from GVA consists of a discrete mechanical unit consisting of 8 thyristors connected anti-parallel in series.
- It is equipped with a trigger module and an auxiliary voltage supply as well as a protective network for static and dynamic voltage sharing
- The highest permitted connection voltage is 12 kVEFF and the highest permitted pulse current is up to 32KA with a pulse duration of up to 100ms
- The switch is air-cooled(self ventilated) and therefore one of the weakest versions in terms of continuous current carrying capacity
- The mechanical design is such that much higher current carrying capacities can be achieved by using forced ventilation or liquid cooling and by using larger disc-type thyristors. The status monitoring and error feedback signals are transmitted via fibre optic cables in a potential free way.

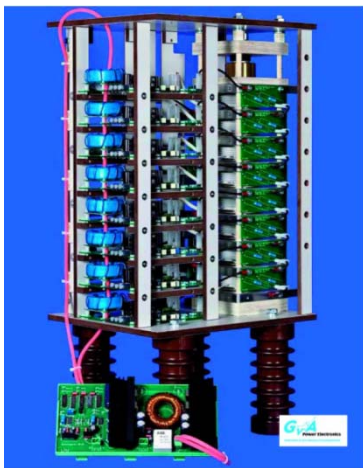


Fig. 102 GVA Thyristor pulser

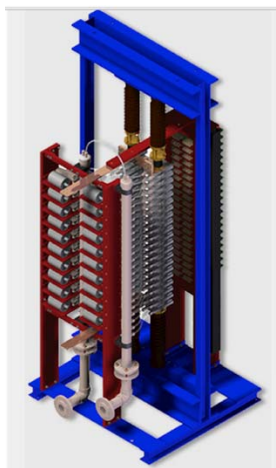
Fig. 103 Thyristor
Controlled Reactors

Fig. 104 Static VAR compensator

- Thyristor Controlled Reactors are used usually in combination with Fixed or Mechanically Switched Capacitors to provide Static VAR Compensation
- Typical example applications include flicker reductions and power factor compensation of Electric ARC furnaces in steel mills
- The SVC valve from Fig. 103 is water cooled. It is designed for operation at 35 kV and the range extends from 10MVAR up to 300MVAR
- All the thyristor modules used in the TCR valves are matched to improve static and dynamic sharing whilst N+1 redundancy is included as standard to ensure consistent availability of supply, even in the harshest of operating conditions

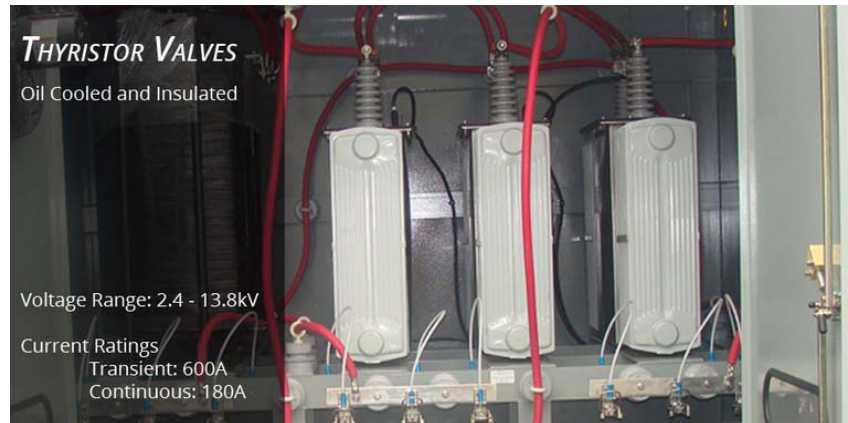
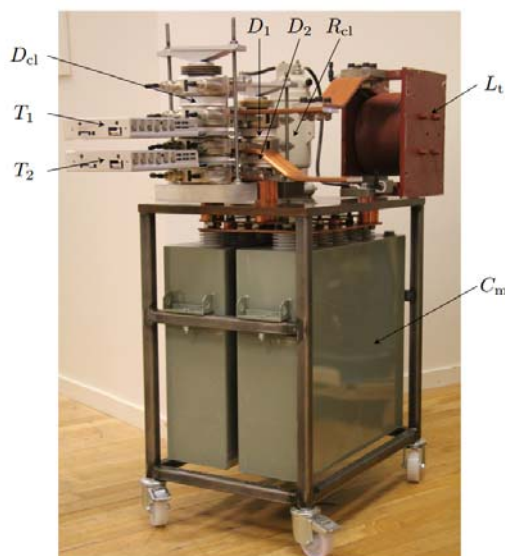


Fig. 105 Oil cooled thyristor valve [50]

➤ Thyristor valves with oil cooling from NEPSI

- Interesting valve concept due to simple oil cooled system
- Thyristor switched stages are equipped with single phase oil cooled and insulated thyristor valves that provide single cycle transient free switching
- The valve tank is constructed of 16Gauge stainless steel and is equipped with a removable 6.3mm thick stainless steel cover.
- The valve is designed with N=1 device redundancy and is furnished with a redundant firing circuit and misfire prevention protection
- Valve controls enter the tank via an oil tight military connector for ease of testing and connection

➤ High power IGCT cell [51]



IGCTs	T1, T2	ABB 5SHY 35L4510
Diodes	D1,D2,Dc1	ABB 5SDF 16L4503
Storage capacitors	Cm	2 x 4mf, 2.65 kV
Clamp inductor	Lt	5uH
Clamp resistors	Rc1	0.6Ω

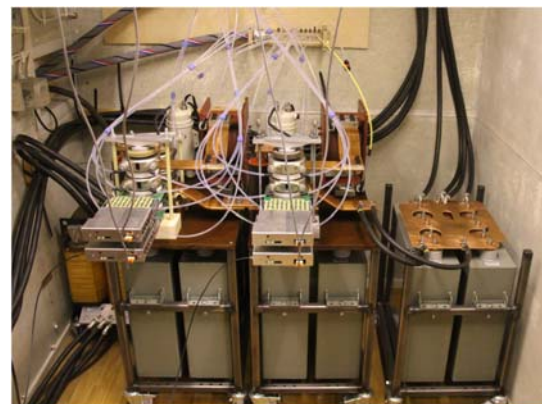


Fig. 106 IGCT-based cascaded converter cells showing the main components [51]

- The cell design, being based on IGBTs, is similar to a power electronic building block (PEBB) for medium voltage industrial drives, but also contains energy storage capacitors and di/dt reactors typically not included in a PEBB
- The cooling system employs de-ionized water
- The prototype cell in [51] is designed for HVDC applications
- Switching frequency is close to 200Hz
- The cell design is based on an asymmetric IGBT rated to 4.5 kV and a maximum turn-off current of 4kA
- The mechanical design incorporates input and output terminals, two diodes in parallel with the IGBTs
- The cell contains di/dt-limiting reactor and clamping circuits in order to limit the turn-off di/dt of the diodes
- All the semiconductors are press-pack devices, which are robust and with low risk of explosion, even in the case of severe over-current conditions
- All the interconnections are made with copper clad aluminium bus bars

➤ High Voltage IGBT Valve

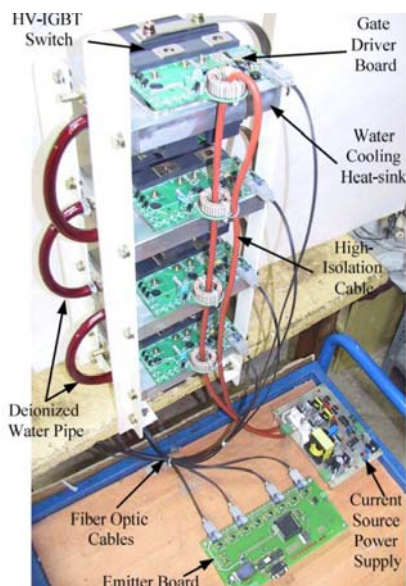


Fig. 107 IGBT valve [52]

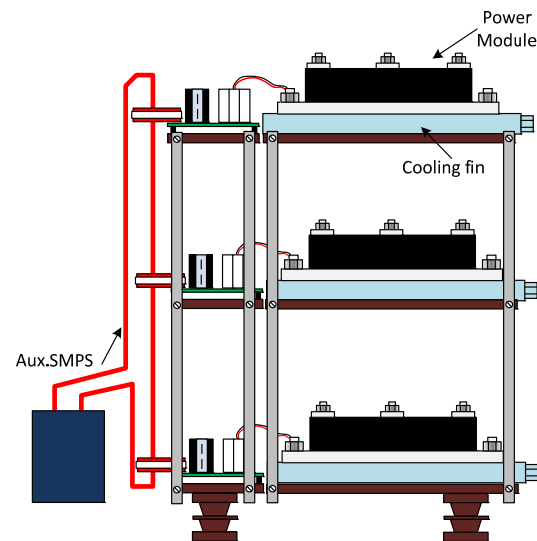


Fig. 108 GVA IGBT valve

- Valve designed for 22 kVDC, 200A at $t_p=5\mu s$, $di/dt=100A/\mu s$
- Switching frequency is set to 1 kHz
- There are 8 devices: CM400HB-90H
- De-ionized water is used for cooling
- 24V Auxiliary power supply with proper isolation
- Optical trigger for devices
- To obtain an appropriate steady state voltage sharing between the 8 IGBTs, a set of 8 resistors (each one in parallel with a switch) are used

- A power cable with high isolation capability carrying an AC current of 4Arms @25 kHz is used
- The cable passes through toroidal transformers placed in every driver's board
- The primary winding of toroidal transformers consists of only 1 turn
- The current injected to the cable is generated by a current source SMPS
- 4 different protection mechanism are considered:
 - Overcurrent and short circuit protection
 - Dynamic and static over voltage protection
 - Power supply under voltage protection
 - Over temperature protection
- Over current protection is performed by one circuit. The current is sensed by a CT and then compared with a constant protection level. When the protection circuit detects an over current occurrence a set of turn-off pulses are transmitted to the series switches

Thyristor HVDC valve concepts

To easily adapt thyristor valves to the HVDC or FACTS applications and to standardize the valve design a strictly modular design is used to compose a customized thyristor valve resulting in a cost optimized design [53]. The thyristor modules are self supporting units with a frame of aluminium profiles, which mechanically supports all components within the modules (see Fig. 109). In HVDC thyristor modules, the frame also serves as a corona shield. Its electrical potential is that of the centre cross beam so that the module is divided into two symmetrical areas. Each area accommodates a complete valve section, consisting of thyristor stack, snubber circuits, valve reactors, monitoring boards, grading capacitor, water circuit and the routing of the optical fibres [53]. The arrangement of the thyristors and heat sinks in the stack and their equipment is a straightforward image of the electric circuit diagram. A uniform voltage grading and ease of testing are advantages of this design. A typical multiple valve unit structure is shown in Fig. 111. Voltage distribution between different levels of the series connected thyristors of a converter valve is a fundamental issue for the valve design for HVDC application. Voltage distribution across the series semiconductors is highly influenced by the valve stray capacitance.

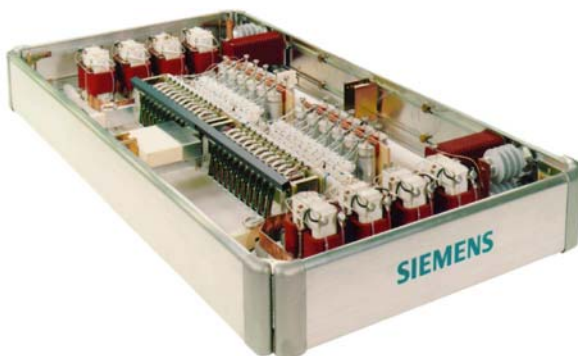


Fig. 109 Modular Unit used in HVDC applications

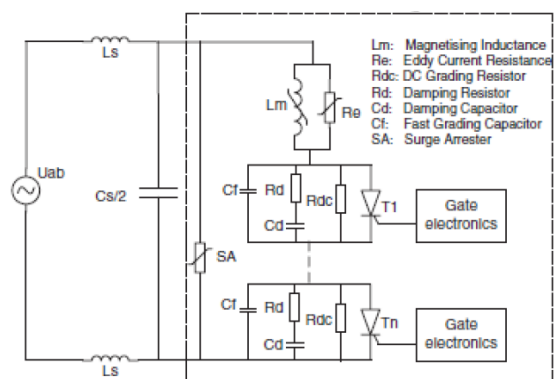


Fig. 110 Equivalent circuit for a single valve

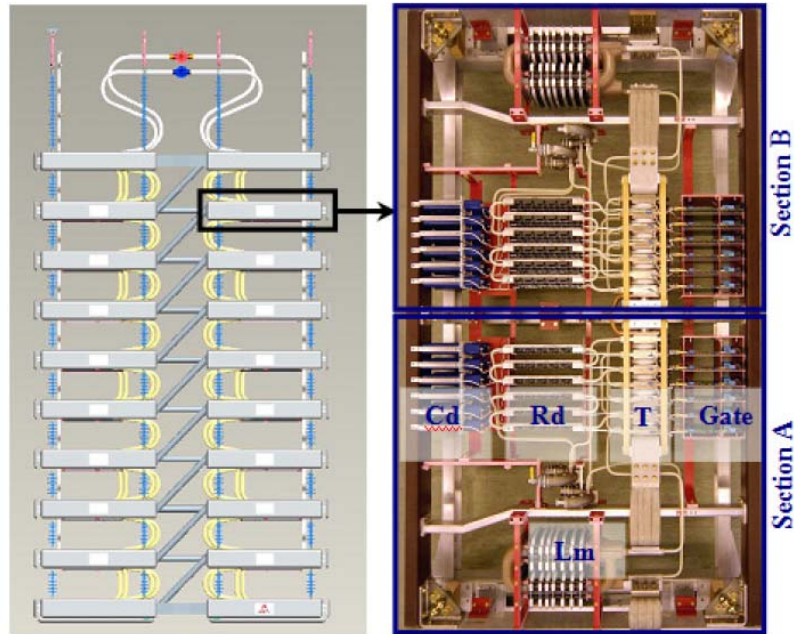


Fig. 111 Typical Valve Unit

7

7. Cooling

This chapter gives a review of used cooling methods for power semiconductors and transformers. Classification of cooling methods can be done according to the mechanism or medium used to transfer heat during the cooling process. Two common ways of cooling power semiconductors are air and liquid cooling. Liquid cooling is in most of the cases done with water or a water/glycol mixture to perform thermosiphon or forced cooling. Other agents, such as oil can also be used.

a. Air cooling for semiconductors [54]

i. Natural and forced air cooling

Air has a thermal conductivity of 0.026 W/mk . It is not an outstanding thermal conductor. Its main advantages are the ability to insulate and it's not corrosive.



Fig. 112 IGBT heat sink with bonded

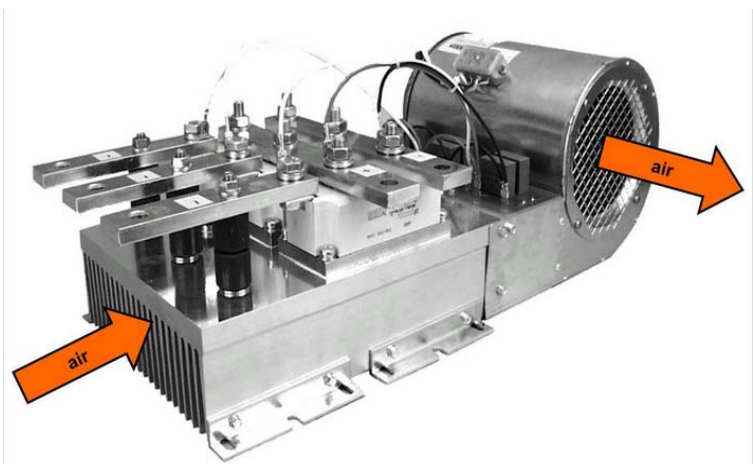


Fig. 113 Forced air cooling using a radial fan [54]

process

It is common knowledge that air rises as it is heated due to its resulting decrease in density (convection). The air flow resulting from this convection process is referred to as laminar flow. This process provides a natural means of removing heat generated by power electronics components [54]. Air cooling requires low to now maintenance, no wear or tear and no noise emission. The main disadvantage consists in very low levels of cooling.

Fans are used in forced air cooling in order to increase the air velocity. This aims to produce turbulent air flow, rather than laminar flow, increasing thus the heat dissipation to the surrounding ambient. Forced air cooling has better effect than natural air cooling. But the high amount of noise and resulting wear and tear are the main disadvantages. Fans and filters require maintenance regularly.

b. Liquid cooling for semiconductors [54]

i. Water cooling of power modules and press pack

Water cooling in power modules or press pack is normally used for very high power ranges as well as for low power devices which already have a water cycle for operating reasons (car drivers, galvanic installations, inductive heating)[55]. In most cases, the admission temperature of the coolant values is as much as 50..70°C when the heat of the coolant is directly dissipated to the atmosphere; in industrial plants with active heat exchangers, the temperature is about 15..25°C. The temperature difference between heatsink surface and coolant, which is lower than for air cooling, may be utilized in two ways:

- Increased power density
- Low chip temperature, long module life



Fig. 114 Semikron water cooled heatsink [54]

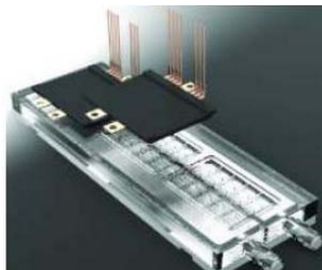


Fig. 115 Danfoss Mold Module, direct liquid cooled with highly efficient double sided Shower Power Turbulators



Fig. 116 Stack of presspack diodes cooled using Vortex

Existing and emerging liquid cold plate solutions[56] :

- Tube type and fin type liquid cold plates to cool packages with DBC substrates with and without copper base plates
- Liquid flow through fins formed directly on copper and AlSiC base plates
- Direct cooling of the base plate or DBC substrate using concepts such as the Danfoss “shower power” design using jet impingement or liquid flow through meandering channels Fig. 115

- Direct double sided cooling of back to back modules with and without fins integrated with DBC substrates
- Micro-channel coolers built into base plates or integrated with DBC substrate or into specially customized package designs
- Stacked power modules and liquid cold plates using extruded channel type, folded fin and micro-channel type cold plates.
- Fig. 116 is showing an interesting concept developed by Aavid. The Vortex Liquid Cold Plate uses helicodal flow paths to create strong secondary flow with high vorticity to achieve high heat transfer coefficients at the flow channel wall and parallel flow paths to reduce liquid velocities and the corresponding pressure gradient. Area enhancement is achieved by orienting the helical path so that its axis is normal to the base. This design is ideal for cooling a stack of press pack IGBTs, thyristors or diodes in series.

The following factors influence the thermal resistance in a liquid cooler [55]:

- The contact area to the coolant (eg. Number of cooling channels)
- The volumetric flow rate as a function of the pressure drop
- The heat storage capability of the coolant
- Turbulence in the water flow
- Heat conduction and spreading in the heatsink
- The coolant temperature (depending on viscosity and density)

Enlarging the contact area of heatsink/coolant will result in improved heat transfer. The particular shape of the liquid cooler and a sufficiently high flow velocity creates a turbulent flow which substantially reduces the heat transfer resistance between heatsink and liquid. An even distribution of heat sources across the heatsink surface is important for low thermal resistance. Due to the high heat transfer coefficient of some $1000\text{W}/(\text{m}^2\text{K})$, the heat flow is dissipated to the cooling liquid with only minor cross-conduction. This means that essentially only those areas on which power semiconductor modules are mounted are used for cooling. Copper rather than aluminium as heatsink material will reduce the volume resistance, increase cross-conduction, thus increasing the effective cooling area. A cooler made of copper allows for a reduction in $R_{\text{th}(j-a)}$ by approximately 20% for a standard IGBT module [55].

In water-glycol mixture, the glycol viscosity influences the $R_{\text{th}(s-a)}$. For a mixture of 50% glycol and 50% water in the temperature range of 10°C to 70°C , the $R_{\text{th}(r-a)}$ was reduced by about 25% between the temperature sensor and coolant.

The typical heat transfer medium to be used for liquid cooling is often water or a glycol/water solution (anti-freeze). More rarely, deionized water or insulation oil (fluorocarbons and PAO=synthetical hydrocarbons) is used. It is important to choose a liquid that is compatible with the cooling circuit and provides wither corrosion protection or a minimum risk of corrosion. To ensure corrosion protection in water cooled aluminium heatsinks, the glycol content must amount to at least 10%.

	Water	Glycol Mixtures	Deionized water	Non-conductive liquids (Fluro-inert,PAO)
Copper	X	X		X
Aluminium		X		X
Stainless steel	X	X	X	X

Tabel 12 Materials and compatibility of liquids

Deionized water is free from ions such as sodium, calcium, iron, copper, chloride and bromide. The deionization process removes harmful minerals, salts and other impurities which may cause corrosion or limescale. Compared to tap water and most other liquids, deionized water has a high electric resistance and is an excellent insulator. But it easily turns acidic when it comes into contact with air. It may be necessary to use anticorrosives in application with deionized water. Connection pieces should be nickel coated. Copper leads as incompatible with the use of deionized water for cooling plates or heat exchangers. Leads made of stainless steel are recommended. [55].

ii. Mounting direction and venting [54]

When setting up the cooling circuit, care must be taken that cooling is not blocked by air bubble build-up. The best mounting setup consists of vertical channels, while the worst is horizontal channels on top of each other.

The preferred flow direction is upwards with the inlet at the bottom and the outlet at the top in the control cabinet.

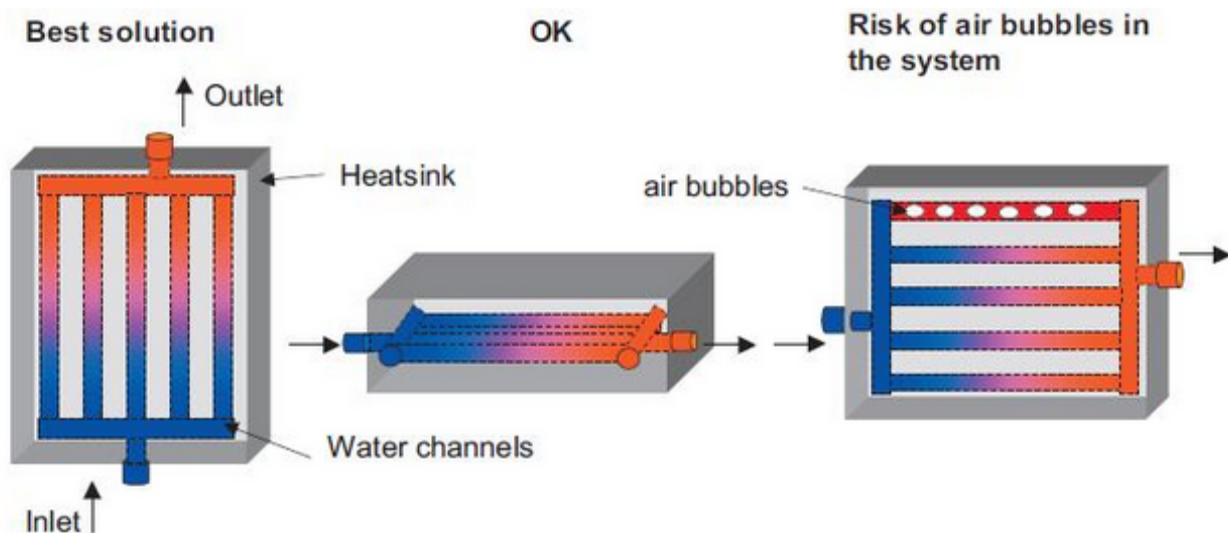


Fig. 117 Mounting direction and venting

iii. Turbulent flow [54]

One way of increasing the thermal efficiency of a water cooling system is by placing coils inside the cooling channel to induce a turbulent flow of the cooling liquid (Fig. 118). The turbulent flow created by the coils can increase the thermal efficiency of the cooling system by 15-20%. Turbulent flow can also be created by the presence of microchannels in the cooling channel (Fig. 119).

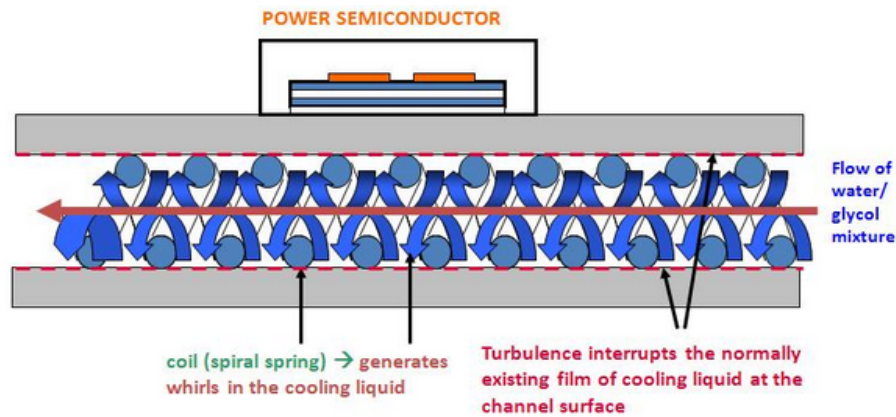


Fig. 118 Use of coils in liquid cooling system
Cooled power device

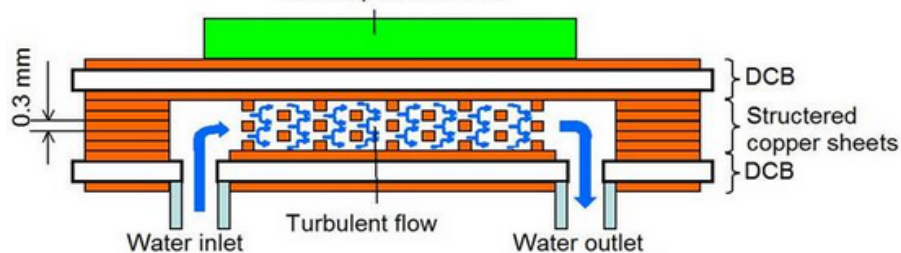


Fig. 119 Use of microchannels in liquid cooling system

One disadvantage of this method is the high risk of channel blockage by particles in the cooling liquid

iv. Thermosiphon Cooling [54]

In thermosiphon cooling, the heat transfer is done by natural convection of water due to gravity. This will result from the fact that heated water is less dense than the colder water and therefore rises to the top of the cooling system causing natural circulation of the cooling liquid (Fig. 120).

The advantage of this system is a minimum amount of maintenance, no wear or tear and the cooling process produces no noise. On the other hand, the disadvantage is that the system requires a large amount of space and it needs to be positioned vertical.

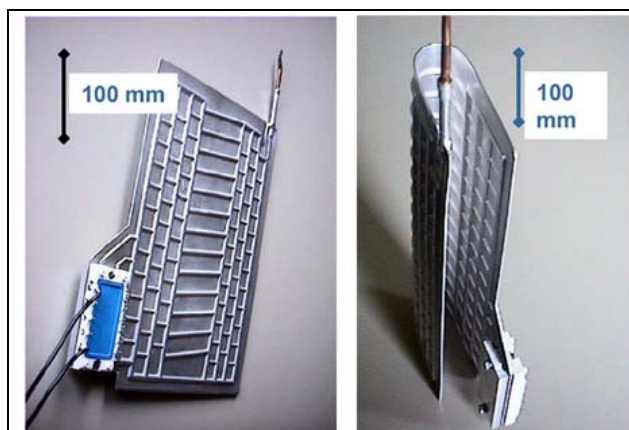


Fig. 120 Thermosiphon Cooling System

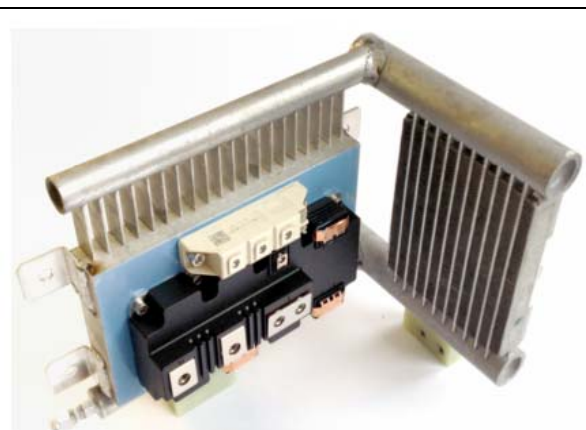


Fig. 121 MMC cell cooling with thermosiphon system

v. Phase transition Cooling [54]

The enthalpy of vaporization is the amount of heat that must be absorbed by a given quantity of liquid in order to transition to the gas state. The opposite of this is referred to as enthalpy of condensation. The same amount of heat is used up or dissipated in each process respectively.

The cooling fluid evaporates at the location of the heat source. The vapor carries the heat to a condenser (which acts as a heat exchanger), where the fluid is then condensed back to its liquid form. Examples of application of this method are described below:

1. Pool Boiling

In pool boiling, the cooling medium evaporates at the heat source, has bubbles rise and condense on the cooler upper surface (Fig. 122). In traction applications, TGC locomotives are employing this process for cooling GTOs (Fig. 123)

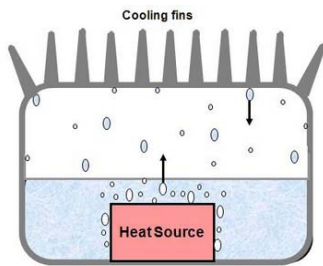


Fig. 122 Pool boiling

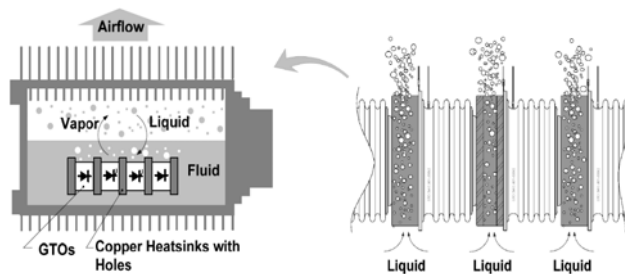


Fig. 123 Cross section of a 2-phase immersion-cooled GTO traction inverter [57]

At high heat stream density, a layer of vaport might build up ath the heat source. This reduces or prevents contact between the heat source and the cooling fluid which inevitably leads to a great reduction in cooling. This is reffered to as the Leidenfrost effect.

2. Heat Pipes [54]

Another method of heat transfer is to use heat pipes. Heat pipes also rely on natural forces to transfer heat. Heat pipes are made of hermetically sealed copper filled up with a small amount of fluid under low pressure. The inner part of the heat pipe is lined with a capillary structured wick (Fig. 124).

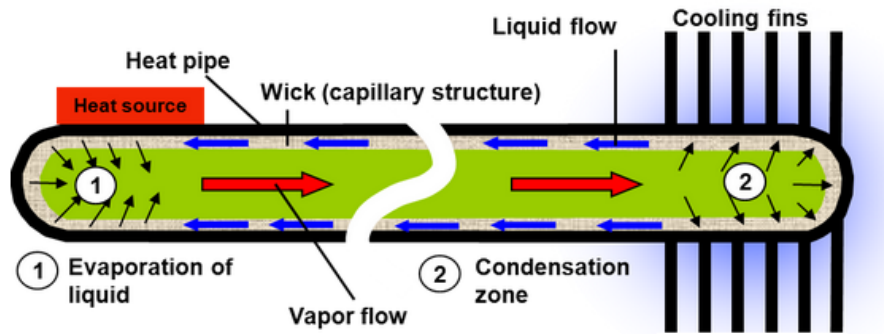


Fig. 124 Liquid cooling with heat pipes

The cooling liquid is evaporated by the heat source at one end of the heat pipe. The vapor is transferred to the opposite end by convection where cooling fins are located. The vapor cools and condenses into liquid form and is carried back to the heat source through the capillary wick structure along the perimeter of the heat pipe.

To form the capillary structure of the heat pipe, a porous material is applied on the inner wall of the pipe. This can be done using either metal foams (steel, aluminium, copper or nickel) or using carbon fibres.

Different heat transfer media can be used within the heat pipes. Water cannot be used below 0°C. Acetone or alcohol is commonly used.

Advantages of using heat pipes include:

- Extremely high heat transfer ability (100 to 1000 times higher than copper at small temperature gradients)
- No parts need to be moved mechanically
- Heat pipes offer enough flexibility to be produced in all forms and sizes.

c. Natural and forced oil cooling for transformers [58]

Different cooling methods of transformers are:

For dry type transformers: Air Natural (AN) and Air Blast

This method is used in small transformers (up to 3MVA). The transformer is cooled by natural air flowing around it. Air blast is used for powers higher than 3MVA, with the help of fans or blowers. The air supply must be filtered to prevent the accumulation of dust particles in ventilation ducts. This method can be used up to 15MVA.

- For oil immersed transformers Fig. 125:
 - i. Oil Natural Air Natural (ONAN)

This method is used for oil immersed transformers. The heat generated in the core and windings is transferred to the oil. Due to convection, the heated oil flows upward direction and then in the radiator. The vacant place is filled up by the oil from the radiator. Afterwards the heat of the oil is dissipated in the atmosphere. This method can be used for transformers up to 30MVA.

ii. Oil Natural Air Forced (ONAF)

The heat dissipation can be improved further by applying forced air on the dissipating surface. Forced air provides faster heat dissipation than natural air. This cooling method can be used for large transformers up to about 60MVA.

iii. Oil forced Air Forced (OFAF)

In this method, oil is circulated with the help of a pump. The oil circulation is forced through the heat exchangers. Then compressed air is forced to flow on the heat exchanger with the help of fans. This type of cooling is provided for higher rating transformers at substations or power stations.

iv. Oil forced Water Forced (OFWF)

This method is similar to OFAF method, but here forced water flow is used to dissipate heat from the heat exchangers. The oil is forced to flow through the heat exchanger with the help of a pump, where the heat is dissipated in the water which is also forced to flow. The heated water is taken away to cool in separate coolers. This type of cooling is used very large transformers having ratings of several hundreds of MVA.

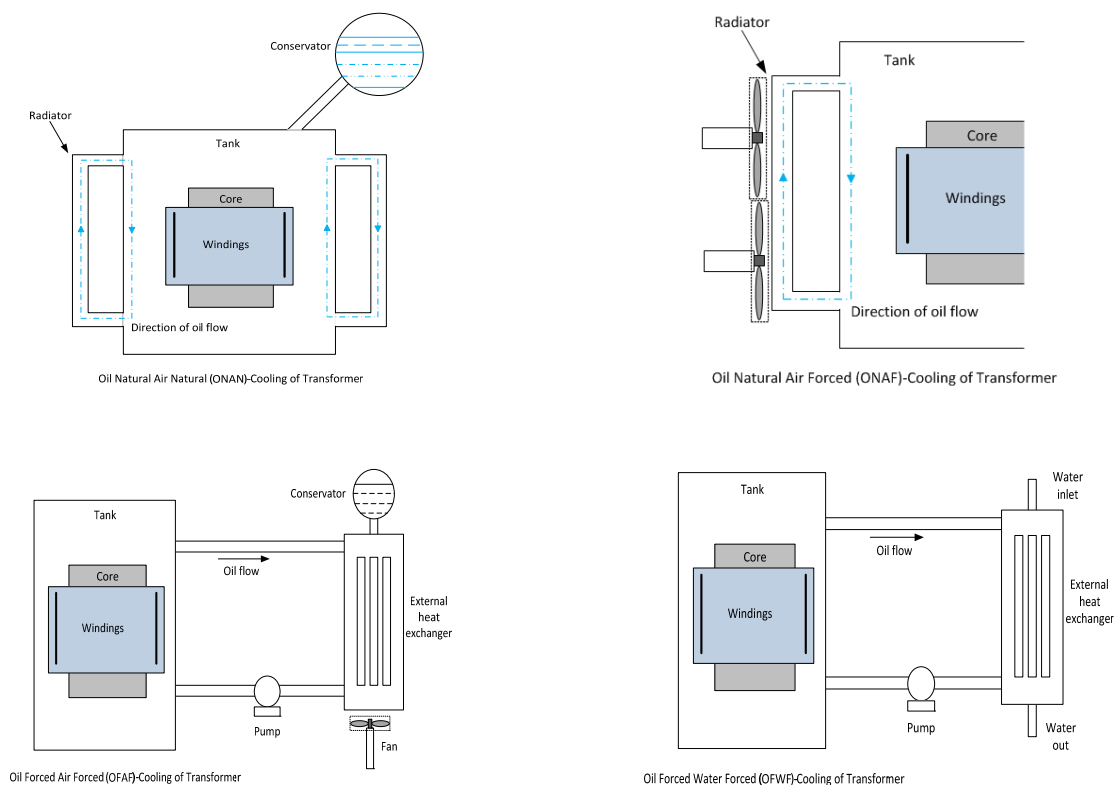
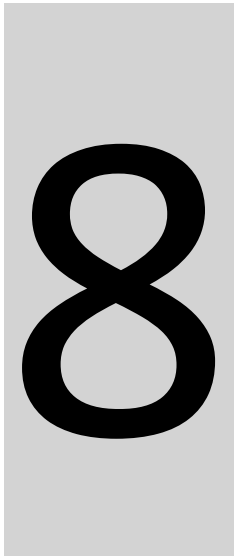


Fig. 125 Oil cooling systems for transformers

Conclusions on cooling

To be added



The purpose of this chapter is to present methods of determination and description of insulation strengths.

8. Insulation coordination

Insulation coordination is the selection of the strength of the insulation. Normal and standard conditions must be known in order to specify the strength. There are different methods of describing it, like: BIL (Basic Lightning Impulse), BSL (Basic Switching Impulse) or CFO[59]. The overall aim of insulation coordination is to reduce to an economically and operationally acceptable level the cost and disturbance caused by insulation failure. In insulation coordination method, the insulation of the various parts of the system must be so graded that flash over if occurs it must be at intended points[60].

Types of insulation

Insulation can be classified as internal or external and also as self-restoring and non-self-restoring.

External Insulation

External insulation is the distance in open air or across the surfaces of solid insulation in contact with open air that are subjected to dielectric stress and to the effects of the atmosphere. Examples of external insulation are the porcelain shell of the bushing, bus support insulators and disconnecting switches.

Internal Insulation

Internal insulation is the internal solid, liquid, or gaseous parts of the insulation of the equipment that are protected by the equipment, enclosures from the effects of the atmosphere. Examples are transformer insulation and the internal insulation of bushings. Equipment may be a combination of internal and external insulation. Examples are a bushing and a circuit breaker.

Self restoring insulation (SR)

Insulation that completely recovers insulating properties after a disruptive discharge (flashover) caused by the application of a voltage is called self-restoring insulation. This type of insulation is generally external insulation.

Non-Self-Restoring Insulation

This is the opposite of self restoring insulators, insulation that loses insulating properties or does not recover completely after a disruptive discharge caused by the application of a voltage. This type of insulation is generally internal insulation.

Basic Lightning Impulse Insulation Level (BIL)

The BIL level is the electrical strength of insulation expressed in terms of the crest value of the “standard lightning impulse”. The BIL is tied to a specific waveshape in addition being tied to standard atmospheric conditions.

Basic Switching Impulse Insulation Level (BSL)

The BSL is the electrical strength of insulation expressed in terms of the crest value of a standard switching impulse.

Standard Waveshapes

The general lightning and switching impulse waveshapes are illustrated bellow:

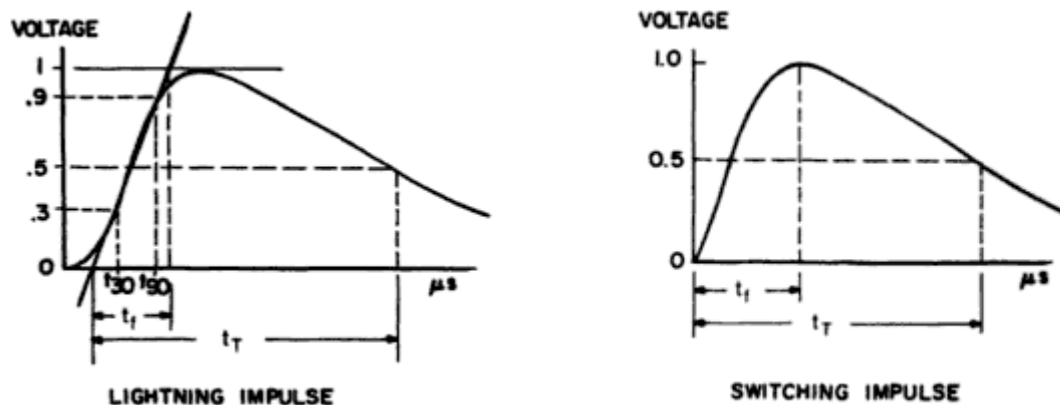


Fig. 126 Standard Waveshapes [59]

Insulation coordination has become a well developed engineering practice. This practice is where the characteristics of the system, insulation of all forms and arresters of all forms cross paths. System performance can be modeled using simple formula presented in IEC 60071-1, 60071-2 and 60071-4. These three standards are very well written and easy to use. They cover 99% of what a person needs to know to perform a lightning or switching surge insulation coordination study. IEEE 1313.1 and 1313.2 are another excellent source for better understanding this engineering practice. A third and highly acclaimed reference is “Insulation Coordination of Power Systems” by Andrew Hileman [61].

There are two coordination methods used in the practice of insulation coordination. The deterministic method is used exclusively when applied to non-self-restoring insulation. When coordinating self-restoring insulation, statistical (or probabilistic) methods are used. The basic difference between these two methods is that in the deterministic method, absolute maximum and minimum values are coordinated[61].

9

9. Conclusions

This state of the art report has investigated concepts and demonstrators for dc/dc converters rated at megawatt and kilovolt levels. Focus has been on dc turbine, traction and solid state transformers. Different topologies have been presented, showing that resonant and phase shift topology are mostly employed. Hardware aspects of transformer, semiconductors, cooling and insulation coordination have also been briefly studied.

Based on the review of concepts and demonstrators from traction and MV distribution, a list of conclusions is shown:

- Modularity is an easy path to follow, when building kV, KHZ and [MW] setups, despite applications specifications. That is why most of the demonstrators are build using this philosophy but also because redundancy is required
- Commissioning of the converters begins from component level (semiconductor characterization, transformer loss model, etc) and goes up to sub-system level, where control and protection are implemented and finally on the system level.
- The highest challenges were on hardware issues like: transformer design, semiconductors device selection and cooling. Not so much on control and protection
- Transformer design has been (and still is) a great issue. Different materials and core shapes have been investigated and clearly c-core nanocrystalline seems to be the preferred option. And the main reason is to reach high power density.
- Transformer mechanical complexity was influenced mainly by cooling and insulation.
- Different cooling methods have been proposed: starting from simple methods like oil immersion to complex de-ionized heat-sinks build around the core and windings or a

combination of this two. Smaller transformers in size at high power levels clearly give high loss density and getting out the heat is no longer a trivial task.

- Efforts for integration of the converters were seen. Due to modularity, it is easier to build 1:1 transformers and integrate it in one PEBB (Power Electronic Building Block), together with the semiconductors and other passives
- It looks like 4.5 kV and 6.5 kV IGBTs were the most employed semiconductors, while only a few choose lower voltage devices, like 1.7 kV or 1.2 kV for the MV side
- It seems that in all demonstrators, soft-switching properties are particularly attractive for MV high-power applications since they allow for further increases in the switching frequency beyond values usually associated with semiconductors used in the applications (several hundred of hertz). This is of importance for isolated dc-dc converters as an increased switching frequency usually leads to a reduction of the transformer size.

What remains to investigate?

Most of the investigations need to be done on engineering aspects. There is a lot of conceptual work, but the real hardware challenges are not yet addressed of offshore dc wind farms.

- **Transformer design** for higher power and voltage: [MW] power levels, kV range and high switching frequency are though design specifications for the transformer. It needs to be proven that with high efforts, a robust, economic and viable design for these levels is achievable, while using one monolithic core. Otherwise, it will be quite difficult not to choose a modular or cascaded converter topology. And this will mean a high number of components, thus low reliability and in the end high OPEX. We know that classic 50Hz transformer technology has overcome the challenges on all power and voltage levels, so it could be interesting to evaluate how they were solved and maybe use or get inspiration from those methods for medium frequency transformers.
- **Valve design** with series connected switches for voltages 25 kV. There isn't really much work done in this area with elevated switching frequency in soft-switching. If active switches like IGBT, IGCT or even IEGT should be use, then the mechanical complexity increases proportional with the voltage, as gate drivers, snubbers, monitoring circuits, resistors, capacitors need to be incorporated. But, it is expected that the turbine converter will be uni-direction, therefor fast rectifying diodes will be employed. Nevertheless, the work on valve design with active switches will be useful for the substation converter.
- **Protection** for overvoltage and short circuit concepts need to be evaluated.
- **High voltage aux smps** topologies, active switches, magnetics and concepts have to be investigate. A low cost, MV connected aux supply will help advancing the state of the art
- **Voltage and currents sensors** with high voltage insulation and low mechanical complexity for medium voltage side
- **Failure rate estimation and mechanism** for power electronics used in offshore wind turbines. The knowledge build up will help the design for reliability
- **Uncover the design principles that lead to high availability**

A preliminary ranking of 3 main design challenges for high power medium voltage dc/dc converter is presented bellow:

Challenge	Rank
Transformer design with low loss density, reduced partial discharge and monolithic core	3
MV Valve design with robust performance and economic value	2
Selection of topology to reach high availability, high efficiency but low component ratings	1

The goal of this work was to down select from a wide pool of possible candidates to only a few. Conclusions on advantages and disadvantages of some topologies are presented bellow:

Hard switching converters

This family of converters has a few advantages like: the technology is proven, has tracking record, limited R&D would be required to implement a full scale dc turbine (by adding a rectifier on medium voltage) and time to market could be faster then other solutions. The down side would be high weight, volume, costs, lower efficiency and reliability. Therefore, it is not a viable solution at the present. Implementing a topology with hard switching will not bring any advantages compared to a classic MVAC turbine, which is what we would like achieve.

Matrix convertes

This topology seems attractive by offering fewer power stages. But it has no tracking record at elevated power and voltage, control seems to be complex and the use of commercial bidirectional switches is limited. Therefore, this option is not attractive as long as challenges on medium frequency transformer and medium voltage valve design exist also here.

High gain converters

Even if this category can offer high voltage gain and has no use of transformer, thus increasing power density, the lack of galvanic separation will only shift engineering effort on generator and nacelle insulation coordination. The tracking record is limited on small scale prototypes (smaller then 30kW), where mainly functionality has been proved. It is considered that the elevated version will not be viable due to the high number of switching cells, composed mainly of electrolytic capacitors and air inductors.

MMC converters

This type of converters is attractive for HVDC levels. They are able to provide low switching losses at the cost of increased controllability, but if the fundamental frequency is increased from 50Hz to kHz level then the main advantage will be lost. It is hard to see how with high availability, power density and low costs can be achieved with a high number of semiconductors and passives.

Phase shift converters

Single and Dual active Bridge converters are interesting options due to soft switching possibilities, high power density and high efficiency. The down side is the transformer design, which needs to withstand high di/dt. The SAB has the disadvantage of voltage drop across the stray inductance due to current dependence, while the DAB will require a complex medium voltage valve design. Nevertheless, the

topology has been implemented on scaled demonstrator and has good tracking record, therefore will be considered as an option in this project.

Resonant topologies

Considering high efficiency, sinusoidal excitation for the transformer and lower MV valve complexity, resonant topologies like SRC and LLC promise to be a good candidate to achieve high power density. Tracking record in traction for MW prototypes exist which brings the technology readiness to a higher level compared to other families. Anyway, there are big disadvantages which need to be conquered: medium voltage capacitors will have to withstand kilo amps, high availability and long life time. Efficiency at partial load is low, while controllability for no load conditions is hard to achieve. But, it is considered that this drawback can be overcome, so this family of converter is considered as an option to continue.

Therefore, two candidate families are selected for down selection: phase shift and resonant converters.



10. Bibliography

- [1] C. Zhao, M. Weiss, A. Mester, S. Lewdeni-Schmid, D. Dujic, J. K. Steinke, and T. Chaudhuri, "Power electronic transformer (PET) converter: Design of a 1.2MW demonstrator for traction applications," *SPEEDAM 2012 - 21st Int. Symp. Power Electron. Electr. Drives, Autom. Motion*, pp. 855–860, 2012.
- [2] N. Soltau, H. Stagge, R. W. De Doncker, and O. Apeldoorn, "Development and demonstration of a medium-voltage high-power DC-DC converter for DC distribution systems," *2014 IEEE 5th Int. Symp. Power Electron. Distrib. Gener. Syst.*, no. 978, pp. 1–8, 2014.
- [3] C. Meyer, *Key Components for Future Offshore DC Grids*. 2007.
- [4] S. Kenzelmann, "Modular DC / DC Converter for DC Distribution and Collection Networks PAR," vol. 5430, 2012.
- [5] R. U. Lenke and R. U. Lenke, E . *ON Energy Research Center A CONTRIBUTION TO THE DESIGN OF ISOLATED DC-DC CONVERTERS FOR UTILITY APPLICATIONS A Contribution to the Design of Isolated DC-DC Converters for Utility Applications*. .
- [6] S. Meier, "Novel Voltage Source Converter based HVDC Transmission System for Offshore Wind Farms," *Electronics*, 2005.
- [7] L. Max, *Design and Control of A DC Grid for Offshore Wind Farms*. 2009.
- [8] A. Garc, *Alejandro Garcés Ruiz Design , Operation and Control of Series-Connected Power Converters for Offshore Wind Parks*, no. August. 2012.

- [9] A. Q. Huang and R. Burgos, "Review of Solid-State Transformer Technologies and Their Application in Power Distribution Systems," *IEEE J. Emerg. Sel. Top. Power Electron.*, vol. 1, no. 3, pp. 186–198, 2013.
- [10] S. Madhusoodhanan and A. Tripathi, "Solid State Transformer and MV Grid Tie applications enabled by 15 kV SiC IGBTs and 10 kV SiC MOSFETs based Multilevel Converters," 2014.
- [11] W. Chen, A. Q. Huang, C. Li, G. Wang, and W. Gu, "Analysis and comparison of medium voltage high power DC/DC converters for offshore wind energy systems," *IEEE Trans. Power Electron.*, vol. 28, no. 4, pp. 2014–2023, 2013.
- [12] Abb, "Power Electronic Transformer for railway on-board applications – an overview," 2013.
- [13] L. Heinemann, "An actively cooled high power, high frequency transformer with high insulation capability," *APEC. Seventeenth Annu. IEEE Appl. Power Electron. Conf. Expo. (Cat. No.02CH37335)*, vol. 1, no. c, 2002.
- [14] H. Hoffmann and B. Piepenbreier, "Medium frequency transformer for rail application using new materials," *2011 1st Int. Electr. Drives Prod. Conf.*, pp. 192–197, 2011.
- [15] T. Kjellqvist, S. Norrga, and S. Östlund, "Design considerations for a medium frequency transformer in a line side power conversion system," *PESC Rec. - IEEE Annu. Power Electron. Spec. Conf.*, vol. 1, pp. 704–710, 2004.
- [16] M. Steiner and H. Reinold, "Medium frequency topology in railway applications," *2007 Eur. Conf. Power Electron. Appl. EPE*, 2007.
- [17] G. Ortiz, M. Leibl, J. W. Kolar, and O. Apeldoorn, "Medium Frequency Transformers for Solid-State-Transformer Applications - Design and Experimental Verification," *Int. Conf. Power Electron. Drive Syst.*, pp. 1285–1290, 2013.
- [18] G. Ortiz, J. Biela, D. Bortis, and J. W. Kolar, "Converter for Renewable Energy Applications Converter for Renewable Energy Applications," *Int. power Electron. Conf.*, pp. 3212–3219, 2010.
- [19] R. Grinberg, S. Ebner, and O. Apeldoorn, "Reliability in Medium Voltage Converters for Wind Turbines," pp. 1–4.
- [20] R. Pena-Alzola, G. Gohil, L. Mathe, M. Liserre, and F. Blaabjerg, "Review of modular power converters solutions for smart transformer in distribution system," *2013 IEEE Energy Convers. Congr. Expo. ECCE 2013*, pp. 380–387, 2013.
- [21] N. Hugo, P. Stefanutti, M. Pellerin, and A. Akdag, "Power electronics traction transformer," *2007 Eur. Conf. Power Electron. Appl. EPE*, 2007.
- [22] I. Villar, L. Mir, I. Etxeberria-Otadui, J. Colmenero, X. Agirre, and T. Nieva, "Optimal design and experimental validation of a Medium-Frequency 400kVA power transformer for railway traction applications," *2012 IEEE Energy Convers. Congr. Expo. ECCE 2012*, pp. 684–690, 2012.
- [23] M. K. Das, C. Capell, D. E. Grider, S. Leslie, J. Ostop, R. Raju, M. Schutten, J. Nasadoski, and A. Hefner, "10 kV, 120 a SiC half H-bridge power MOSFET modules suitable for high frequency,

- medium voltage applications,” *IEEE Energy Convers. Congr. Expo. Energy Convers. Innov. a Clean Energy Futur. ECCE 2011, Proc.*, pp. 2689–2692, 2011.
- [24] G. Wang, S. Baek, J. Elliott, A. Kadavelugu, F. Wang, X. She, S. Dutta, Y. Liu, T. Zhao, W. Yao, R. Gould, S. Bhattacharya, and A. Q. Huang, “Design and hardware implementation of Gen-1 silicon based solid state transformer,” *Conf. Proc. - IEEE Appl. Power Electron. Conf. Expo. - APEC*, pp. 1344–1349, 2011.
- [25] J. Clare, “Modular high power converter topologies,” *Power Electron. 2010 Improv. Effic. Power Grid, IET Semin.*, pp. 1–57, 2010.
- [26] M. Pavlovsky, S. W. H. De Haan, and J. a. Ferreira, “Concept of 50 kW DC/DC converter based on ZVS, quasi-ZCS topology and integrated thermal and electromagnetic design,” *2005 Eur. Conf. Power Electron. Appl.*, 2005.
- [27] D. Aggeler, J. Biela, and J. W. Kolar, “A compact, high voltage 25 kW, 50 kHz DC-DC converter based on SiC JFETs,” *Conf. Proc. - IEEE Appl. Power Electron. Conf. Expo. - APEC*, pp. 801–807, 2008.
- [28] H. Cha, Q. Tang, and F. Z. Peng, “Metro Vehicle System Converter for,” pp. 1613–1618, 2007.
- [29] L. Max and T. Thiringer, “Control method and snubber selection for a 5 MW wind turbine single active bridge DC/DC converter,” *2007 Eur. Conf. Power Electron. Appl. EPE*, 2007.
- [30] L. Yang, T. Zhao, J. Wang, and A. Q. Huang, “Design and analysis of a 270kW five-level DC/DC converter for solid state transformer using 10kV SiC power devices,” *PESC Rec. - IEEE Annu. Power Electron. Spec. Conf.*, pp. 245–251, 2007.
- [31] W. Chen, A. Huang, C. Li, and G. Wang, “A High Efficiency High Power Step-Up Resonant Switched-Capacitor Converter for Offshore Wind Energy Systems,” pp. 235–239, 2012.
- [32] J. Robinson, D. Jovcic, and G. Joós, “Analysis and design of an offshore wind farm using a MV DC grid,” *IEEE Trans. Power Deliv.*, vol. 25, no. 4, pp. 2164–2173, 2010.
- [33] A. Parastar and J. Seok, “High-Gain Resonant Switched-Capacitor Cell-Based DC / DC Converter for Offshore Wind,” vol. 30, no. 2, pp. 644–656, 2015.
- [34] K. Park and Z. Chen, “Analysis and design of a parallel-connected single active bridge DC-DC converter for high-power wind farm applications,” *2013 15th Eur. Conf. Power Electron. Appl. EPE 2013*, vol. 8, pp. 665–671, 2013.
- [35] F. Deng, “Design and Control of A DC Grid for Offshore Wind Farms,” p. 133, 2012.
- [36] K. Park and Z. Chen, “Analysis and design of a parallel-connected single active bridge DC-DC converter for high-power wind farm applications,” *2013 15th Eur. Conf. Power Electron. Appl. EPE 2013*, 2013.
- [37] S. Lundberg and T. Thiringer, *Wind farm configuration and energy efficiency studies-series DC versus AC layouts*, vol. Doctor of . 2006.

- [38] S. S. Gjerde, *Sverre Skalleberg Gjerde Analysis and Control of a Modular Series Connected Converter for a Transformerless Offshore Wind Turbine*, no. October. 2013.
- [39] D. J. S.M.Fazeli, "LUND 2015 Demonstration of 30kW IGBT LCL DC / DC converter as proof of concept for interconnecting HVDC systems into a future DC grid S . M . FAZELI , seyedmahdifazeli@abdn.ac.uk , School of Engineering , University of Aberdeen , Aberdeen , AB24 3UE , UK," pp. 1–6, 2015.
- [40] I. Villar, "Multiphysical characterization of medium-frequency power electronic transformers," vol. 4622, p. 234, 2010.
- [41] E. Agheb and H. K. Hoidalen, "Medium frequency high power transformers, state of art and challenges," *2012 Int. Conf. Renew. Energy Res. Appl.*, pp. 1–6, 2012.
- [42] S. Balci and I. Sefa, "Core Material Investigation of Medium-Frequency Power Transformers," pp. 861–866, 2014.
- [43] K. Venkatachalam, C. R. Sullivan, T. Abdallah, and H. Tacca, "Accurate prediction of ferrite core loss with nonsinusoidal waveforms using only Steinmetz parameters," *2002 IEEE Work. Comput. Power Electron. 2002. Proceedings.*, no. June, 2002.
- [44] "www.hivolt.com." .
- [45] G. Ortiz, J. Biela, and J. W. Kolar, "MegaCube," 2010.
- [46] Y. Zhou, D. E. Macpherson, W. Blewitt, and D. Jovcic, "Comparison of DC-DC converter topologies for offshore wind-farm application," *6th IET Int. Conf. Power Electron. Mach. Drives (PEMD 2012)*, pp. A12–A12, 2012.
- [47] O. S. Senturk, *High Power Density Power Electronic Converters for Large Wind Turbines*, no. November. 2011.
- [48] K. Lee, K. Jung, Y. Suh, C. Kim, H. Yoo, and S. Park, "Comparison of high power semiconductor devices losses in 5MW PMSG MV wind turbines," *Conf. Proc. - IEEE Appl. Power Electron. Conf. Expo. - APEC*, pp. 2511–2518, 2014.
- [49] H. a. Toliyat, "Recent advances and applications of power electronics and Motor Drives - Electric machines and motor drives," *2008 34th Annu. Conf. IEEE Ind. Electron.*, 2008.
- [50] "http://nepsi.com/products/thyristor-switched-harmonic-filter-banks/components/thyristor-valves.html." .
- [51] I. C. Cells and T. Modeer, "Implementation and Testing of High-Power," pp. 5355–5359, 2014.
- [52] M. Ranjbar, M. Farzi, A. A. Ahmad, and A. Abrishamifar, "Theoretical and practical considerations relating to design high-voltage IGBT valve," *2011 19th Iran. Conf. Electr. Eng.*, pp. 1–1, 2011.
- [53] H. Huang and M. Uder, "Application of high power thyristors in HVDC and FACTS systems," *17th Conf. Electr. Power Supply Ind.*, 2008.
- [54] Semikron, "http://www.powerguru.org/cooling-methods-for-power-semiconductor-devices/." .

- [55] “<http://www.powerguru.org/water-cooling-of-power-modules/>.” .
- [56] S. S. Kang and A. Thermalloy, “Advanced Cooling for Power Electronics Power Module Packages,” *Cips*, vol. 9, 2012.
- [57] P. E. Tuma, “Passive 2-Phase Liquid Techniques to Control Temperatures in Microelectronics and Power Systems,” no. Figure 1.
- [58] “<http://www.electricaleasy.com/2014/06/cooling-methods-of-transformer.html>.” .
- [59] A. R.Hileman, *Insulation Coordination for Power Systems*. 1999.
- [60] “<http://www.electrical4u.com/insulation-coordination-in-power-system/>.” .
- [61] J. Woodworth, “ArresterWorks,” 2012.

10

11. Appendix

a. Historic summary of high power dc/dc converters

To be added.